

DEVELOPMENT OF CATALYST MATERIALS BASED ON CARBON NANOFIBERS FOR ELECTROCHEMICAL CELL APPLICATIONS

Teză destinată obținerii
titlului științific de doctor inginer
la
Universitatea Politehnica Timișoara
în domeniul INGINERIE CHIMICĂ
de către

Ing. Roxana Muntean

Conducător științific: prof.univ.dr.ing Nicolae Vasilcsin
Referenți științifici: prof.univ.dr.ing Waltraut Brandl
prof.univ.dr.ing. Florica Manea
prof.univ.dr.ing. Petru Ilea

Ziua susținerii tezei: 09.12.2016

Seriile Teze de doctorat ale UPT sunt:

- | | |
|---|--|
| 1. Automatică | 10. Știința Calculatoarelor |
| 2. Chimie | 11. Știința și Ingineria Materialelor |
| 3. Energetică | 12. Ingineria sistemelor |
| 4. Ingineria Chimică | 13. Inginerie energetică |
| 5. Inginerie Civilă | 14. Calculatoare și tehnologia informației |
| 6. Inginerie Electrică | 15. Ingineria materialelor |
| 7. Inginerie Electronică și Telecomunicații | 16. Inginerie și Management |
| 8. Inginerie Industrială | 17. Arhitectură |
| 9. Inginerie Mecanică | 18. Inginerie civilă și instalații |

Universitatea Politehnica Timișoara a inițiat seriile de mai sus în scopul diseminării expertizei, cunoștințelor și rezultatelor cercetărilor întreprinse în cadrul Școlii doctorale a universității. Seriile conțin, potrivit H.B.Ex.S Nr. 14 / 14.07.2006, tezele de doctorat susținute în universitate începând cu 1 octombrie 2006.

Copyright © Editura Politehnica – Timișoara, 2016

Această publicație este supusă prevederilor legii dreptului de autor. Multiplicarea acestei publicații, în mod integral sau în parte, traducerea, tipărirea, reutilizarea ilustrațiilor, expunerea, radiodifuzarea, reproducerea pe microfilme sau în orice altă formă este permisă numai cu respectarea prevederilor Legii române a dreptului de autor în vigoare și permisiunea pentru utilizare obținută în scris din partea Universității Politehnica Timișoara. Toate încălcările acestor drepturi vor fi penalizate potrivit Legii române a drepturilor de autor.

România, 300159 Timișoara, Bd. Republicii 9,
Tel./fax 0256 403823
e-mail: editura@edipol.upt.ro

Foreword

The present thesis was elaborated based on the scientific work accomplished in Laboratory of Electrochemistry, Corrosion and Electrochemical Engineering from Faculty of Industrial Chemistry and Environmental Engineering, University Politehnica Timișoara and in Laboratory of Materials Science from Westphalian University of Applied Sciences, Gelsenkirchen, Germany.

This work deals with the development of catalyst materials based on carbon nanofibers decorated with platinum and platinum cobalt alloy particles for electrochemical cell applications. During three years, it would have been impossible for me to accomplish this work without the help, encouragement and support of coordinating professors, colleagues, friends and family.

First and foremost, I would like to express my deeply gratitude to Prof. Dr. Eng. Nicolae Vaszilcsin from University Politehnica Timișoara, for giving me the possibility to study an interesting subject under his academic guidance and support and for his invaluable help throughout my PhD study.

I would like to thank Prof. Dr. Eng. Waltraut Brandl from Westphalian University of Applied Sciences, Gelsenkirchen, for all the support, valuable scientific advices and for offering me the opportunity to conduct my research in an international environment, in a modern and well equipped laboratory.

Special thanks to Prof. Dr. Eng. Gabriela Mărginean from Westphalian University of Applied Sciences, Gelsenkirchen, for her permanent help, for always having time to offer me advices and to teach me and for giving me a lot of opportunities to learn new things.

Furthermore, I would like to thank Prof. Dr. Eng. Cornelia Păcurariu, Assoc. Prof. Dr. Eng. Andrea Kellenberger and Assist. Prof. Dr. Eng. Narcis Duțeanu from University Politehnica Timișoara for being part of my committee and for their great suggestions and advices regarding my scientific research.

Many thanks to my colleagues and friends from Gelsenkirchen and Timișoara for the constructive discussions, their moral support, advices and friendship.

Finally, last but not least, I am extremely grateful to my family for their kind support, for trusting me and encouraging me to make important steps in my life.

Timișoara, December, 2016

Eng. Roxana MUNTEAN

Muntean, Roxana

DEZVOLTAREA UNOR MATERIALE CATALITICE PE BAZĂ DE NANOFIBRE DE CARBON PENTRU APLICAȚII ÎN CELULE ELECTROCHIMICE

Teze de doctorat ale UPT, Seria 4, Nr. 85, Editura Politehnica, 2016, 124 pagini, 66 figuri, 15 tabele.

ISSN:1842-8223

ISBN:978-606-35-0117-3

Cuvinte cheie: nanofibre de carbon, electrocatalizatori, aliaje platină-cobalt, plasmă de oxigen, funcționalizare cu plasmă, plasmă de microunde.

Rezumat,

Nanoparticulele de platină pe suport de carbon sunt utilizate în domenii extrem de variate, însă una dintre cele mai importante aplicații o constituie pilele de combustie. În această lucrare, atenția a fost îndreptată spre obținerea de materiale catalitice pe bază fibre de carbon decorate cu particule de catalizator. În acest scop, s-a urmărit îmbunătățirea reactivității CNF prin expunerea acestora unui proces de funcționalizare folosind plasmă de oxigen. Acest tratament generează pe suprafața exterioară a fibrelor grupări funcționale pe bază de oxigen (carboxil, carbonil sau hidroxil), crescând astfel dispersabilitatea acestora în solvenți polari. Depunerea particulelor de catalizator a fost realizată prin aplicarea unei metode electrochimice, folosind curent pulsatoriu, dintr-un electrolit acid. Electrozi CNF-Pt/Pt-Co cu conținut scăzut de platină rezultați în acest studiu au fost analizați în vederea determinării morfologiei, compoziției chimice, distribuției și cantității de particule de catalizator depuse pe suportul de carbon. Investigațiile au relevat o distribuție uniformă a particulelor de catalizator cu dimensiuni nanometrice reduse. Metoda prezentată conduce la o modalitate rapidă și facilă de dezvoltare a electrozilor cu o activitate catalitică ridicată, datorată prezenței platinei, metalul cel mai electroactiv.

DEVELOPMENT OF CATALYST MATERIALS BASED ON CARBON NANOFIBERS FOR ELECTROCHEMICAL CELL APPLICATIONS

Keywords: carbon nanofibers, electrocatalysts, platinum-cobalt alloys, oxygen plasma, plasma functionalization, microwave plasma.

Abstract,

Carbon-supported Pt nanoparticles are used in different fields, but one of the most important applications is as electrocatalyst for fuel cells. In this work, the attention was focused on the development of catalyst materials based on carbon nanofibers decorated with catalyst particles. In this regard, the improvement of handling and wettability of CNF, by subjecting them to a functionalization process using oxygen plasma was performed. By employing this treatment, different oxygen containing functional groups (carboxylic, carbonylic or hydroxylic) are generated on the outer surface of CNF, enhancing their dispersibility in a polar solvent. The catalyst deposition was performed using an electrochemical method, applying a pulsed current technique from an acidic solution. The resulted CNF-Pt/Pt-Co electrodes with low platinum loading were further analysed to determine the morphology, chemical composition, distribution and amount of catalyst particles deposited onto the carbonic support material. SEM investigations revealed a homogeneous distribution of the catalyst particles with a nanometric size range. The presented method leads to a facile and rapid way to develop electrodes with an improved catalytic activity promoted by the presence of platinum, the most electroactive metal.

Content

Abstract.....	7
Abbreviations.....	9
1 INTRODUCTION.....	11
1.1 Background and motivation.....	11
1.2 Aim of the work.....	14
2 STATE OF THE ART.....	16
2.1 Theoretical aspects regarding catalyst materials.....	16
2.1.1 Definition of the catalyst.....	16
2.1.2 Catalysts classification.....	17
2.1.3 Applications.....	18
2.2 PEMFC - A brief description of the technology.....	18
2.3 PEMFC catalysts.....	22
2.4 Support materials for PEMFC catalysts.....	25
2.5 Synthesis methods of platinum based catalysts.....	28
2.6 Polymer electrolyte membrane.....	31
2.7 Degradation mechanisms for PEMFC components.....	32
2.7.1 Membrane degradation.....	32
2.7.2 GDL degradation.....	33
2.7.3 Catalytic layer degradation.....	33
2.7.4 Bipolar plates degradation.....	34
3 METHODOLOGY AND EQUIPMENT.....	35
3.1 Equipment and Materials.....	35
3.2 Physical Characterization.....	36
3.2.1 Scanning Electron Microscopy (SEM).....	36
3.2.2 Energy Dispersive X-ray Spectroscopy (EDX).....	37
3.2.3 X-ray Diffraction (XRD).....	38
3.2.4 Thermogravimetric Analysis (TGA).....	39
3.2.5 X-Ray Fluorescence (XRF).....	41
3.3 Electrochemical Techniques.....	41
3.3.1 Linear Sweep Voltammetry (LSV).....	42
3.3.2 Tafel Slope Method.....	43
3.3.3 Cyclic Voltammetry (CV).....	44
3.3.4 Pulsed Current Deposition Method (PCD).....	45
3.4 CNF Treatment.....	46
3.4.1 Low-pressure Plasma Treatment.....	47
3.4.2 Titrimetric Analysis.....	48
3.5 Membrane Electrode Assembly (MEA) Testing.....	49
4 EXPERIMENTAL PROGRAM.....	50
4.1 Preparation of the support electrode.....	51
4.1.1 CNF functionalization treatment.....	51
4.1.2 CNF thermal behaviour.....	53
4.1.3 CNF corrosion investigations.....	56
4.2 Synthesis of platinum based catalysts.....	61

4.2.1	Pulsed current deposition of Pt nanoparticles on CNF support material.....	66
4.2.1.1	Influence of the functionalization on the Pt/CNF morphology.....	68
4.2.1.2	Influence of the current density on the Pt/CNF morphology.....	69
4.2.1.3	Influence of the duty cycle on the Pt/CNF morphology.....	70
4.2.1.4	Influence of the number of cycles on the Pt/CNF morphology.....	71
4.2.2	Characterisation of the obtained platinum catalysts.....	72
4.2.3	Applications of the Pt/CNF catalysts.....	77
4.2.3.1	HER on Pt/CNF electrodes.....	77
4.2.3.2	In situ PEMFC polarization curves on Pt/CNF catalysts.....	80
4.3	Synthesis of platinum - cobalt based catalysts.....	83
4.3.1	Pulsed current deposition of Pt-Co alloy on CNF support material...	86
4.3.1.1	Influence of the bath composition on the Pt-Co/CNF morphology...	86
4.3.1.2	Influence of the current density on the Pt Co/CNF morphology.....	87
4.3.1.3	Influence of number of cycles on the Pt-Co/CNF morphology.....	89
4.3.1.4	Influence of the duty cycle on the Pt-Co/CNF morphology.....	90
4.3.2	Characterization of the obtained Pt-Co catalysts.....	91
4.3.3	Applications of the Pt-Co/CNF catalysts.....	96
4.3.3.1	OER on Pt-Co/CNF electrodes.....	96
4.3.3.2	In situ PEMFC polarization curves on Pt-Co/CNF catalysts.....	98
5	CONCLUSIONS.....	100
	OUTLOOK.....	104
	REFERENCES.....	105
	APPENDIX.....	115

Abstract

The main goal of the present study was to develop catalyst materials with high catalytic activity for electrochemical cell applications, based on carbon nanofibers decorated with platinum and platinum-cobalt alloy particles.

The thesis has been structured into 5 chapters:

Chapter 1 presents a short introduction, highlighting the background and motivation of the chosen topic.

Chapter 2 deals with state of the art in the field of catalysts, succinctly presenting some theoretical aspects regarding catalysts production, current fabrication methods, classification and main applications. Moreover, a brief description of the PEMFC technology is realized, emphasizing the key components and reaction mechanisms that appear during operation.

Chapter 3 describes the methodology and equipment used to accomplish the experimental program. This chapter offers an overview regarding the applied investigation methods and presents different analytic techniques, which can provide important information on quality and performance of the developed catalyst materials.

Chapter 4 presents the experimental program concerning the functionalization treatment of the carbon support material, catalyst material deposition, reporting the detailed steps in order to obtain the catalyst electrodes and furthermore exhibits the results attained during this study, highlighting the important aspects.

Chapter 5 reveals the conclusions and original contributions achieved through this work.

In the actual state of the art, platinum is considered the most effective catalyst material for electrochemical reactions, but due to its prohibitive price, the use of this metal in industrial purposes is limited. Therefore, during last years, several materials have been investigated, in order to obtain efficient catalyst materials for electrochemical systems. Lately, scientists have endeavoured to reduce the platinum amount without affecting the desired characteristics like catalytic activity, structural stability, high electrical conductivity and good corrosion resistance. Carbon based materials, such as carbon nanofibers, are suitable support materials for catalyst particles, providing an increased available surface area, good mechanical properties, high electrical conductivity and nevertheless, good interaction with the catalyst particles. The high graphitization degree of the fibers provides a good corrosion resistance and assures a defect free crystalline material.

In the present study, the possibility of bringing together the unique characteristics of CNF with high graphitization degree and the special properties of the noble Pt nanoparticles was tested.

The **original contributions** of this study refer to the possibility of combining the oxygen plasma functionalization treatment of the support material with the electrochemical deposition method (pulsed current deposition) to develop low platinum and platinum-cobalt loading catalysts, suitable for electrochemical devices, like fuel cells or water splitting electrolyzers. In this regard, investigations on the degradation mechanism (corrosion resistance, thermal stability, graphitization degree) of the CNF support material after the functionalization treatment are performed. Studies on the deposition mechanisms of platinum and

platinum-cobalt codeposition respectively, from a self-developed electrolyte are accomplished by analysing the linear and cyclic polarisation curves, carried out onto the support material. Moreover, the evaluation of the dual catalytic effect of the developed electrodes is investigated by determination of the kinetic parameters for HER and OER in a three-electrode cell, from acid and alkaline electrolytes. Additionally, the performance of the electrodes as catalyst for PEMFC was verified in a single-cell test bench at room temperature.

Carbon-supported Pt nanoparticles are used in different fields, but one of the most important applications is as electrocatalyst for fuel cells. Several studies during the last years have revealed that there is a strong correlation between size and distribution of the catalyst particles on the surface of support material and the efficiency of the catalyst. In this work, the attention was focused on the improvement of handling and wettability of CNF, by subjecting them to a functionalization process using oxygen plasma. The advantages of this method are various. Through this treatment, different oxygen containing functional groups (carboxylic, carbonylic and hydroxylic) are generated on the outer surface of CNF, enhancing their dispersibility in a polar solvent. The presence of such functional groups leads to favourable changes regarding their reactivity and improves considerably the catalyst deposition process. After functionalization, CNF were dispersed into isopropanol and the obtained ink was sprayed onto a gas diffusion layer. The obtained uncatalysed electrode represents the support material for platinum and platinum-cobalt particles, which are subsequently deposited onto its surface. The catalyst deposition was performed using an electrochemical method, applying a pulsed current technique from an acid solution. The electrolyte was developed by mixing K_2PtCl_4 as source for platinum ions, KCl which assures an optimum electrical conductivity and H_3BO_3 for stabilizing the pH value. The deposition parameters were adjusted in order to obtain a uniform distribution and reduced size catalyst particles on the CNF surface. The effect of several deposition parameters, such as current density, deposition time, duty cycle and number of cycles on the morphology of the obtained catalysts was also investigated. The resulted CNF-Pt/Pt-Co electrodes with low platinum loading were further investigated by means of SEM combined with EDX, XRF, XRD and TGA to determine the morphology, chemical composition, distribution and amount of catalyst particles deposited onto the carbonic support material. The electrochemical surface area was determined by cyclic voltammetry in 0.5 M H_2SO_4 solution. SEM investigations revealed a homogeneous distribution of the catalyst particles with a nanometric size range for the samples prepared with a previous functionalization treatment of the CNF. The optimized electrodes were investigated by electrochemical means, in order to analyse the catalytic activity regarding the HER and OER in acid and alkaline solutions. Moreover, the behaviour of the electrodes as electrocatalysts for fuel cells is analyzed performing in situ polarization curves in a PEMFC test bench, at low temperatures. The characteristics (structure, chemical composition and morphology) of the deposited catalyst particles have a strong influence especially on the catalytic activity over the electrode surface during operation in water splitting electrolyzers as well as fuel cells.

The presented method leads to a facile and rapid way to develop electrodes with an improved catalytic activity promoted by the presence of platinum, the most electroactive metal and by the employment of a support material with high specific surface area. Moreover, alloying platinum with transitional metals like cobalt reduces significantly the production costs and improves substantially the durability of the catalysts.

Abbreviations

ACL	Anodic Catalytic Layer
AFC	Alkaline Fuel Cell
<i>b</i>	Tafel Slope
CB	Carbon Black
CCL	Cathodic Catalytic Layer
CE	Counter Electrode
CNF	Carbon Nanofiber
CNT	Carbon Nanotube
CV	Cyclic Voltammetry
<i>d</i>	Average Diameter of the Particles
d.c	Duty Cycle
DAFC	Direct Alcohol Fuel Cell
DTA	Differential Thermal Analysis
E°	Standard Electrode Potential
E_{corr}	Corrosion Potential
ECSA	Electrochemical Active Surface Area
EDX	Energy Dispersive X-Ray Spectroscopy
<i>F</i>	Faraday constant ($F = 96500 \text{ C mol}^{-1}$)
GANF	Grupo Antolin Nanofibers
GDE	Gas Diffusion Electrode
GDL	Gas Diffusion Layer
HER	Hydrogen Evolution Reaction
HOPG	Highly Oriented Pyrolytic Graphite
HOR	Hydrogen Oxidation Reaction
<i>i</i>	Current Density
i_{corr}	Corrosion Current Density
i_0	Exchange Current Density
LSV	Linear Scan Voltammetry
MEA	Membrane Electrode Assembly
OCP	Open Circuit Potential
OER	Oxygen Evolution Reaction
ORR	Oxygen Reduction Reaction
PAFC	Phosphoric Acid Fuel Cell
PCD	Pulsed Current Deposition
PEMFC	Polymer Electrode Membrane Fuel Cell
PFSA	Perfluorinated Sulphonic Acid
PTFE	Polytetrafluoroethylene
<i>R</i>	Ideal Gas Constant ($R = 8.314 \text{ J K}^{-1} \text{ mol}^{-1}$)
RE	Reference Electrode
SCE	Saturated Calomel Electrode
SEM	Scanning Electron Microscopy
SHE	Standard Hydrogen Electrode
SOFC	Solid Oxide Fuel Cell
SSA	Specific Surface Area
<i>T</i>	Absolute Temperature

TGA	Thermogravimetric Analysis
t_{on}	Deposition time, during which potential/current density is applied
t_{off}	Time between pulses, during which no current flow is applied
WE	Working Electrode
XRD	X-Ray Diffraction
XRF	X-Ray Fluorescence Spectroscopy
α	Charge Transfer Coefficient
η	Overpotential
u	Scan Rate
θ	Diffraction angle
ρ	Density

1 Introduction

"It is not the strongest of the species that survives, nor the most intelligent that survives. It is the one that is most adaptable to change."

- Charles Darwin

1.1 Background and motivation

Building a sustainable future has lately become a priority. The economic development during the last period led to discovery of new energy sources as well as new viable alternatives for replacing the fossil fuels as coal, oil and natural gas [1], which are finite, non-renewable and have a negative impact on the environment. These facts, correlated with the increase of world population and demand, thrust into the necessity of finding alternative energy sources. On the other hand, it is necessary to defeat the environmental issues, which are associated with the use of conventional sources above mentioned. CO₂ emissions that result from fossil fuel combustion are known to cause the "greenhouse effect" which is the main reason for global warming. From this point of view, eco-friendly technologies are demanded, that can produce constant energy, without affecting the environment [2].

Recently, due to the great concern and intensive studies, several types of clean and renewable energy technologies have entered markets. It is expected that in a short time, the classic energy sources that produce undesired emissions will be slowly replaced by the new revolutionary clean sources [3]. Worldwide, at this moment, the main energy sources are based on fossil fuels (80%), the other part is represented by alternative energy suppliers (Figure 1.1) [2]. In present, from total global energy consumption, around 13 % is provided from renewable energy. A large variety of renewable resources are nowadays used for energy production as sunlight, wind, geothermal heat, hydropower or biomass. Among these alternative energy suppliers, fuel cells can provide an important contribution to the global energy consumption, as it can reduce our dependence on fossil fuels and can be used in various applications from portable power to transport and stationary systems [3].

Fuel cells are electrochemical devices that directly transform chemical energy into electrical energy, without any intermediary processes [4]. These devices operate with hydrogen and oxygen to produce electricity, water and heat, and unlike batteries, the process remains continuously, as long as the fuel is supplied [5]. The possibility of combining hydrogen and oxygen within a fuel cell provides a convenient opportunity to generate clean electrical energy. Fuel cells were first developed mainly to cover the need of providing electricity in areas where the infrastructure is not favourable and furthermore this technology expanded very fast once the aerospace programs were implemented [2].

Fuel cells are a unique technology, an effective source of clean and sustainable energy, both for stationary and mobile applications. These days, they are assessed to be very performant, developing high power densities [2, 4]. Moreover, they have reduced sizes, are silent, need a very easy maintenance and they fit into a various

range of fields. Fuel cell technology is divided into three main markets, namely portable power, transportation and stationary power [5].

Regarding these aspects, six types of fuel cells have been developed and tested during time, such as: alkaline fuel cells (AFC), polymer electrolyte membrane fuel cell (PEMFC), direct alcohol fuel cells (DAFC), molten carbonate fuel cells (MCFC), phosphoric acid fuel cells (PAFC) and solid oxide fuel cells (SOFC) [6]. Each of these types has its own specific characteristics, presented in Table 1.1.

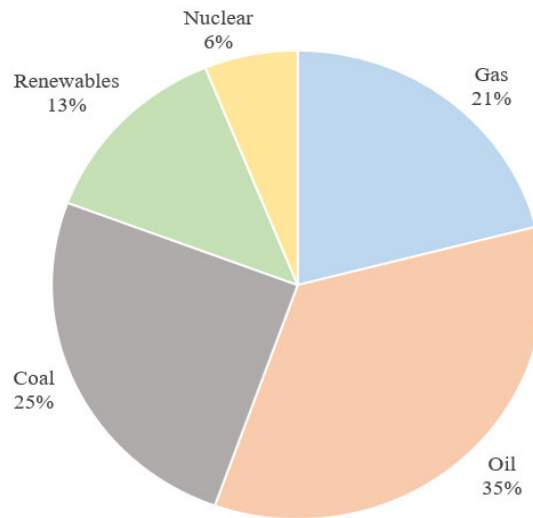


Figure 1.1. The main types of energy sources

Table 1.1. Types of fuel cells and typical characteristics [4]

Type of fuel cell	Electrolyte	Operating temperature [°C]	Electrical efficiency [%]	Power [kW]	Applications
AFC	Potassium hydroxide	70 – 100	45-60	> 20	submarine, spacecraft
PEMFC	Polymer membrane	50 – 80	40-60	< 250	vehicles, stationary devices
DAFC	Polymer membrane	60 – 130	40	< 1	portable
MCFC	Liquid molten carbonate	630 – 650	45-60	> 200	stationary devices
PAFC	Phosphoric acid	150 - 220	35-45	> 50	stationary devices
SOFC	Ceramic	977 - 1000	50-65	> 20	stationary devices

PEMFC distinguishes by its simple design, the main component being the membrane electrode assembly (MEA). MEA consists essentially in a proton exchange membrane (PEM) that represents also the electrolyte in contact, on both sides, with two porous electrodes loaded with catalytic particles [7]. Another important feature, that needs to be mentioned, is the low operation temperature (under 90°C) and the compact modern design. MEA is situated between two pole plates provided with gas flowing channels. All the components together form "a single cell" [7]. The fuel and the oxidant are fed from an external source, unlike the conventional batteries. Hydrogen is delivered on the anodic side of the cell and oxygen on the cathodic region. The PEM is impermeable for gases and very stable in these particular working conditions. The hydrogen oxidation takes place at the anode side and represents the main reaction inside the fuel cell. This reaction is accelerated by the catalyst particles, which are attached on the surface of a gas diffusion layer (GDL). Protons, once they have been formed, pass through PEM, towards the cathode and the electrons are carried through an external circuit, producing electric energy [8]. On the cathodic side of the cell, the hydrogen ions, (H^+) interact with oxygen molecules (O_2), forming water.

A major current disadvantage of this technology is the high cost of the catalysts involved into the fuel cells production. Up to now, important progress has been realized in this field in order to reduce the production costs and also to increase the efficiency and durability. Other fundamental problems encountered in fuel cells production and employment are represented by the slow reaction rates as well as the fact that hydrogen is not an available fuel on the market [2]. Moreover, most of the actual hydrogen production employs fossil fuels both for energy and source. Concerning these facts, water electrolysis is considered a promising option for a clean hydrogen production using renewable sources. This process is based on splitting the water molecules into hydrogen and oxygen using electricity. The reaction of transforming electrical energy into chemical energy takes place in an electrolyser, which presents a similar construction as a fuel cell. Likewise, electrolysers consist of an anode and a cathode, which are separated by an electrolyte. Moreover, several types of electrolysers have been developed due to the differences in the operation mode and electrolyte material or membrane involved in the process.

The best materials for HER and OER are noble metals like Pt, Pd, Rh or Ir. Moreover, first-row transition metal such as Ni, Co, Mn and Fe and their oxides have been widely studied for their relatively good activity for OER.

There are several aspects which contribute to a proper conversion of chemical energy into electricity (or reverse conversion). The catalyst type, more exactly the catalyst efficiency, lifetime, stability and corrosion resistance, the flow field design, the thickness of the membrane, humidity and temperature are just a few factors that influence the performance and efficiency of an electrochemical cell [2].

Intense research in this field have revealed that platinum is the metal with the highest catalytic activity for both HOR/HER and ORR [1-7]. Moreover, platinum has a good stability and an improved corrosion resistance. At the same time, its prohibitive price (approx. 30 € per gram) represents a big disadvantage that limits the use of this metal for industrial and commercial purposes [9]. The high rate of usage and the big amounts of platinum lead to significant costs of the fuel cells. Due to this fact, it is necessary to find cheaper alternatives to replace platinum, which involve new materials or convenient solutions to reduce the costs without affecting the fuel cells performance.

The first PEMFC developed in 1960 by General Electrics, USA, used 28 g Pt cm^{-2} loading, but during time, a value of 0.2 g Pt cm^{-2} was achieved, which is 100 times

smaller than the initial one. Nanotechnology brought new advantageous solutions regarding this inconvenient, offering the possibility to deposit very small catalyst particles on a compatible support material with a high surface area, improving in this way the electrochemical active surface area and reducing the catalysts amount simultaneously. These developments led to important cost reductions. Several convenient methods for platinum deposition are available nowadays. Chemical, physical and electrochemical methods are the most frequently used catalyst deposition technologies [10].

Suitable materials as support for platinum deposition are the carbon-based structures due to their unique characteristics, excellent mechanical and electrical properties and good interaction with metal particles [11]. The main disadvantage of these materials is the low surface energy as well as their hydrophobicity and consequently it is necessary to subject them to a functionalization treatment prior to the catalyst deposition. Another inconvenient is the corrosion resistance of these materials in respect to the applied working conditions.

Summarizing, the great interest in developing clean technology for energy production brought remarkable progress in this field. Moreover, the promising role of fuel cells in providing clean energy has been proven within a great variety of studies.

1.2 Aim of the work

Considering the actual knowledge in the field of PEM cells, the main goal of this study was to develop catalyst materials suitable for electrochemical devices in order to catalyse either the HOR/ORR or HER/OER, by depositing noble metallic nanoparticles on a carbonaceous support material using an electrochemical method. Carbon materials, such as carbon nanofibers (CNF), are emerging as exciting for supporting the catalyst particles inside the electrochemical cells. Thus, in this work, CNF with a high graphitization degree were employed as support material for Pt and Pt-Co catalyst particles. CNF require a functionalization treatment prior to catalyst deposition. During this step, the surface energy is enhanced and handling and wettability is improved simultaneously. As functionalization process, the oxygen plasma treatment was taken into consideration, due to fact that it is a facile, cheap and clean process. To determine the best functionalization parameters, an accurate titration method was performed, to estimate the concentration of acidic groups formed onto the carbon structures during the oxygen plasma treatment. The thermal behavior was investigated using TGA measurements and the corrosion resistance of the support material was tested in acidic solution. All these investigations lead to an appropriate evaluation of the CNF stability and lifetime in the desired working conditions.

Regarding the development of the catalysts, a pulsed current plating method (PCD) is used. This electrochemical method has been proved to be a very efficient technique, since it is a clean process that requires only a few seconds to deposit a sufficient catalyst amount, in comparison to other available deposition methods. In addition, applying this technique, small metallic catalyst particles (<100 nm) can be deposited onto the substrate material, improving considerably the utilization degree of the catalyst.

Two different types of catalyst particles are deposited onto the CNF support material. Platinum based catalysts are suitable to be applied on the anodic side of the fuel cell, where the HOR takes place or in the cathodic side of an electrolyser, where the HER occurs. On the other hand, platinum-cobalt based catalysts are appropriate

for the cathodic side of a fuel cell, for ORR and on the anodic side of an electrolyser for OER, respectively.

The optimization of Pt and Pt-Co particles electrodeposition is performed by applying linear voltammetry at normal temperatures, by using several electrolytes, scan rates and concentration ratios of the metallic cations in the developed electrolyte.

The morphology, structure and chemical composition of the electrodes obtained in this study are investigated using Scanning Electron Microscopy (SEM) combined with Energy Dispersive X-Ray Spectroscopy (EDX). The catalyst content is determined using Thermogravimetric Analysis (TGA). The ratio of Pt and Co of the developed alloy is measured using X-Ray Fluorescence Spectroscopy (XRF) and X-Ray Diffraction (XRD). The electrochemical active surface area (ECSA) is obtained conducting Cyclic Voltammetry (CV) measurements in 0.5 M H₂SO₄ solution.

The influence of the functionalization degree of the CNF on the support material degradation and distribution of the catalyst particles is also evaluated by comparing the corrosion resistance, thermal behaviour, platinum loading and the electrochemical surface area of the tested samples. Through the functionalization step, the catalyst distribution is improved and this fact, associated with reduced particle sizes obtained using EPCP method, confers a high active surface area and an increased sensitivity of the catalyst. All the above-mentioned steps are realized with the purpose to obtain advanced catalyst materials for electrochemical devices, to catalyse either the hydrogen oxidation/evolution reaction and/or oxygen reduction/evolution reaction.

The thesis has been structured into 5 chapters:

Chapter 1 presents the background and motivation of the chosen topic.

Chapter 2 deals with the state of the art in the field of catalysts, presenting some theoretical aspects regarding catalysts production, current fabrication methods, classification and applications. Moreover, a brief description of the PEMFC technology is realized, highlighting the main components and functions as well as reaction mechanisms that appear during utilization.

Chapter 3 describes the methodology and equipment used in order to accomplish the experimental program. This chapter offers an overview regarding the applied investigation methods and presents different analytic techniques, which can provide important information on the quality and performance of the catalyst materials.

Chapter 4 presents the experimental program concerning the functionalization treatment of the carbon support material, catalyst material deposition, reporting the steps followed with the aim to develop the catalyst electrodes and additionally exhibits the results obtained during this study, highlighting the most important aspects.

Chapter 5 reveals the conclusions of this study and the original contributions achieved through this work.

The present thesis aims to contribute to several research questions regarding the development of catalyst materials for electrochemical cell applications.

2 State of the art

2.1 Theoretical aspects regarding catalyst materials

As it has been mentioned in the previous chapter, either the conversion of chemical energy into electricity inside a PEMFC or the complementary conversion from an electrolyser occurs by several electrochemical reactions that require a catalyst material. Until this moment, platinum still represents the best option for the cathodic and anodic reactions inside a fuel cell. During time, intense studies have been performed in order to develop high performance PEMFC, by using different advanced catalyst layers and materials, applying several fabrication techniques, or changing the catalyst layer architecture. Nevertheless, a proper understanding of the reaction mechanism regarding the optimization and evaluation of the fuel cell performance in relation to the MEA structure is strongly necessary.

2.1.1 Definition of the catalyst

Catalysts are the key for the chemical transformations, since they are directly involved in the process, bringing several important advantages like environmental protection, a good efficiency of the process and furthermore they are able to influence the selectivity of the chemical reactions [12].

The term "catalysis" was first introduced in 1835 by Berzelius and it was defined as the ability of substances to "*awaken affinities which are asleep at a particular temperature by their mere presence and not by their own affinity*". The concept was used to describe several catalysed reactions as fermentation of sugar to ethanol by employing enzymes, decomposition of hydrogen peroxide using metals or conversion of ethanol to acetic acid employing platinum as catalyst [12].

60 years later, in 1895, another definition of the catalysis, which is still valid today was stated by Ostwald: "*A catalyst accelerates a slow chemical reaction without affecting the position of equilibrium*" [13]. Nowadays, catalysts are materials or substances that enable a chemical reaction to start with an increased rate or to take place in different conditions than is normally possible [13]. Moreover, a catalyst can be considered an agent that improves significantly the rate of a reaction or a process. In the presence of a catalyst, the reaction occurs faster and requires less activation energy.

In theory, a catalysed reaction can be described as a cyclic process, in which the catalytic material participates without being consumed and can be recovered in its original form at the end of the process. In practice, in many cases, the catalyst materials are destroyed or deactivated after a certain amount of time by the secondary reactions that occur during the process and their activity becomes lower or even inexistent [12]. In the case of an uncatalysed reaction, a higher activation energy is required to overcome the energy barrier. By employing a catalyst, the activation energy is significantly decreased and the transition state is easier achieved than in the first case. The reaction rate of an uncatalysed chemical reaction depends on the rate-determining step. The catalyst participates to the slowest step, improving the reactivity between species.

In this way, catalysts fulfil several functions:

- provide a new path for the reaction that is more complex but requires less energy;
- decrease the activation energy and increase the reaction rate simultaneously;
- maintain the overall free energy change as for the uncatalysed reaction;
- accelerate both the forward and backward reactions [14].

Catalysts have three important properties:

- activity;
- selectivity;
- stability.

The **activity** of the catalyst represents the capacity of the material to increase the reaction rate [15]. The activity can be measured using the number of moles that are transformed in a certain amount of time and on a certain surface area (intrinsic activity), or the number of moles that are transformed in a certain amount of time and on a certain catalyst volume (specific activity), or the number of molecules which are transformed in a certain amount of time (turnover number). The catalytic activity depends on several process parameters and on the physical properties of the catalyst, as temperature, pressure, concentration, specific surface area or porosity. The activity of the catalyst material can be usually regenerated.

The **selectivity** of the catalysts represents the property of the material to be suitable for the reaction system. Depending on the catalyst type used in a process, different reaction products can be obtained.

The **stability** of a catalyst represents the capacity of the material to be attainable during a reaction for a long time without any activity and selectivity modifications [14]. Catalysts stability is influenced by the material decomposition or poisoning. The catalyst lifetime is an important aspect regarding the economy.

2.1.2 Catalysts classification

Catalysts are available in numerous forms and types, varying from a few molecules to large structures as enzymes and zeolites [16]. Based on the structure of the materials, chemical composition, state of aggregation, applications, type of the catalytic reaction or precursor structure, several criteria for classifying catalysts are known today.

Generally, two major catalysts groups are available: **homogeneous**, when the catalyst material is in the same phase as the reaction occurs and **heterogeneous**, when catalyst material is in a different phase as the reaction takes place [15].

Most commonly, homogeneous catalysts are liquids and are predominantly used in liquid state processes, whereas the heterogeneous catalysts are usually solids and are involved either in liquid or gaseous state reactions, separated by a phase boundary. Heterogeneous catalysts can be split in two parts, the support material and the catalytically active component. This type of catalysis has several advantages in comparison to the homogeneous catalysis, mainly the fact that the catalyst recovery can be easier performed and the thermal stability is increased. On the other hand, homogeneous catalysts are well defined systems due to their molecular nature, having a better activity and selectivity compared to heterogeneous catalysts [14, 16].

Each of these main groups have their own special properties and characteristics, which make them suitable for different applications and processes.

2.1.3 Applications

Catalysts have been efficiently used in chemical industry for over 100 years. At this moment, over 75% of the chemicals are produced in the presence of a catalyst and over 90% of the processes are accelerated by employing different catalytic materials [15].

Although, homogeneous catalysts are less frequently used in industrial purposes, the most eloquent examples for this type of catalysts relate to the petrochemical industry. Moreover, different types of acids are used in organic synthesis to manufacture phenol, ethanol, in polymerization reactions and oil refining [16].

On the other hand, heterogeneous catalysts are intensively used (around 80% of the industrial catalytic processes) in a wide range of applications. Frequently, heterogeneous catalysts are found in reactions that involve gases or liquids, which are passed over the surface of a metal, a metal oxide or an alloy. In general, these catalysts consist of nano-sized metal particles deposited on a support material, the metal particles expose the active sites and the support material acts as an anchor for the particles. Since the main reaction takes place onto the catalyst surface, gas molecules interact with the surface of the catalyst particles and several adsorption processes can occur [14]. The total surface area of the catalyst has a significant effect on the reaction rate and therefore, larger surface areas are required, involving finely divided metals, metal oxides, sulphides, halides or supported metallic particles and films. As important applications, production of several chemicals can be mentioned (ammonia, sulphuric acid), purification of exhaust gas streams (environmental catalysis) or energy conversion such as fuel cells, electrolysers or batteries [16].

2.2 PEMFC - A brief description of the technology

Regarding the energy conversion applications, fuel cells are the most representative and studied devices that are used in this purpose, being one of the most promising technologies for both mobile and stationary devices [17].

The idea of an equipment that converts chemical energy in electricity was first highlighted in 1839, by Sir William Grove, a physicist, who has been recognized as "*the father of the fuel cell*" [8]. The operation principle of a fuel cell is built on the reaction between two gases, hydrogen as fuel and oxygen as oxidant, obtaining electricity, water and heat. This fundamental principle is valid for all types of cells, the main differences consisting in the employed electrolyte, which also determines the operating temperature, cell design, reactants and type of ion that assures the ionic conduction [18]. As the main reactions are similar inside each type of fuel cell, the major attention of actual research is focused on improving the efficiency of the hydrogen oxidation reaction (HOR) and mostly of the oxygen reduction reaction (ORR). Important studies are nowadays performed, to overcome several deficiencies regarding the operation temperatures, heat and water management, durability and contamination of the catalyst material [18]. Other significant research targets are strongly related to the possibility of reducing the overpotential for the oxygen

reduction reaction on the cathodic side, along with the decrement of the catalyst amount by increasing the utilization degree and decreasing the degradation rate [19].

Polymer electrolyte membrane fuel cell (PEMFC) distinguishes from the other types of fuel cells by the low operating temperature (under 90°C), that enables a fast start of the device and a stack efficiency over 50%. Another notable advantage is that the electrolyte is solid and due to this fact, there is no risk of electrolyte leakage, such devices being better adapted to mobile applications. On the other hand, polymer membrane needs a special maintenance, as a proper hydration degree is necessary to achieve a convenient proton transfer. The degradation of the membrane leads to serious damage for the fuel cell. Moreover, the increased susceptibility of contamination with by-products like carbon monoxide, create another important problem that should be overcome [7].

Currently, more than 80% of the research activity in this field deals with the improvement of the polymer membrane and only a few studies are performed regarding the improvement of the catalyst layer. Regarding this approach, three important directions are needed to be taken into consideration:

- development of cost-effective catalysts with an improved activity and durability;
- determination of the catalyst material structure;
- clarification of reaction mechanisms which occur on the surface of the catalyst layers.

A PEMFC consists mainly of two fundamental components: the membrane electrode assembly (MEA) which is called "*the core of the fuel cell*" [20] and bipolar plates (Figure 2.1).

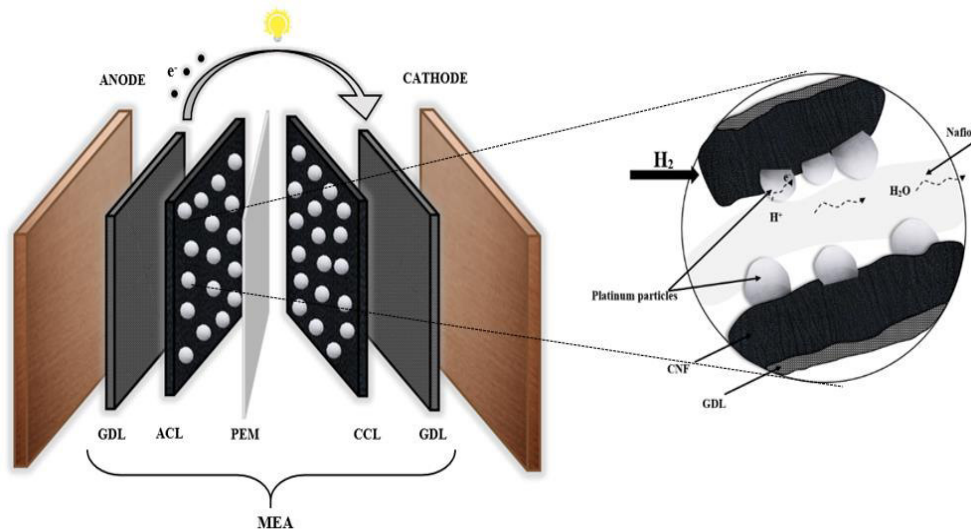


Figure 2.1. PEMFC components and triple contact zone

Both main components have a crucial function, assuring the basic operations inside the fuel cell. Bipolar plates facilitate the gas transport and simultaneously provide mechanical support [18]. MEA consists of two diffusion layers (GDL) placed on the anodic and cathodic side, which ensure the gas transport from the pole plates towards the reaction sites, two catalytic layers (ACL and CCL) both on the anodic

and cathodic side, where the catalyst particles are located, comprising the active reaction region, and the ion conducting membrane (PEM), that transports hydrogen cations from the anode to the cathode.

At the surface of the electrodes, both anode and cathode respectively, two different electrochemical reactions occur (Eq. 2.1 and Eq. 2.2). Hydrogen, which is fed to the anode, is adsorbed onto the catalyst surface, being oxidized and split into protons and electrons. Electrons flow to the cathode through an external circuit. The protons pass through PEM, towards the cathode, where the oxygen is fed and adsorbed onto the catalyst surface. Oxygen is protonated by the H^+ and reduced to water by electrons from the external circuit [18].

Fuel cell performance is generally characterized by a polarization curve, which is a plot of cell voltage as a function of current density, as shown in Figure 2.2. The theoretical open circuit voltage (OCV) of the PEM fuel cell is around 1.23 V, at standard conditions (1 atm, 25°C). As the current is drawn from the cell, the cell voltage drops gradually from the OCV due to various losses, including anode and cathode kinetic loss.

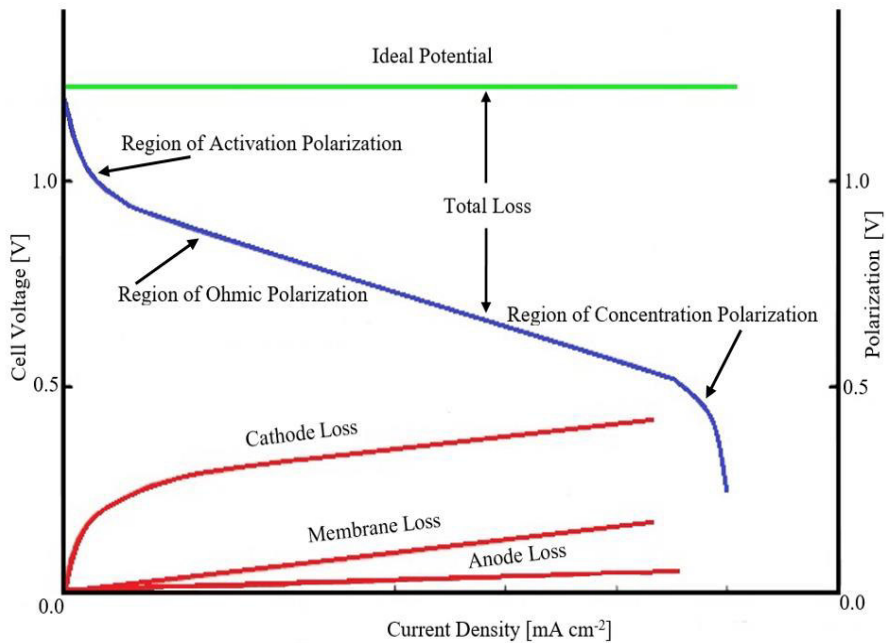
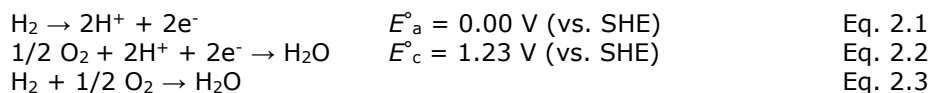


Figure 2.2. Polarization curve of a PEMFC

The anode and cathode half-reactions together with the overall reaction of the fuel cell are given in Eq.2.1 – Eq. 2.3.



The active region is the place where the electrochemical reactions occur. Generally, the main condition for a reaction to take place is that the electrolyte, reactants and catalyst to be in contact one to each other. Regarding the fuel cell, this condition can be fulfilled just in certain regions called "*triple contact zones*". This is the place where the fuel (hydrogen), the catalysts and the membrane (PEM) are in contact [21]. This intersection point is essential for the performance of the fuel cell because it assures the gas arrival from the GDL to catalyst particles, where hydrogen oxidation reaction takes place and released protons are directly transported through the membrane towards the cathode [22]. These zones are the most important regions regarding the performance of the fuel cell. It is strongly necessary to have a large active surface, to enable an efficient hydrogen oxidation on the anodic side or oxygen reduction on the cathodic side, respectively. Moreover, a high electric conductivity is strongly recommended for minimizing the ohmic loss and a long lifetime of the components, to overcome the costs. At this moment, the state of the art regarding PEMFC technology is hampered by two important aspects, namely the decreased durability of the fuel cell components and the high production costs [22]. Regarding the production expenses, an important reduction can be performed by enhancing the fuel cell performance or by diminishing the platinum loading of the catalyst. More than 55% from the total production costs represent the catalyst price, while the membrane, pole plates and gas diffusion layers around 10% each. Therefore, a substantial reduction can be achieved from the catalysts costs, by employing alternative materials, innovative preparation methods or improving the cell design [20].

Numerous strategies have been tried to reduce the production costs and to increase the performance of the fuel cell. Several approaches regarding the reduction of Pt loading for PEMFC technology have been tested during the last period.

Decreasing the Pt amount, by alloying with other transition metals (bimetallic or ternary catalyst alloys) or non-noble electrocatalysts, has been proved to be an efficient method. Non-noble metals, employed as catalysts, can considerably reduce the production costs of the fuel cell [23], but the main disadvantage is the activity targets and performances which are not fulfilled yet, especially regarding commercial applications. Furthermore, taking into consideration that the main reactions inside a fuel cell occur only on the catalyst surface and the core of the catalyst is basically not involved into the reaction, a feasible alternative is to cover completely a less noble metal or metal particles as Fe, Co, Ni, Cu with a thin Pt coating, such as Pt skins, Pt monolayers or Pt nanostructured thin films. This method, known as the "*core-shell*" approach leads to significant costs reduction and can diminish the platinum amount consumption up to 80% [24].

Reducing the Pt loading by manufacturing ultra-low loading catalysts or diminishing the catalyst particle size can be as well considered a suitable method to achieve considerable cost reductions. These approaches can be accomplished by improving the catalyst dispersion, using novel fabrication techniques or developing new MEA production methods to enable a better catalyst utilization. In addition, improving the PEMFC performance by optimization of the operating parameters has been also tested [25].

Furthermore, an important improvement of the performance can be obtained by employing carbon-based catalyst support materials or developing novel non-carbonaceous support materials with increased surface area. This efficient method reduces the platinum consumption and maintains or even improves the catalytic activity. This approach can be accomplished by depositing platinum nanoparticles on

a compatible material, with an increased surface area that acts as support [8, 26]. Not only in this situation, platinum particles should be very finely dispersed onto the surface support, in order to attain a large platinum active surface area, which comes in contact with the reactant and electrolyte [8].

2.3 PEMFC catalysts

Platinum, as it has been mentioned before, represents an excellent catalyst for both anode and cathode fuel cell reactions, even if there are considerable differences regarding the kinetics between these fundamental reactions [8, 27]. A great concern of the scientists has been recently raised to develop convenient catalyst materials, mainly for the oxygen reduction reaction (ORR). The hydrogen oxidation reaction (HOR) and hydrogen reduction reaction (HER) are fundamental electrochemical reactions with a great importance for a wide range of applications. Due to this fact, these reactions have been intensively investigated during the last years and many aspects are still a concern for the scientists, such as reaction and adsorption mechanisms.

HOR on platinum takes place in three steps, with an increased kinetic rate, having a low oxidation overpotential [2, 8, 17]. Voltage losses are insignificant, even for a low platinum amount. In the current state of the art, platinum content varies from 0.1 - 0.4 mg cm⁻² [27]. To meet the targets for a profitable commercialization, it is necessary to be reduced under 0.1 mg cm⁻².

The accepted mechanism for HOR is presented in Eq. 2.4 - Eq.2.6. The exchange current density is around 0.1 A cm⁻², being extremely high in comparison to the ORR exchange current density (6 μA cm⁻²).



The total reaction for HOR in acid environment is presented in Eq. 2.7:



The hydrogen adsorption is considered the rate-determining step for the entire HOR mechanism. In addition, recent studies have shown that Tafel - Volmer mechanism is rate limiting at low potentials, while Heyrovsky - Volmer mechanism occurs at higher potentials [28].

Within a fuel cell, the cathodic reaction is considered more complicated than the anodic one, because it consists in two distinct routes. The major voltage losses in a PEMFC system (more than 50%) are caused by the high oxygen reduction overpotential (300 - 400 mV) [28]. The catalyst material needs to be very resistant for the increased corrosive conditions that occur on the cathodic side of the fuel cell. Consequently, the cathode needs a higher platinum loading than the anode, to overcome the afore mentioned difficulties [2].

Two distinct mechanisms are available regarding the ORR. The first one, which is also the desired route, consists in a four-electron pathway, which directly leads to the formation of water. The second route is an incomplete oxygen reduction, through a two-electron pathway, resulting in hydroperoxyl or hydrogen peroxide. The two-electron pathway is undesired because it leads to low energy

conversion efficiency and the intermediary and final products (HO_2 , H_2O_2) are poisonous for the membrane.

In the first case, O_2 molecules adsorb onto the platinum surface, $\text{O}=\text{O}$ bond is broken (Eq. 2.8), oxygen atoms are protonated by hydrogen protons that come from the anode across the membrane and the reduction takes place with the aid of the electrons that come through the external circuit (Eq. 2.9). The OH groups are further protonated and reduced respectively, resulting water that leaves the platinum surface (Eq. 2.10).



In two-electron pathway, the $\text{O}=\text{O}$ bond is not broken, but the O_2 is adsorbed as a molecule to the platinum surface (Eq. 2.11). Once the O_2 is adsorbed, the protonation and the reduction reaction occurs, obtaining an intermediary product $\text{HO}_{2\text{ads}}$ (Eq. 2.12). This compound is further protonated and reduced, resulting $\text{H}_2\text{O}_{2\text{ads}}$, (Eq. 2.13), which is finally desorbed from the catalyst surface (Eq. 2.14) [29].



Regarding the above-mentioned reactions, the main characteristics that catalyst material should accomplish in order to be efficient for PEMFC are the activity, selectivity, stability and poisoning resistance.

Regarding PEMFC catalysis, the activity consists in the ability of the material to adsorb the reactant (hydrogen or oxygen) and to break its chemical bonds, to promote the reaction. When the reaction starts, it is necessary to allow the products to be released, providing new free spots for the next reactant molecules. A very strong adsorption can lead to catalyst blockage and consequently the reaction is interrupted. Therefore, a balanced interaction between the reactant and the catalyst is strongly necessary. In the case of hydrogen adsorption, platinum exhibits the highest activity among all the other metals, for the oxygen adsorption, platinum has also a high activity, but the adsorption is considered too strong [30].

The selectivity as it was mentioned before, refers to the ability of the catalyst material to promote only the desired reaction and to reduce the other secondary reactions and side products. In the case of hydrogen oxidation, the selectivity is not essential, because the only possible reaction is in the direction of H^+ and e^- production. Contrarily, the oxygen reduction, as it was previously mentioned, can follow one from the two pathways. In this case, platinum is the most selective metal (almost 100%), having a real positive effect since it promotes only the atomic oxygen adsorption, avoiding the H_2O_2 formation [27, 30].

The stability of the catalyst materials is the key for the whole fuel cell system durability. The strong oxidant medium, pH, temperature as well as the reactive radicals inside the fuel cell lead to a very aggressive environment for almost all the transitional pure metals, which makes them unsuitable as catalysts. The dissolution of the metals can occur especially at high electrode potentials that appear during the fuel cell operation. Moreover, a formation of an oxide layer can defend the corrosion problems, but on the other side, it inhibits the catalytic properties

regarding the oxygen reduction reaction. This aspect can be successfully overcome by employing noble metals as platinum, iridium or gold, which are very stable in the fuel cell conditions in comparison to metals like nickel, cobalt or iron [30].

Regarding the stability, selectivity and activity, platinum is the most suitable metal for PEMFC catalyst material. The poisoning resistance is the only drawback for this metal because the sulphur species and carbon monoxide can damage the catalytic properties of platinum. There are different methods to avoid poisoning, either maintaining a clean medium or alloying platinum with other metals to reduce the susceptibility of contamination. Unsupported and supported platinum alloys proved to exhibit an increased tolerance to carbon monoxide poisoning [27]. Alloys with several transition metals like nickel, cobalt, chromium or iron have been tested toward the oxygen reduction reaction, to increase the durability and to reduce the production costs [31].

There is a continuous effort among the scientists to reduce the costs of the fuel cell catalysts and in this direction, two major approaches can be taken into consideration. The first one consists in reduction of platinum content either by alloying this metal with other transition metals or increasing the active surface area using high surface materials as support. The particle size effect on ORR has been intensely investigated and the results have shown that there is an optimum particle size of around 3.5 nm, under which the surface activity and stability starts to decrease [32]. Another alternative is to employ non-noble metals, to develop a suitable catalyst material. In the latter case, despite of the several encountered disadvantages, as poor stability and limited catalytic activity, the non-noble catalysts are considered convenient for the future, due to their low price and availability [8].

During last years, a considerable number of scientific works have presented studies regarding the employment of non-platinum group metals as catalyst for PEMFC. Tantalum and tantalum oxide [33], ruthenium [34], molybdenum [35] or palladium [36] based catalysts are just a few of tested alternative metals regarding the HOR and ORR, although the mechanisms are still unclear and the activity needs considerably to be improved. In addition, several approaches for developing non-noble electrocatalysts are based on transition metal carbides and nitrides, such as tungsten carbide [37] or molybdenum nitride [38, 39]. These materials have good electrochemical properties and stability within a wide pH range, which make them suitable for PEMFC applications.

On the other hand, alloys of platinum with light transition metals like cobalt [40], nickel [41], chromium [42], manganese [43], iron [44] or titanium [45] have been found to exhibit a favourable electrocatalytic activity towards the ORR in comparison to normal platinum - carbon catalyst in low temperature fuel cells. The enhancement of ORR activity is attributed to the geometric changes of the Pt structure due to alloying, which improves the adsorption strength of reactants. These types of alloys increase also the performance and the resistance of the catalyst to sintering and coalescence. Alloys of platinum with transition metals that modify the oxophilicity of the particles surface seem to improve the kinetics of the ORR by impeding the formation of the oxide layer that competes with the oxygen adsorption [46]. Pt-Co alloy catalysts have been proved to be more effective and exhibit increased performance regarding the ORR in PEMFC. It is believed that the bimetallic Pt-Co catalyst improves the durability by reducing Pt dissolution and migration during the fuel cell operation [40]. Moreover, the possibility of preparing ternary platinum-rich alloys like Pt-Fe-Ni [47] or Pt-Fe-Co [48], Pt-Co-Cr [49], Pt-Co-Ni [50] with variable compositions have attracted attention due to their

enhanced performance and durability within the fuel cell. Metal oxide electrocatalysts like spinel type oxides, have been also studied for their catalytic activity and the results are superior in comparison with the classical Pt-C catalysts, but their main disadvantage is the low stability in acidic media [50]. In one of their studies, Li and the team developed a Pt-Fe-Ni alloy catalyst. The deposition had been performed in two steps, firstly the electrodeposition of Fe-Ni alloy on porous carbon electrode was carried out and subsequently a galvanic displacement process in order to form the Pt-Fe-Ni alloy [47] was realized. In a similar study [49], Pt-Co-Cr alloy was obtained through a thermochemical synthesis process on dispersed carbon support using nitrogen-containing precursors of the transition metals.

Core-shell catalysts [51] have particular characteristics due to the fact that platinum is deposited onto the surface of a less expensive metal, reducing considerably the production costs. Several recent studies have presented different types of core-shell catalysts, with Pt rich shell and Pt-Co alloy core, with an increased activity for the fuel cell reactions due to their high surface area [52].

Another important aspect in the fuel cell production and performance is the support material for the catalyst particles. Materials with a porous structure and a high surface area, with good interaction with platinum particles are suitable as catalyst support. It is recommended to use materials with good electrical conductivity and high mechanical resistance. It is well known that the specific activity of platinum metal to ORR is also related to the carbon support. To enhance the activity of ORR, one strategy is to explore highly active catalysts with novel carbon material as a support [53].

2.4 Support materials for PEMFC catalysts

The support material generally provides a physical surface for dispersion of small metal particles and moreover, it is strongly necessary to accomplish the high surface area condition [54]. In addition, the material needs to be stable in the working conditions and usually it is necessary to have a good electrical conductivity. The most used support materials in industry are refractory oxides, like alumina (Al_2O_3) or silica (SiO_2) since these materials exhibit a large accessible surface area, an increased porosity, as well as thermal stability. Metallic nanoparticles such as Pt or Rh supported on SiO_2 or Al_2O_3 have been lately used in heterogeneous catalysis. Regarding fuel cell applications, the above-mentioned materials are not suitable because the electrical conductivity is low or rather inexistent [55].

The main purpose for employing nanostructured catalyst particles supported on different materials is to reduce catalyst loading by increasing the utilization, improving the activity and the total performance of the cell consequently. It has been reported that carbon materials with both high surface area and good crystallinity may not only provide a high dispersion of Pt nanoparticles, but also facilitate electron transfer, resulting in a better device performance. A wide variety of support materials like carbon based materials: graphite, carbon black (CB) [56], carbon nanotubes (CNT) [57] carbon nanofibers (CNF) [58], highly ordered pyrolytic graphite (HOPG) [59], metallic materials such as copper [60], nickel [61], titanium [62] or metal oxides like titanium oxide [63], tin oxide [64], have been lately tested regarding the fuel cell applications. In each of these studies, support materials were successfully decorated with catalyst particles and they have proved to be efficient regarding the electrochemical activity.

During the last years, due to their unique properties, carbon based structures became intensively studied, considering their availability, physical and chemical properties, processability, and relatively low costs. Carbon nanostructured materials are suitable as catalyst support in respect to their properties, like high surface area, excellent electrical conductivity and chemical inertness in strongly basic and acidic environments [53]. From the other point of view, the inert surface of carbon needs an additional treatment in form of a suitable surface modification in order to create a favourable interaction with the catalyst particles [65].

Carbon blacks are considered suitable support materials due to their high activities and long lifetime in comparison to the other carbonaceous structures with low activity or rapid deactivation [66]. Commercially available Pt/C powders containing carbon black (Vulcan XC 72) have been almost exclusively used as catalyst supports in low-temperature fuel cells and are still currently employed in numerous fuel cell devices on market [67]. The high surface area, the low cost and availability make this material very attractive for fuel cell applications [66]. Carbon black is widely used as support, but still has drawbacks regarding the catalytic activity, due to impurities and micropores. Catalyst particles can be blocked in the pores and this fact may lead to considerable reduction of three-phase reactive sites, consequently reducing the Pt utilization and catalytic activity. Carbon black exhibits also instability in acidic/alkaline conditions and moreover presents poor corrosion resistance [66]. In this context, several studies have revealed that higher catalytic activities can be achieved using other allotropic forms of carbon, like CNT or CNF supported catalysts in comparison with the same catalyst particles supported on CB. This fact was attributed to the special structure of the CNF and CNT, due to the high surface area, good electronic conductivity and chemical stability [54]. Various tests carried out in PEM fuel cell conditions indicate that these materials are more durable and exceed the lifetime of the most widely used Vulcan XC 72.

The graphitic structure of CNF or CNT has a relatively large and accessible external surface area without impurities such as sulphur or inorganic compounds. These structures, having usually a diameter up to 100 nm and a length reaching few μm , represent a suitable support material for catalyst deposition. Several characteristics of these materials can be adjusted by synthesis conditions like temperature, pressure or time, the growth catalyst metal, or the carbon source. The orientation of the graphitic planes, either in fishbone (CNF) or in a parallel way (CNT), the diameter and length of the structures can be finely adjusted to obtain the desired characteristics. In comparison with the conventional Vulcan XC 72 carbon support that presents an electric conductivity of 4 S cm^{-1} and specific surface area of $250 \text{ m}^2 \text{ g}^{-1}$, CNT and CNF have significantly higher electric conductivities of around 100 S cm^{-1} and extremely high specific surface areas between $100 - 900 \text{ m}^2 \text{ g}^{-1}$ respectively [54].

The main disadvantage of carbon-based materials like CNF and CNT is the fact that they are chemically inert and have a low surface energy. In order to overcome this aspect, it is necessary to subject them to a functionalization treatment prior to catalyst deposition process. This step will considerably improve the catalyst distribution onto their surface. Without additional treatments, the amount of oxygen groups on the surface of as-synthesized CNT or CNF is usually too low to be used in catalysis, for anchoring metal particles. Thus, after the growth of carbon structures, the non-polar surface of the graphitic material can be activated by introduction of oxygen-containing groups using different treatments that involve an oxidizing agent [68]. The oxygen-containing groups ensure wettability with water and other polar solvents and enable the anchoring of catalyst particles.

The nature of functional oxygen groups is not completely known, but several studies regarding this aspect using different methods like FTIR spectroscopy, XPS or using an acid-base titration technique have demonstrated that multiple types of surface oxygen groups (acidic, neutral and basic) can be distinguished, as presented in Figure 2.3 [69].

Oxygen activated carbon materials contain significant amounts of oxygen and hydrogen groups, which give rise to various surface complexes. Electrochemical and catalytic properties of carbon materials is strongly dependent on chemical species that exist onto their surfaces. Oxygen based functional groups such as carbonyl ($>C=O$), hydroxyl and/or phenols ($-OH$), and carboxyl ($-COOH$), can increase the catalyst deposition rate and dispersion in solvents.

The functionalization treatment can extend the application alternatives of these materials and therefore, it is strongly necessary to understand the changes that occur on the carbon external surface. It has been proved that the concentration of specific carbon surface groups, such as carboxyl, can be improved applying chemical, physical or thermal treatments. By introducing suitable functional groups, carbon materials can be made either hydrophobic or hydrophilic. Various studies have tried to understand the influence of oxygen containing groups and their concentration on the catalyst dispersion and activity [70]. On the other hand, oxygen-containing functional groups might alter the surface acidity, corrosion resistance and adsorption ability for other molecules.

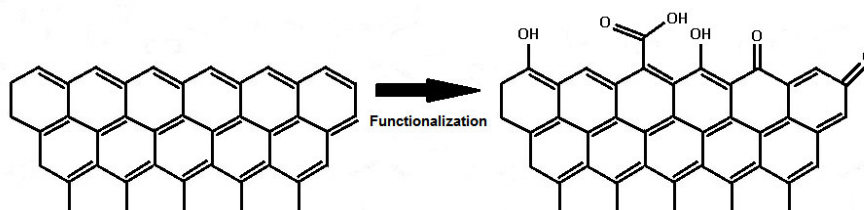


Figure 2.3. Oxygen containing surface groups on CNF

The functionalization methods can be classified in two main categories, depending on the nature of interactions between the surface of carbon material and functional groups [71]. The covalent functionalization is based on the formation of covalent bonds between functional entities and carbon surface. This type of treatment is non-reversible and may produce defects in the material structure. Direct covalent functionalization is associated with a change in hybridization from sp^2 to sp^3 . On the other side, non-covalent functionalization is based on Van der Waals π - π interactions. The great advantage of non-covalent functionalization relies upon the possibility of attaching various groups without disturbing the electronic structure of the carbon material and keeping unchanged the bulk properties of the material [72]. The formation of non-covalent functionalities using surfactants can be a suitable method for dispersing the carbon structures in aqueous or organic solvents. Carbon structures usually tend to agglomerate in bundles or other aggregates resulting in poor solubility in most solvents and poor chemical compatibility, which greatly hinders their applications. To improve their solubility, carbon materials are functionalized by different methods. Functionalization of carbon structures has been reported using several techniques, using strong acids, liquid-phase refluxing in concentrated acid (HNO_3 , H_2SO_4 , or their mixture) [73], plasma oxidation [74] or electrochemical treatments [75]. An easy and clean way to

covalently attach chemical groups is by plasma oxidation. This method is emerging as a superior efficient treatment for high surface materials. Studies regarding plasma functionalization method [76, 77] have revealed that this type of treatment is a feasible way to modify the fibers surface. Moreover, the oxygen plasma treatment increases the surface energy of the fibers and improves the wettability in different solvents. Beside the surface functionalisation, an additional undesired etching process has been noticed when a higher value of power was applied.

The functionalization process is strong related to the catalyst deposition method. Due to this fact, it is necessary to correlate the deposition technique with the appropriate functionalization treatment in order to achieve improved catalysts materials.

2.5 Synthesis methods of platinum based catalysts

The activity of a catalyst depends considerably on the size of the active particles and their dispersion configuration over the support structures as well as the particle interactions with the support material. It has been demonstrated that the optimal dispersion pattern of the catalyst correlated with reduced particle sizes can be obtained by employing an appropriate fabrication procedure and choosing the ideal support material [54].

In the actual state of the art, different deposition methods are employed to obtain PEMFC catalysts. For low temperature fuel cells, catalysts require nano-sized dimensions and are usually deposited onto support materials with increased surface area [8]. Among the convenient methods, chemical and electrochemical deposition [78], colloidal [79], impregnation [80], electroless [62] or chemical and physical vapour deposition [81] are frequently used.

The electrodeposition method was first used to deposit a catalytic layer onto a support for a PEMFC in 1992 by Vilambi Reddy [22]. Through this method, it was possible to produce electrodes with a platinum loading about 0.05 mg cm^{-2} . The resulted electrodes exhibited an increased utilization degree, providing also high performance. Electrodeposition offers a unique way to deposit several types of metals in precise locations on the substrate material and furthermore confers an easier control for the nucleation and growth of the metal particles. Different electrochemical techniques can be used for deposition, as galvanostatic electrodeposition (direct current, pulsed current), potentiostatic deposition or cyclic voltammetry to obtain Pt in a form of nanoparticles or thin layers [82]. The electrochemical method has been extensively used to deposit Pt onto carbon substrates both for anodes and cathodes in PEMFC, to improve the Pt utilization and to reduce the catalyst loading without any significant performance loss of the cell, compared to the conventional deposition techniques. The electrodeposition technique provides a simple fabrication of electrodes and guarantees that the ions from the plating bath, pass through the electrolyte towards the support material and they are deposited on the areas where protonic and electronic conduction coexist. This method proved to be an efficient way to synthesize platinum nanoparticles with high density of atoms and clean surfaces, since this process does not require the addition of stabilizers and additives which may be adsorbed onto the surface, poisoning the active area of the catalyst [83].

The deposition occurs at the interface of the electric conductive substrate (support material) and the electrolyte that contains metal ions that need to be deposited. This process is accomplished in five steps, as follows:

- transport of the metal ions towards the support material;
- electron transfer;
- adsorption of atoms onto the support material;
- nucleation and growth on two or three dimensions;
- growth of the three-dimensional bulk phase.

To obtain nanostructured particles, it is necessary to stop the process after the fourth step. In pulse electrodeposition, the potential or current is alternated swiftly between two different values. This results in a series of pulses of equal amplitude, duration and polarity, separated by zero current. Each pulse consists of an on-time (t_{on}) during which potential or the current is applied, and an off-time (t_{off}) during which zero current is applied. The peak current density and the pulse duty cycle control the nucleation rate and decrease the dendritic growth [84].

It is also possible to control the deposited composition and thickness by setting the pulse amplitude and width. These parameters favour the initiation of growth nuclei and greatly increase the number of grains per unit area, leading to finer grained deposit with superior properties than conventionally deposited coatings [85].

Electrodeposition of Pt nanoparticles on carbon based structures has recently been intensive reported by several groups [86, 87]. Choosing the proper substrate, deposition potential or current and growth time, it is possible to deposit nanoparticles with a high degree of monodispersity and narrow particle size distribution.

Kim and co-workers presented a new approach based on pulse electrochemical deposition for preparation of catalysts for PEMFC using a H_2PtCl_6 plating bath. The results indicate that the duration of the pulse (t_{off}) plays an important role in the deposition process. A longer pause between pulses resulted in a decreased nucleation rate. Moreover, samples prepared using a higher current density (200 mA cm^{-2}) showed a better performance than samples deposited at lower current densities [84].

Duarte and team deposited platinum on carbon support using an impregnation-reduction method. The reduction was achieved either chemically or electrochemically. A potential pulse method was employed and the deposition process was carried potentiostatic [86].

Platinum-cobalt catalysts with a low loading, supported on carbon black, having an improved activity for the ORR were electrochemically developed using galvanostatic pulse technique from a potassium tetrachloroplatinate solution and various concentrations of cobalt chloride [31]. In the same purpose, platinum-nickel electrodes were co-deposited onto multi-walled carbon nanotubes through a three-step electrochemical process. An increased resistance to CO poisoning was obtained for the prepared electrodes which was attributed to the presence of nickel in the catalyst structure [41].

The simultaneous reduction of two metal ions from the same electrolyte is possible when the reduction potentials of the metals are equal or have similar values, as the Eq. 2.15 describes:

$$E_1^{\circ} + \frac{RT}{n_1F} \ln a_1 + \eta_1 = E_2^{\circ} + \frac{RT}{n_2F} \ln a_2 + \eta_2 \quad \text{Eq. 2.15}$$

where E_1° and E_2° are the standard reduction potentials for the discussed metals, a_1 and a_2 are the ions activities, η_1 and η_2 are the cathodic overpotentials and n_1 and

n_2 are the number of electrodes involved in the chemical reaction, R is the ideal gas constant, T is the thermodynamic temperature and F is the Faraday constant.

From a simple salt solution, the main condition to achieve the co-deposition of two metals is that their reduction potentials to be similar and if the overpotentials are neglected, by changing the ions activities, the simultaneous deposition can be reached. If the standard potentials are significantly different, the most effective method to achieve the co-deposition is by bringing the both metals in a complex compound. Frequently, as complexing agents are used cyanides, phosphates or ammonia compounds and often, surfactants are added in order to decrease the reduction rate of the more noble metal. It is known that noble metals deposit preferentially, faster than less noble metals, and starting from this premise, a classification of the metals co-deposition can be realised. Brenner has classified the co-deposition of metals into five important types: regular, irregular, at equilibrium, anomalous and induced [88]. The first three types refer to a normal co-deposition in which the ions ratio in the deposition bath influences the metal percent in the alloy structure. Moreover, the metal with the more positive redox potential is preferentially deposited to the less noble metal. In the case of regular co-deposition, the process is diffusion rate limited, the irregular co-deposition appears when the system is not limited by the diffusion of ions, but due to some irregularities that appear in the deposition potentials of the metals. Typical to the equilibrium co-deposition is that the metal percent in the electrolyte influences the metal ratio in the deposit. The last two co-depositions kinds refer to an atypical electroreductions of the alloys because the less noble metal deposits preferentially to the noble metal.

Electroless deposition is a method for obtaining a coating or supported metallic nanostructures by chemically reducing the metal ion or its complex onto the substrate material without applying an external current. In the electrochemical method, reduction takes place by supplying current externally and the sites for the anodic and cathodic reactions are separate. For the chemical deposition method, electrons required for the reduction are supplied by a reducing agent and the anodic/cathodic reactions are on the inseparable work piece. Moreover, as these reactions take place only on catalytically active surfaces, the support needs be catalytically active in order to promote the redox reactions [89].

Due to its simplicity, impregnation method is among the most frequently used techniques for Pt-based catalysts deposition on carbon support materials to produce PEMFC electrodes. The impregnation technique is a clean method to synthesize catalysts, the reduction reactions occur at room temperatures, with low energy consumption. Disadvantages of the impregnation technique are related to the possibility of particle agglomeration in solution. Carbon structures can be successfully impregnated with catalyst precursors by mixing both in an aqueous solution. A reduction step (chemically or electrochemically) is required, to reduce the catalyst precursor to the metallic state. As reduction occurs after the impregnation step, the nature of the support material has an important role in controlling the particles size [90]. Carbon xerogel-supported catalysts have been prepared by impregnating various supports with hexachloroplatinic acid aqueous solutions. The reduction process was performed under hydrogen flow at 350°C for 3 hours. A very good dispersion of Pt particles was associated with the texture of the support material and the surface composition of the carbon xerogels [80].

Lately, a great interest for development colloidal methods to prepare Pt catalysts supported on carbon structures has been shown. Usually, this method comprises the preparation of a platinum metal colloid, followed by adsorption on support, or formation of a Pt oxide colloid, followed by reduction and adsorption, or

adsorption followed by chemical reduction. In the colloidal method, the size of the Pt nanoparticles is controlled and stabilized by special agents, such as ligands, surfactants or polymers. Though the colloidal method, a narrow size distribution of metal nanoparticles can be provided, the only problem is the presence of the used agent, which can be difficult removed once the particles are adsorbed onto the support and may impede the catalytic performance of the nanoparticles. One further disadvantage is that the colloidal particles are prepared at high dilution, which is not suitable for its scale up [90].

Sputtering techniques are quite simple and efficient deposition methods that can produce uniform particle distribution. The size of the particles is controlled by adjusting the working time and current values. Sputtering deposition techniques have been employed to obtain thin platinum films on the surface of carbon materials. This technique can lead to uniform Pt nanoparticles on carbon support in comparison to other deposition methods as impregnation or electrodeposition.

2.6 Polymer electrolyte membrane

Proton exchange membranes (PEM) are a key component for a PEMFC. Generally, the lifetime of the membrane determines the lifetime of the fuel cell. In order to have a great performance within a PEMFC, a membrane should accomplish the following conditions:

- high proton conductivity;
- impermeable to gases;
- proper water transport;
- high thermo-mechanical and chemical stability for the fuel cell conditions;
- electrical insulator.

The most suitable material, that exhibits the all above mentioned conditions is the perfluorinated sulphonic acid (PFSA). This material, named Nafion[®] is one of the most widely used membranes, being commercially available at DuPont Company, USA [8].

"Nafion[®] perfluorosulfonic acid (PFSA) membranes are non-reinforced films based on chemically stabilized PFSA/polytetrafluoroethylene (PTFE) copolymer in the acid (H⁺) form" [91].

Nafion[®] membrane has an aliphatic perfluorinated backbone with side chains and a semi-crystalline structure (Figure 2.4). This membrane is proton conductive and thermally stable up to 80°C. When the membrane absorbs water, the ionic domains swell to form proton-conducting channels and as the water content increases, the concentration of transferred protons decreases. The strong bonds between the fluorine and the carbon make it durable and resistant to chemical attack.

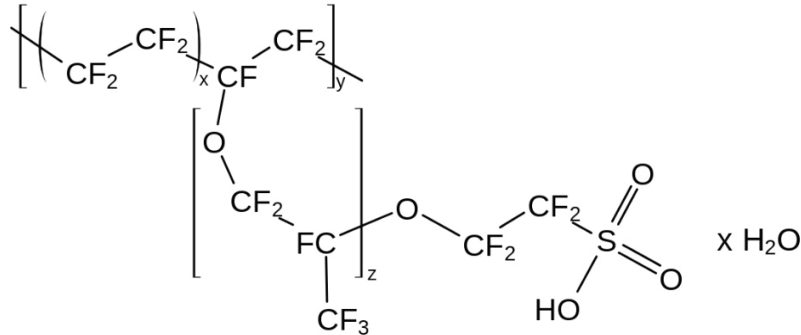


Figure 2.4. Nafion® structure

2.7 Degradation mechanisms for PEMFC components

The degradation of a fuel cell is a combined deterioration effect of each of the cell components like bipolar plates, polymer membrane, catalyst material or gas diffusion layer.

The MEA is mainly susceptible to degradation, since the polymer membrane is both electrolyte and splitter for the reactants (hydrogen and oxygen). An early degradation of the membrane can occur due to an inadequate humidification, mechanical stresses or reactant high pressure. Another type of deterioration can be assessed to the decomposition of the membrane or a chemical degradation caused by the H_2O_2 formation in the cathodic region. It is widely known that the presence of hydrogen peroxide and HO_2^- radicals is poisonous for the membrane, destroying the polymer matrix [92].

2.7.1 Membrane degradation

Among the degradation effects from all the components of a fuel cell, one of the important factors that determines the PEM fuel cells life time is the membrane degradation or failure. As the polymer membrane has several important roles inside a fuel cell, as proton conductor, electric insulator and gas separator, a proper maintenance is highly recommended.

The most common degradation mechanisms related to the polymer membrane are:

Mechanical degradation that can be achieved by perforations and cracks caused by improper manipulation or defects from manufacture, tension or no uniform compression. This lead to hot spots and gas crossover, which produce an early degradation of the membrane.

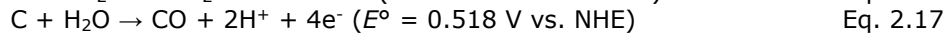
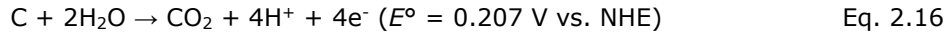
Chemical degradation represents the polymer membrane deterioration by the $-\text{OH}$ and $-\text{OOH}$ radicals generated from the electrochemical and chemical reactions. These radicals lead to “*unzipping reactions*” caused by gas crossover and electrochemical oxygen reduction correlated with the formation of H_2O_2 .

Contamination of ionic species – Nafion membrane has a stronger affinity to metal ions than for protons, resulting in ion exchange of protons with metal ions. This leads to reduction of proton conductivity, reduction of water transport associated with drying out of membrane and water management issues.

2.7.2 GDL degradation

GDL carbon based materials frequently represent the support structure for catalyst particles, assuring the gas access, transport of electrons and protons as well as removal of water. Carbon black presents significant mass transfer limitations due to its dense structure. The pore size and distribution of carbon black affects the interaction between Nafion and catalyst nanoparticles, resulting in failure of achieving the three-phase zone between gas, electrolyte and electrocatalyst, leading to a very low Pt utilization. Additionally, carbon black is known to endure severe electrochemical oxidation, forming surface oxides, which react finally to CO₂ at the cathode of the fuel cell. The formation of CO₂ is accelerated when a lower pH value and higher potential is reached, combined with the humidity and temperature factor, resulting in a reduced life time of the electrocatalyst and detachment of the catalyst particles [54]. Moreover, the graphitization degree directly influences the corrosion resistance of the carbon-based material [93]. Recently, studies have presented that non-graphitised carbon may not satisfy the durability requirements for PEMFC conditions.

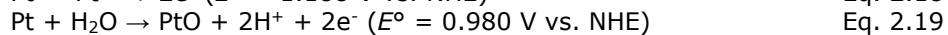
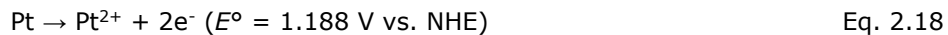
The electrochemical oxidation of carbon is presented in Eq. 2.16 - 2.17:



Carbon corrosion is susceptible during fuel starvation or at start/stop cycles and it is thermodynamically possible also during the fuel cell operation, but is considered insignificant at normal temperatures. It was found that the operating temperature can increase the loss of GDL hydrophobicity. Moreover, carbon corrosion can lead to a significant decrease in the electronic conductivity of the support material.

2.7.3 Catalytic layer degradation

Inside a fuel cell, catalyst materials are normally subjected to severe conditions that promote oxidation like, high potential (> 0.75 V), temperature and the most important aspect, the presence of oxygen. Although Pt particles are stable in acidic electrolytes at low potentials, surface oxidation of the catalyst particles has been reported to decrease the electrocatalytic activity especially for oxygen reduction reaction. Several degradation mechanisms as agglomeration of catalyst particles, catalyst detachment or poisoning can lead to severe loss of activity. These aspects facilitate sometimes the catalyst dissolution or particle growth, facts that lead to loss of electrochemical surface area, catalyst particles migration into the membrane, redeposition of catalyst on other particles, increasing the catalyst size. The corresponding reactions are presented in Eq. 2.18 – Eq. 2.20.



2.7.4 Bipolar plates degradation

Metallic materials such as bipolar plates of the fuel cell stack assembly corrode under a warm (65°C - 90°C), acidic (pH 2-3) and humid environment. Metal cations from the bipolar plates, such as Fe^{2+} , Ni^{2+} or Cr^{3+} , Cu^{2+} can be released during the process and can deteriorate the polymer membrane. To avoid the corrosion process, the metallic parts are coated with noble or corrosion resistant films or inert graphite plates can be taken into consideration.

3 Methodology and equipment

3.1 Equipment and materials

The necessary **equipment** for the experimental program is composed of:

- Potentiostat/Galvanostat (Ivium Technologies Vertex);
- Thermostated electrochemical cell (Radiometer Analytical CEC/TH);
- Ultrasonic Bath (Bandelin Sonorex);
- Oven (Heraeus);
- Plasma Reactor (Plasma Finish RFG 300 RF);
- Scanning Electron Microscope (ESEM XL 30, Philips);
- Energy-Dispersive X-Ray Spectrometer (EDAX);
- X-Ray Fluorescence Spectrometer (Spectro Analytical Instruments);
- X-Ray Diffractometer (X'Pert Philips);
- Thermogravimetric Analysis Instrument (Netzsch STA 449 F1 Jupiter);
- PEMFC Test Bench;
- Electronic Load (Höcherl & Hackl ZS1806NV);

The **materials and chemicals** used for the experimental program are:

- Carbon Nanofibers, GANF, Grupo Antolin, Spain;
- Gas Diffusion Layer, GDL, H2315 I2C6, Freudenberg, Germany;
- Isopropanol 99.8% purity, Merck, Germany;
- Ethanol, 96% vol., VWR Chemicals, Belgium;
- Sulphuric acid, H₂SO₄, 98% purity, Rotipuran®, Carl Roth, Germany;
- Potassium tetrachloroplatinate, K₂PtCl₄, 99.99% trace metals basis, Sigma-Aldrich, Germany;
- Boric acid, H₃BO₃, 99% Analytical Reagent, Merck, Germany;
- Potassium chloride, KCl, >99.5% purity, ACS, ISO, Carl Roth, Germany;
- Cobalt (II) chloride hexahydrate, CoCl₂ · 6 H₂O, ACS reagent, 98%, Sigma-Aldrich, Germany;
- Sodium hydroxide, NaOH, >99% purity, ISO, Carl Roth, Germany;
- Hydrochloric acid, HCl 0.1 M, Reag. Ph. Eur., Sigma-Aldrich, Germany;
- Distilled water;
- Nafion® membrane, type NR-212, DuPont, USA.

The results were acquired and processed using the following **software**:

- Ivium Soft by Ivium Technologies for Linear and Cyclic Voltammetry;
- STA 449 F1 Software Netzsch Data Collector;
- Proteus Thermal Analysis, Netzsch Data Processing;
- X'Pert Data Collector, XRD Philips;
- X'Pert HighScore 3.0, PANalytical;
- X-Lab Pro 5.1 Spectro Midex XRF;
- Origin 8® for Data Processing;
- Microsoft Office® 2016.

3.2 Physical Characterization

Samples have been characterized using Scanning Electron Microscopy (SEM) combined with Energy Dispersive X-Ray Spectroscopy (EDX) for morphology and chemical composition identification, X-Ray Diffraction (XRD), as well as X-Ray Fluorescence Spectroscopy (XRF). Moreover, Thermogravimetric Analysis (TGA) was employed to evaluate the thermal stability of the electrodes at different temperatures and for determination of the catalyst content of the developed electrodes.

3.2.1 Scanning Electron Microscopy (SEM)

The types of signal produced by the Philips XL 30 ESEM used for this work, are namely, secondary and back-scattered (reflected) electrons.

The most important characteristics of the employed SEM are [94]:

- acceleration voltage up to 30 kV;
- resolution up to 2 nm;
- magnification ranges between 25 x – 250 000 x.

The working principle of the SEM (Figure 3.1) consists in scanning a sample with a beam generated by an electron gun, which is guided through two or more electron lenses. The whole process is carried out under a high vacuum level. Electrons are accelerated through a voltage difference between the anode and cathode. The beam will be demagnified by an electron lens system, which will generate an electron beam of 1-10 nm on the specimen surface [95].

A deflection coil, installed before the last lens, scans the sample in a raster across the sample with the electron beam of a separate cathode-ray tube [96]. The intensity of the tube is filtered by one of the signals to form an image. Besides secondary and backscattered electrons, a large variety of electron-sample interactions can be used to form an image, which gives information about the samples. The magnification of the image can be adjusted by setting the scan-coil current.

Secondary Electrons (SE) (energy < 50 eV) are formed by beams of electrons which hit the specimen, while low energy secondary electrons leave the sample with different angles. As they have a negative charge, positive sources will attract them. The secondary electrons are attracted into a Faraday type cage of +300 V and surround the detector [95]. The cage is sufficiently electrically charged to generate flashes of light. The electrical signal is projected on a display as a video image, or can undergo analog-digital conversion to be displayed as a digital image. The value of the angle of low energy secondary electrons beam which are leaving determines the brightness of the signal. If the hitting angle of the beam towards the sample is perpendicular, some electrons leave the sample undetected. As the angle increases, the leave of the electrons on one side will decrease, more secondary electrons being generated.

Backscattered electrons (BSE) (energy > 50 eV) are used for detection between the contrasts of various regions which have different chemical compositions [97]. The accelerated beam which hits the sample produces elastic and inelastic collisions within the sample. Elastic scattering produces changes to the trajectory of the incoming beam when it interacts with the sample but its kinetic energy remains constant. When the beam hits an atom with a greater atomic number the likeliness of collision is higher because of the greater cross-section area. The number of electrons returning to the BSE detector is higher and therefore, a brighter area corresponds with elements of higher atomic number Z.

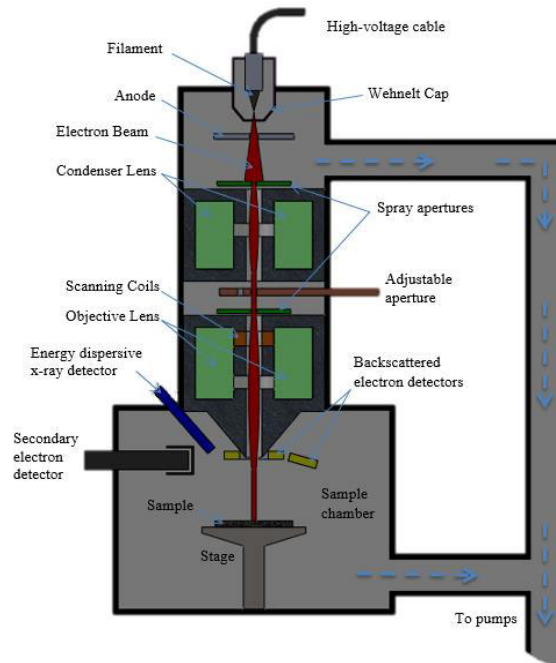


Figure 3.1. Schematics on the SEM

3.2.2 Energy Dispersive X-ray Spectroscopy (EDX)

Nowadays, most SEM devices are equipped with an EDX spectrometer. This technique is used for elemental analysis of a sample. To stimulate the emission of characteristic X-rays from a specimen, a high-energy beam of charged particles such as electrons or protons is focused into the sample. An atom within a sample contains unexcited electrons in discrete energy levels or electron shells bound to the nucleus. The incident beam may excite an electron in the inner shell, ejecting it from its shell, thus creating an electron hole. An electron from an outer higher energy shell then fills the hole and the energy difference between the shells is released in the form of an X-ray (Figure 3.2). Because the energy of the X-ray is characteristic of energy difference between two shells of the atomic structure of the element from which they were emitted, the measurement of the samples elemental composition is possible.

In a spectrometer, X-ray energies are identified by a detecting material, most frequently a lithium-drifted silicon (Si (Li)) crystal [98]. Charged pulses produced in the crystal by the X-rays which are proportional to their energy are detected simultaneously. No focusing of the X-rays are needed, so all the present elements are detected. The pulses will enter to external stages of the preamplifier. In the digital processing system, all processing is performed inside the digital module. Once the signal is digitalized, it is subjected to filtering and finally it is illustrated for interpretation.

The outputs of a scanning electron microscope are usually easy to interpret and can be used to investigate materials of different sizes, forms and shapes. Samples as-polished, etched, rough-surfaces, cross-sections or powders can be easily subjected to SEM or EDX investigations. Because of relative easy manipulation, both SEM and EDX have a wide range of applications in chemistry, materials science and materials development.

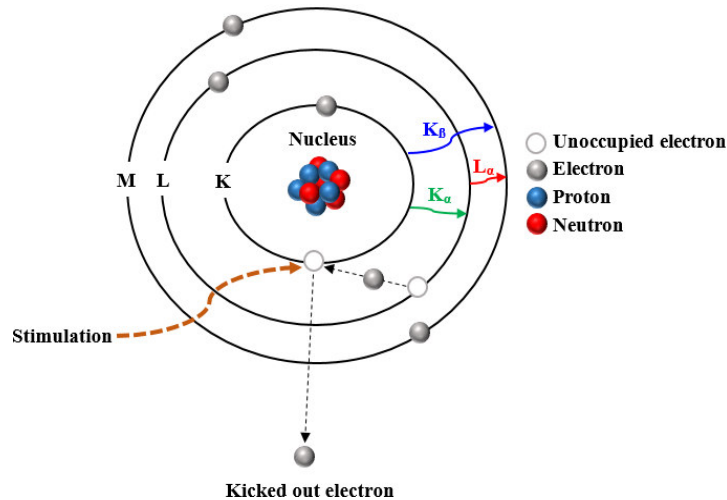


Figure 3.2. EDX Principle

3.2.3 X-ray Diffraction (XRD)

The X-ray diffraction analysis were carried out using an X`Pert MPD System from Phillips, Netherland. This diffractometer is outfitted with a high resolution PW3020/10 vertical goniometer with long fine focus ceramic tube, Cu anode, 1.5406 Å wavelength, and max. 3 kW and 60 kV. This device offers a high-quality phase identification and quantification of pure materials, simple mixtures as well as polycrystalline materials based on their crystalline structure [99].

During X-ray diffraction, a sample is irradiated with a monochromatic beam of X-rays, the beam being diffracted at angles determined by the atomic planes. The intensity and spacing of these diffracted beams are unique function of each type of material and can be identified by comparison to a database. Diffraction effects occur when electromagnetic radiation impinges on periodic structures with geometrical variations on the length scale of the wavelength of the radiation. The interatomic distances in crystals and molecules are situated between 1.5 and 4.0 Å, which correspond to the electromagnetic spectrum, with the wavelength of X-rays having photon energies between 3 and 8 keV.

X-rays are produced when electrons with kinetic energies in the keV range impinge on matter. The emission spectrum comprises from a continuous part, called Bremsstrahlung, and some discrete lines exhibitive of the chemical elements from the target material. The principle of such a tube is presented in Figure 3.3.

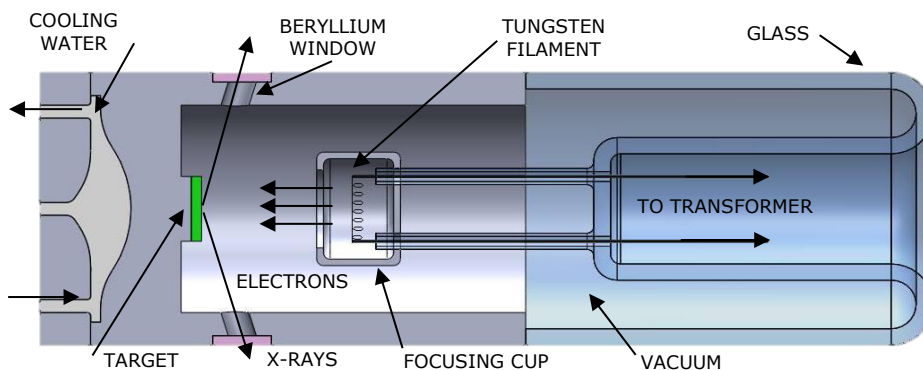


Figure 3.3. Schematic cross-section of an X-ray tube

Electrons are emitted from the cathode filament and accelerated towards the anode plate. The anode is typically fabricated from copper, chromium, aluminium, molybdenum or another metal. The electron current between filament and anode may be adjusted by tuning the filament current in the range of tenths mA. When impinging upon the anode, the electrons are decelerated by their interaction with the target plate atoms, leading to emission of X-rays [100].

There are several X-ray diffraction techniques. Two of the most common are:

Single crystal X-ray diffraction, which are used to identify structures of crystalline materials ranging from simple inorganic compounds to complex molecules. Even though obtaining single crystals is difficult, single crystal X-ray crystallography is a primary method for determining the unit cell dimensions, bond-lengths, bond-angles and site-ordering information.

Powder X-ray diffraction, which are used to characterize crystallographic structure, grain size, and preferred orientation in polycrystalline or powder solid samples. This is a preferred method of analysis for characterization of unknown crystalline materials. Compounds are identified by comparing diffraction data with a database.

The diffraction pattern is collected by varying the incidence angle of the incident x-ray beam by θ and the scattering angle by 2θ while measuring the scattered intensity $I(2\theta)$ as a function of the latter. Two angles have thus to be varied during a $\theta - 2\theta$ scan [100]. A wide range of organic and inorganic powder samples have been measured with this arrangement, thus the name of powder diffractometer was given. Its measurement principle can also be applied for investigation of thin films, especially if the layers are polycrystalline and have been deposited on flat substrates.

3.2.4 Thermogravimetric Analysis (TGA)

Thermal analysis (TGA) is a term frequently used to depict analytical experimental techniques that examine in detail the behaviour of a sample as a function of temperature. Conventional thermal analysis methods include techniques such as thermogravimetric analysis (TGA), differential thermal analysis, differential scanning calorimetry, thermo-mechanical analysis and dynamic mechanical analysis [101]. TGA is based on precise measurements of mass variation,

temperature and temperature change, which requires a precision balance using a thermoresistant crucible loaded with the sample and a precise programmable furnace. A schematic representation of TGA instrument is shown in Figure 3.4.

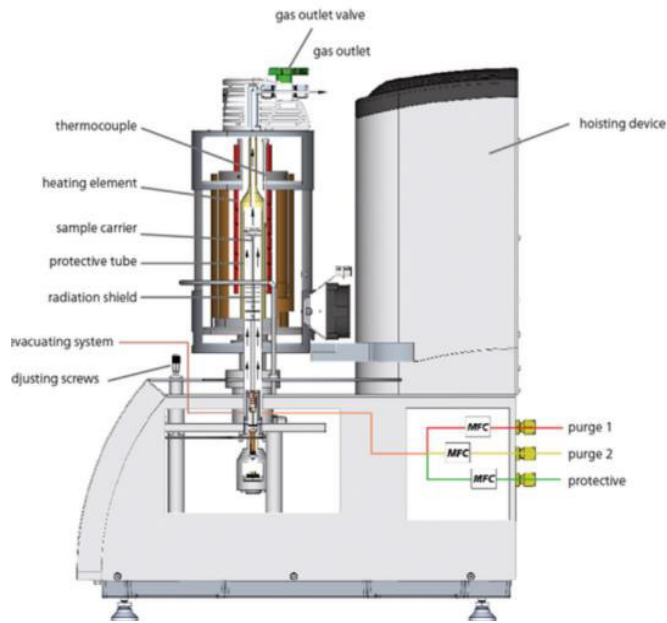


Figure 3.4. Schematic representation of TGA instrument [102]

The advantages of thermal analysis in relation to other analytical methods are numerous. The studies can be performed over various temperature ranges, using diverse temperature programmes, samples of different physical forms (solid, liquid and gel) can be investigated, only small amounts of sample are necessary (typically 0,1 μg -10 mg), the testing atmosphere can be easily controlled and the experimental procedures are fast (from a few minutes to hours) [101].

Atmospheres can be generally divided into two categories, namely interactive and non-interactive. A non-interactive atmosphere such as helium or argon gas is used to create the experimental conditions without affecting the sample. Meanwhile, an interactive atmosphere like oxygen or nitrogen may be directly involved during the thermal events occurring in the sample. Specific atmospheres can be used under static or flowing conditions, the second being employed to eliminate gases evolved in the vicinity of the sample. Gases employed in TG analysis include synthetic air, Ar, H_2 , He, N_2 , O_2 [102].

In this regard, the TGA measurements were carried out using an instrument STA 449 F1 Jupiter[®] from Netzsch (Germany). This instrument has a top-loading system, the silicon carbide furnace (SiC) is operating from ambient temperature up to 1600°C. The system allows measurements of samples up to 5 grams in weight and up to 5 ml in volume, having a digital resolution in the nanometric range (0,025 μg). The built-in gas supply unit, with three mass flow controllers for purge and protective gases, offers optimum control on the atmosphere around the sample. Heating and cooling rates are in the range of 0.001 K min^{-1} to 50 K min^{-1} .

3.2.5 X-Ray Fluorescence (XRF)

The X-ray fluorescence spectroscopy was carried out using a Spectro Midex LD from Spectro Analytical Instruments (Germany). This non-destructive measuring method is one of the most flexible techniques available for the analysis and characterization of materials. Modern XRF instruments can analyse solids, liquids, and coated samples for both major and trace components. The test is rapid and often sample preparation is minimal or not required [103].

Spectro Midex X-ray Fluorescence Spectrometer (Figure 3.5) utilizes an air-cooled low power X-ray tube with micro focus for collimated point sample excitation. With the incorporation of software controlled collimators, the size of the measuring spot can be selected in several fixed steps between 200 μm and 4 mm, enabling it to be optimized for a whole range of applications.

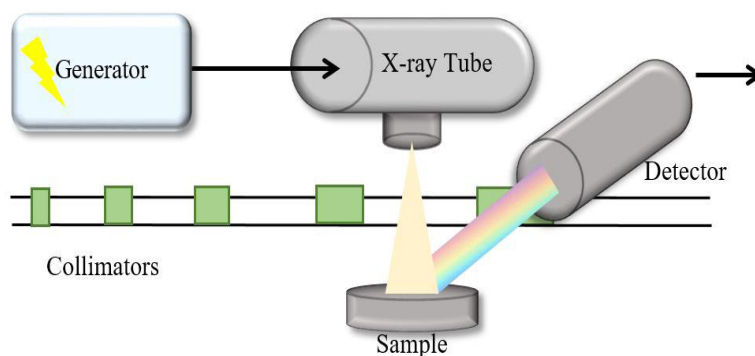


Figure 3.5. Schematic representation of XRF working principle

The high-resolution detection system consists of an X-ray tube with Mo anode, power max. 30 W, voltage max. 48 kV and Si drift detector (SDD) with electrical Peltier-cooling, processing up to 250,000 pulses per second. For a fast point analysis of an unknown sample, it is possible to determine elements from magnesium to uranium in less than 180 seconds.

XRF is based on the principle that individual atoms, when excited by an external energy source, emit X-ray photons of a characteristic energy or wavelength. By counting the number of photons of each energy emitted from a sample, the elements present may be identified and quantitated. The identification of elements by X-ray methods is possible due to the characteristic radiation emitted from the inner electronic shells of the atoms under certain conditions. The emitted quanta of radiation are X-ray photons whose specific energies permit the identification of their source atoms [104].

3.3 Electrochemical Techniques

Several electrochemical characterization methods can be used to evaluate the performance of electrochemical cell catalysts. Characterization of catalyst materials, reaction mechanisms or kinetics can be achieved by linear voltammetry, cyclic voltammetry, chronopotentiometry.

Regarding the electrochemical behaviour, several technics have been applied, to determine the electrochemical surface area of the obtained catalysts, the electrochemical behaviour of the catalysts materials, as well as corrosion behaviour of the carbonic substrate.

The electrochemical measurements were carried out using a Potentiostat/Galvanostat IVIUM Technologies Vertex, in a three-electrode cell, using as counter electrode a platinum disk and as reference, a Saturated Calomel Electrode (SCE).

The studies on the catalyst particles deposition require the use of the following experimental electrochemical techniques:

- Linear sweep voltammetry (LSV)
- Cyclic Voltammetry (CV)
- Galvanostatic pulse current deposition (PCD)

The linear sweep voltammetry was applied to establish the working parameters for the catalyst deposition. For determination of the reaction mechanisms from the electrode-electrolyte solution interface for Pt, Co and Pt-Co deposition, kinetic parameters $1-\alpha$ and i_0 have been determined using the Tafel slope method.

Cyclic voltammetry has been employed for studying the electrochemical reduction of the metallic particles and oxidation processes of the investigated catalysts. Moreover, with using the cyclic polarisation curves, the electrochemical active surface area was calculated.

The deposition process of the catalysts was carried out using the galvanostatic pulse plating method, by applying several current densities and varying the characteristic parameters.

3.3.1 Linear Sweep Voltammetry (LSV)

Potential sweep methods are considered the most widely used methods, providing important information regarding the electrochemical behaviour of the system. Linear voltammetry (LSV) represents an electrochemical technique suitable for a great variety of applications, like identifying unknown species, determination of the solutions concentration, establishing the number of electrons involved in a process. Regarding this technique, the potential of the working electrode is varied in time with a linear scan rate (ν) between 2 different values, the initial (E_i) and final (E_f) and current density (i) is measured (Figure 3.6).

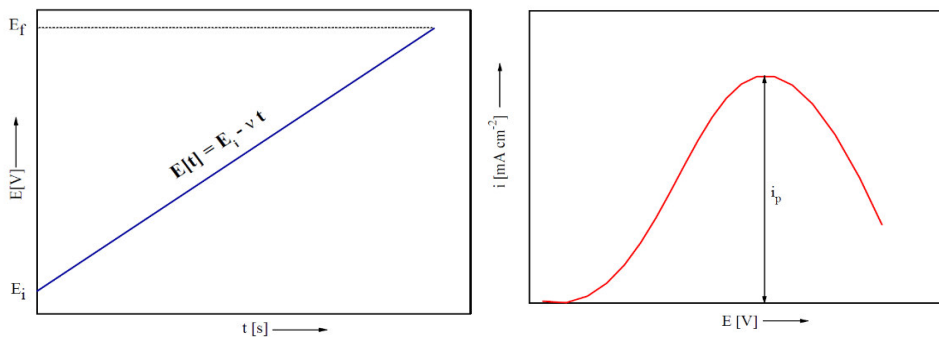


Figure 3.6. LSV Technique

As the potential is constantly changing, gives rise to ohmic currents, due to the capacitive charging of the working electrode double layer.

LSV technique employs a potentiostatic configuration for the electrochemical cell. The cell is composed of three electrodes: working electrode (WE), reference electrode (RE) and counter electrode (CE). The current flows between the CE and WE (Figure 3.7). The (CE) (or auxiliary electrode) is normally used to close the electrical circuit in the electrochemical cell. Usually it is made off inert materials like platinum, gold or graphite and it is practically not involved in the electrochemical reactions. The CE area is necessary to be higher than the WE area in order to avoid the limitation of electrochemical processes. The RE is a stable electrode with a well-known potential, being used for measurement and control of the system potential. In the present experimental work, a saturated calomel electrode (SCE) has been employed as reference. A Luggin capillary is used for the RE to minimize the electrolyte resistance and samples with 1 cm^2 were prepared as working electrodes for the electrochemical investigations.

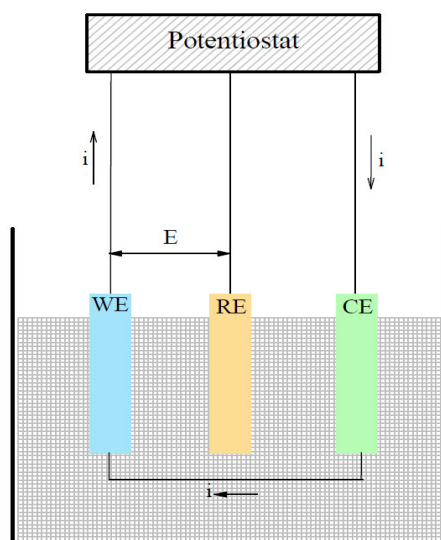


Figure 3.7. The electrochemical cell configuration

3.3.2 Tafel Slope Method

Tafel slope method offers the possibility to determine the corrosion behaviour of tested materials using current density values as well as the identification corrosion/inhibition mechanisms or possible modifications of the electrode surface. The potentiodynamic plot describes the current density dependence on the potential values, being usually represented in logarithmic form as shown in Figure 3.8.

Using this method, the corrosion rate can be calculated using the Tafel slope values as the Eq. 3.1 describes:

$$i = i_o \left\{ \exp \left[\frac{2,303}{b_a} (E - E_{eq}) \right] - \exp \left[-\frac{2,303}{b_c} (E - E_{eq}) \right] \right\} \quad \text{Eq. 3.1}$$

where $\frac{2,303}{b_a}$ and $\frac{2,303}{b_c}$ represents the anodic and cathodic slope, b_a and b_c are the anodic and cathodic Tafel plots constants, E_{eq} – equilibrium potential and i_o – exchange current density.

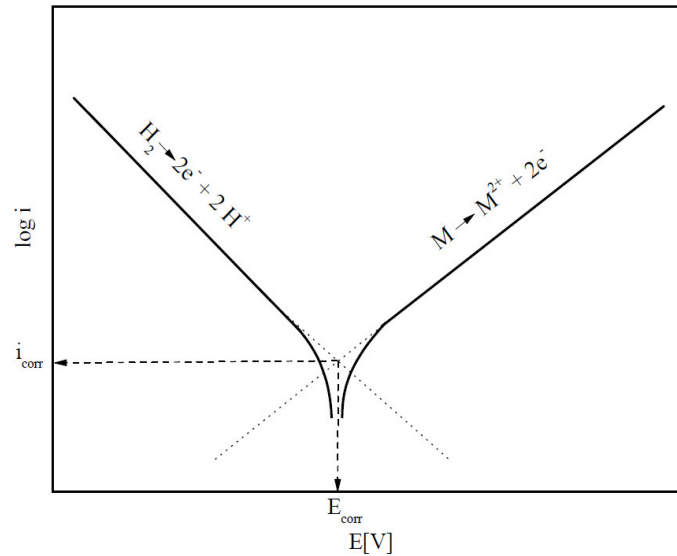


Figure 3.8. Tafel plot

3.3.3 Cyclic Voltammetry (CV)

Cyclic voltammetry (CV) can be regarded as a suitable technique for investigation of the surface reactions, detecting the electrochemical properties of the atoms surface and less for the volume and mass properties.

CV represents a type of potentiodynamic electrochemical investigation for identifying the electrochemical behaviour of a system. It was first introduced in 1938 by Randles.

As principle, a triangular signal with symmetric slopes is applied to the working electrode and the potential is shifted with a constant scan rate from the initial value (E_i) to another potential value (E') called reverse potential, then is restored to the initial value E_i for several cycles (Figure 3.9). The applied scan rate may vary in a large range, depending on the demands from $\mu V s^{-1}$ up to $V s^{-1}$. The registered current is usually related to the surface of the working electrode. The current density is plotted against the potential values, obtaining a cyclic voltammetry. The number of cycles may also vary, depending on the demands.

The registered peaks are characteristic to specific electrochemical reactions at the electrode/electrolyte interface. The height and the width of the characteristic peaks offer important information about the electrochemical process and they are dependent of the scan rate, the concentration of the electrolyte, or the electrode material.

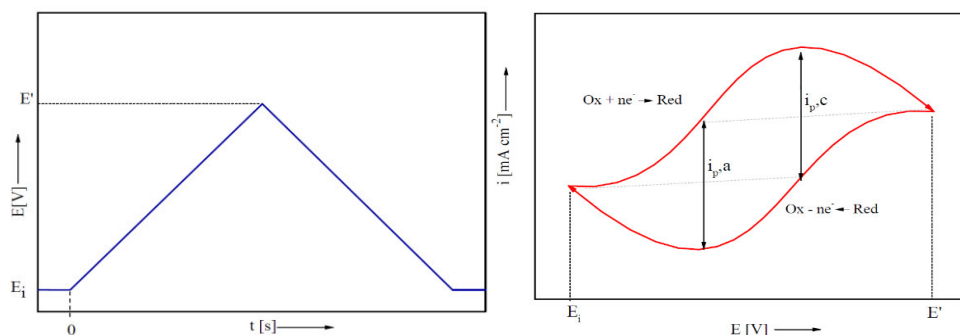


Figure 3.9. CV Technique

Cyclic voltammetry technique offers the possibility to investigate the kinetics of an electrochemical reaction on the surface of the working electrode. Several processes like oxidation/reduction, diffusion, or adsorption/desorption can be highlighted on the cyclic voltammogram.

In this experimental work, CV was applied to determine the potential range for electrochemical reactions that occur during the deposition process for platinum and platinum-cobalt alloy. Moreover, CV gives important information regarding the electrochemical surface area (ECSA) of the studied electrodes, using the hydrogen adsorption/desorption (oxidation) peaks.

3.3.4 Pulsed Current Deposition Method (PCD)

For decorating the CNF support material with catalyst particles, an electrochemical method was applied. By employing this type of deposition, several advantages are achieved. The catalyst particles deposition occurs mainly on the CNF surface which is electrically connected to the system and less in the depth of the material. This fact favours the formation of three-phase reaction zone inside the electrochemical cell and increases the utilisation degree of the catalyst. Within the different types of electrodeposition methods, the pulse current plating method distinguishes from the other techniques by easiness of application, the short time of the process and the possibility to deposit nanoparticles with a good distribution onto the substrate material.

The pulsed current plating method was first introduced in 1950, being mainly an alternative method for 24 karats gold deposition, which exhibited difficulties for deposition with standard direct current method.

In PCD, the applied potential or current density is varied between two different values, resulting in a series of pulses with equal amplitudes, duration and polarity [85]. Each pulse is characterised by three important parameters: the potential/current density applied value (i), deposition time or the time when the potential (E) or current density value (i) is applied (t_{on}) and the period between pulses or the period when there is no current flow in the system (t_{off}).

The duty cycle (d.c) corresponds to the percentage of total time of a cycle and it is described by the Eq. 3.2:

$$\text{d.c [\%]} = \frac{t_{\text{on}}}{t_{\text{on}} + t_{\text{off}}} \times 100 \quad \text{Eq. 3.2}$$

In practice, PCD involves a duty cycle higher than 5% and t_{on} varying from μs to a few ms. The deposition rate is the same as for the direct current method.

A typical square waveform pulse is shown in Figure 3.10. This type of pulse is usually applied in case of alloy deposition or pure metals especially in multilayers. Moreover, there are several types of pulse waveforms that can be applied for the deposition process depending on the desired characteristics.

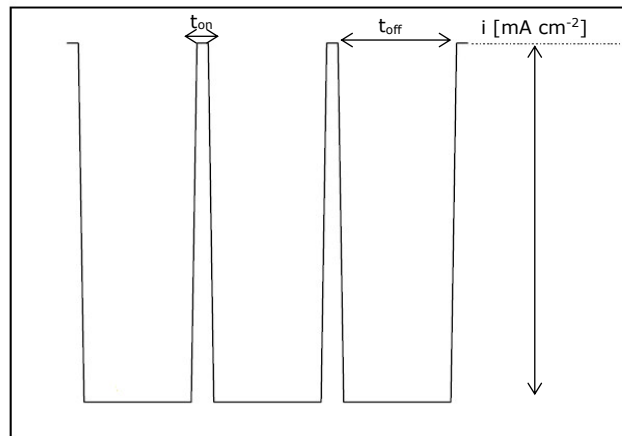


Figure 3.10. Typical pulse-current waveform

Several advantages can be achieved by applying the PCD method in comparison to the standard direct pulse electrodeposition:

- Better current distribution;
- Controlled mass transfer step;
- Controlled microstructure;
- Reduced porosity;
- Uniformity of the layer;
- Lower hydrogen embrittlement;
- Controlled chemical composition in case of alloys.

The current density limit can be significantly raised in comparison to direct current deposition since the replenishing of metal ions concentration in the diffusion layer is realized only during t_{off} . Moreover, PCD reduces the additives requirement, enhancing the bath stability and efficiency [85].

3.4 CNF Treatment

Prior to the deposition process, the CNF require a functionalization treatment to enhance the surface reactivity and hydrophilicity, which further influences the catalyst deposition and distribution. This step was performed using low-pressure oxygen plasma treatment, which is an efficient and rapid process, providing a high functionalization degree onto the exposed material. In addition, no by-products are released during the operation and the treatment is shorter (up to a few minutes) in comparison with other available functionalization methods.

3.4.1 Low-pressure Plasma Treatment

The low-pressure plasma treatment (activation/functionalization) was carried out using a PINK V15-G from PINK GmbH Thermosysteme (Germany).

At atmospheric pressure, plasma is very hot, as in flames and arc discharge (10^3 - 10^4 K). If the pressure is reduced under 100 Pa, plasma can be produced at low temperature. This is called non-thermal plasma. The material treated with low-pressure plasma is only slightly heated because the gas has a very low temperature. However, the energy of the electrons corresponds to a temperature of thousands K. This advantage enables the treatment of temperature sensitive materials. Low-pressure plasma is produced by subjecting a gas to strong electromagnetic fields. The reaction depends on the type of dielectric (ionized) gas and the excitation frequency. Therefore, a treatment in neutral, oxidizing or reducing environment is possible. A schematic representation for the low-pressure plasma treatments is presented in Figure 3.11.

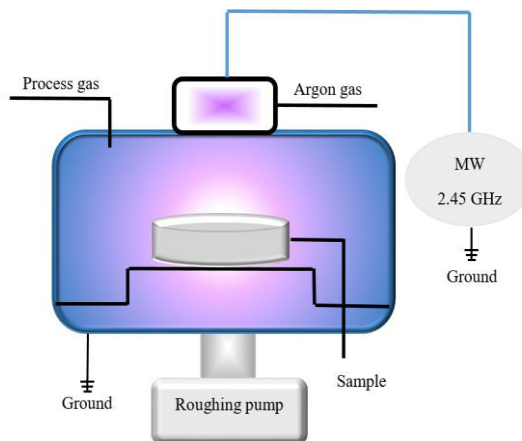


Figure 3.11. Schematic representation of low-pressure plasma treatment

Procedures involving non-thermal plasma technology are not only extremely efficient, but also ecologically neutral and economically useful because no polluting waste products and no disposal costs incur therefore. With the aid of low-pressure plasma, it is possible to obtain simply and efficiently an activation or chemical modification of different materials surfaces (Figure 3.12).

Plasma activation produces covalent chemical bonds between oxygen and carbon atoms allowing interactions between the treated material and other substances and/or the environment because of their polarity. Such chemical bonds are stable over time and there is no degradation under normal storage conditions. However, storage stability is influenced by subsequent contamination from outside and/or inside and physical processes in the material.

The PINK V15-G is a high-quality system, designed for both industrial small batch production as well as low-pressure plasma treatment for R&D test series. The oven is integrated in a 50 cm rack, which is equipped with rollers and height-adjustable feet. A professional control unit serves also as storage for the process parameters. Plasma excitation frequency is provided by a 2.45 GHz microwave

generator, with adjustable power up to 600 W. Low pressure inside the treatment chamber is achieved and maintained with the help of an oil-sealed rotary vane pump. The plasma gas (argon) is introduced through a mass-flow-control inlet. Additionally, three gas inlets provide process gases for surface treatments like: activation and/or modification, cleaning, etching or coating.

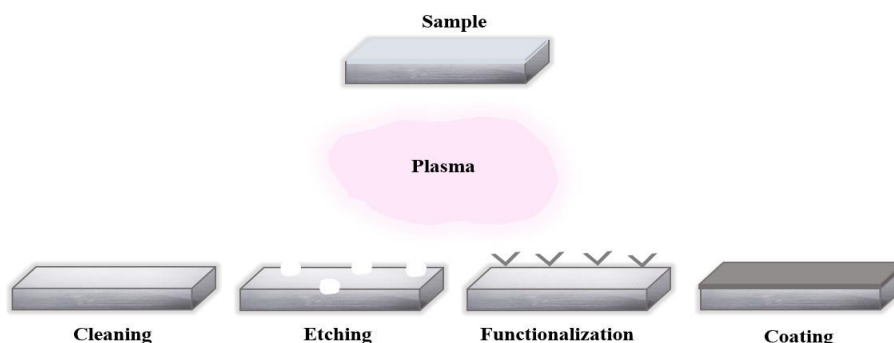


Figure 3.12. Plasma processes

3.4.2 Titrimetric Analysis

As it was already mentioned, the functionalization process of CNF is performed to improve the reactivity of the fibers by attaching reactive groups onto their surface. Functional groups like carbonyl, carboxyl, hydroxyl, lactones, phenols, amines, aldehydes may be produced, depending on the gas involved in the process. Functional groups can be acidic, basic or neutral. Depending on the applied parameters, the types and amount of surface functional groups may vary. In this study, since the functionalization process is conducted under oxygen atmosphere, the main functionalization groups are based on oxygen.

Surface groups for activated carbon can be usually determined by wet or dry methods. The wet methods involve titrations like Boehm [105], acid-basic, or potentiometric. The dry mode involves diffuse reflectance, X-ray photoelectron spectroscopy (XPS), thermal analysis or thermal desorption [106].

Boehm titration provides qualitative and quantitative information about the carbon surface, but only a few of the acidic groups can be detected, like phenols, lactones or carboxylic. This method works on the principle that oxygen containing groups have different acidities and can be neutralized using different bases. Accordingly, the estimation of the acidic groups concentration is successfully performed by the neutralisation titration method.

In the present experimental work, the surface functional groups containing oxygen are determined employing the Boehm titration method. Four different activated CNF samples were tested, related to CNF bulk sample without any functionalization treatment.

3.5 Membrane Electrode Assembly (MEA) Testing

Selected electrodes are further tested as anodes (CNF/Pt) or as cathodes (Pt-Co based catalysts) in a full automatic PEMFC test bench designed at Westphalian Energy Institute, Gelsenkirchen, Germany (Figure 3.13). During operation, a hydraulic medium surrounds each test cell, assuring a homogenous pressure distribution over the active cell area. A single cell is composed of an anode and a cathode fixed on both sides of a PEM membrane (type Nafion® 212) forming the MEA. The test cell is equipped with two graphite pole plates, designed with a symmetric flow fields with four serpentine channels, for a uniform gas distribution. The geometry of the gas flow field is suitable for 20.25 cm² (4.5 cm x 4.5 cm) electrodes. MEA are placed between the graphite pole plates and are tightly pressed against each other by hydraulic compression (up to 5 bar). Each of the two pole plates are equipped with intake and outlet channels for gasses (H₂ as fuel is fed at the anode and air as oxidant at cathode respectively). The H₂ flow rate was set to 500 mL min⁻¹ and the air flow rate was 1000 mL min⁻¹.

The test cell is connected to an electronic load type Höcherl & Hackl ZS1806NV. Polarisation curves are determined at normal temperature (25°C) in constant voltage mode as well as potentiodynamic, by decreasing the cell voltage from the open circuit (OCP) down to 0 V. Before recording the polarisation curves, the electrodes were preconditioned for 45 minutes at different voltage values to activate the catalysts (0.15 V, 0.45 V and 0.65 V).



Figure 3.13. MEA test system with hydraulic compression

4 Experimental Program

For development of catalyst materials based on CNF, three important specific objectives were taken into consideration:

- **Support material preparation (non-catalysed electrode);**
- **Catalyst particles electrodeposition onto the support material;**
- **Characterisation of the obtained structures.**

The experimental program is schematically presented in Figure 4.1.

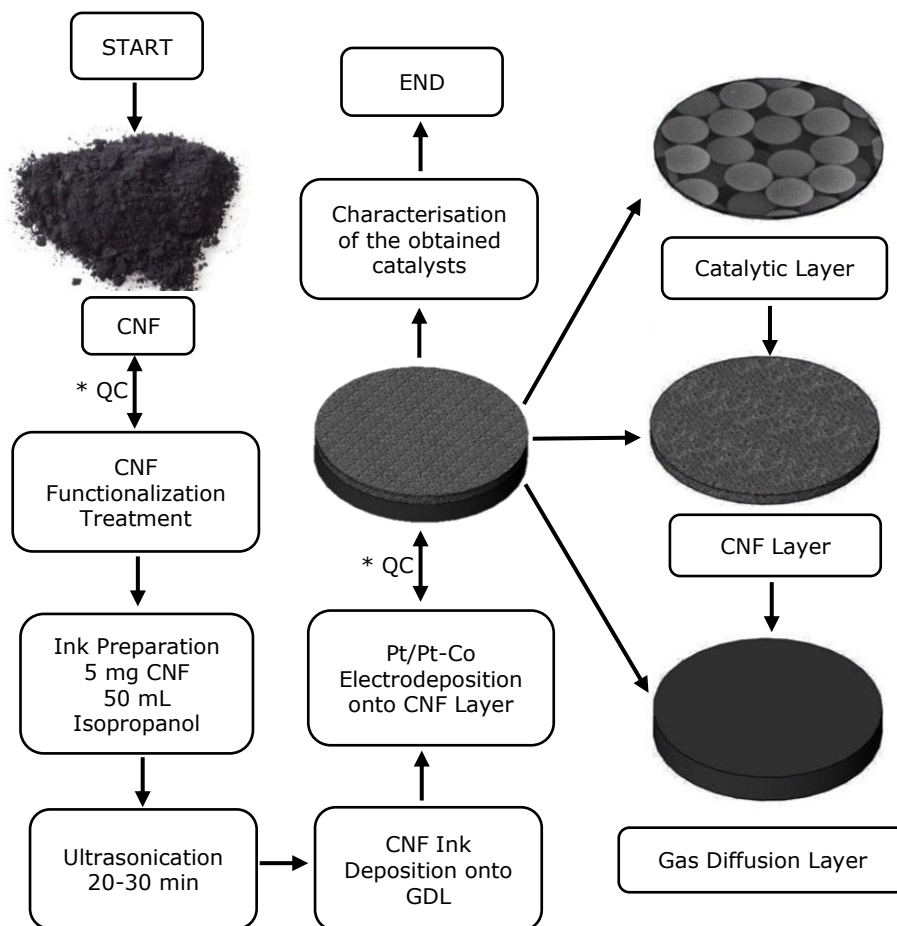


Figure 4.1. Schematic representation of the experimental program

4.1 Preparation of the support electrode

CNF (commercially available as GANF) with a high graphitization degree (up to 100) and a high surface area of about $105\text{-}115\text{ m}^2\text{ g}^{-1}$ from Grupo Antolin, Spain were employed as catalyst support material. CNF are sub-micron Vapour Grown Carbon Fibers (s-VGCF) with a small diameter, being characterized by excellent electric and thermal conductivity (See Appendix 1). The main properties of the employed CNF are presented in Table 4.1.

Table 4.1. Main properties of the employed CNF

Measured Property	CNF (GANF)
Fiber Diameter (TEM) [nm]	20-80
Fiber Length (SEM) [μm]	> 30
Bulk Density [g cm^{-3}]	≈ 2.1
Apparent Density [g cm^{-3}]	0.085
Specific Surface Area (BET - N_2) [m^2g^{-1}]	105 - 115
Graphitization Degree [%]	≈ 100
Electrical Resistivity [$\Omega\text{ m}$]	10^{-4}
Metallic Particles Content [%]	0.1 - 0.2

4.1.1 CNF functionalization treatment

As scheme presented in Figure 4.1 illustrates, prior to catalyst deposition process, CNF need to be fixed onto the GDL surface in order to obtain the support material. A uniform CNF interlayer with around $5\text{ }\mu\text{m}$ thickness is required to be created onto the GDL surface. Thus, it is necessary to bring the CNF in a liquid dispersion to proceed with the spraying process using a manual liquid pulverizer. As produced, CNF exhibit a certain degree of hydrophobicity and inertness that leads to difficulties in mixing them with the liquid medium for obtaining a homogeneous dispersion. Consequently, CNF need a surface modification treatment to improve the wettability, surface energy, as well as to achieve a hydrophilic character and a favourable interaction with the liquid medium. Among the various functionalization methods mentioned in literature, plasma treatment distinguishes by its ease and rapid process. Accordingly, CNF are subjected to a functionalization treatment in oxygen plasma atmosphere. The oxygen-carrying polar functional groups improve the hydrophilicity of the carbon structures, favouring the dispersion in various solvents [65]. Attaching functional groups on the carbonaceous support material can substantially change the surface reactivity, especially the CNF dispersion process in the desired solvent. Moreover, the oxygen plasma treatment improves considerably the catalyst deposition process by creating nucleation anchors for the metal which will be subsequently reduced onto the CNF surface. In addition, oxygen containing groups may build up a protective layer that prevent the further oxidation of the carbon. On the other side, the formation of lattice defects (created by the local etching and burning out of the graphitic structure) may result in decreased conductivity of the material.

Functionalization treatment using plasma is considered an efficient method for surface modification, being a clean and efficient process, which can induce different types of functional groups on the CNF surface by the interaction of plasma-generated excited species with the solid outer surface of carbon. As described in the previous chapter, the type of functional groups depends on the gas mixture involved in the process. Applying oxygen, the C=C bond is broken, and hydroxyl, carbonyl and/or carboxyl groups can be produced, resulting a chemical/physical modification on the first atomic layer of the CNF. The significant parameters (plasma power and treatment time) applied for the functionalization process are presented in Table 4.2. The oxygen and argon flow of 100 mL min^{-1} and a pressure of 60 Pa were kept constant for all investigations.

Table 4.2. Functionalization parameters for oxygen plasma treatment

Plasma parameters	Power [W]	Time [s]
CNF 80	80	1800
CNF 100	100	1200
CNF 120	120	600

Each set of parameters creates onto the CNF surface a certain concentration of functionalities. It is essential to determine the number of functional groups created during the plasma treatment, to establish the optimal treatment parameters that may lead to the desired functionalization degree of the CNF. Similar studies regarding this aspect stated that once the applied power is increased, the functionalization process is intensified and a higher concentration of functional groups is achieved. In addition, a prolonged exposure time correlated with a high applied power affects considerably the CNF surface and may lead to etching effects, destroying considerably the bulk properties of the exposed material [74].

The presence of functional groups can be validated and quantified using several means. Among them, the most simple, cheap, and rapid method to identify the existence of functional groups onto the CNF surface is by mixing them with a polar solvent and determine the required time for sedimentation [107]. Moreover, a comparison between different solvents can be realized to determine the most stable dispersion formulation.

After the functionalization treatment, CNF were investigated in respect to the functionalization degree, particularly regarding the concentration of functional groups attached to their surface. Nowadays, several investigation methods are available to determine the type of the functional groups, as well as their concentration. As the main groups created during the oxygen plasma treatment have been shown to possess an acidic character [68], a suitable method for estimation their concentration is an acid-base titration.

The Boehm titration [105] is regarded as an appropriate chemical method for determination of the functionalities concentration located onto the CNF surface. The oxygen functionalization groups were quantitatively evaluated using a titration method with HCl. CNF functionalized with the parameters presented in Table 4.2 were analysed regarding their functionalization degree in comparison to untreated CNF, considered as reference. 5 mg of each specimen were mixed with 20 mL 0.1 M NaOH solution at normal temperature and stirred for 24 hours under N_2 continuous flow atmosphere with the aid of a magnetic stirrer. Therefore, the mixture was filtered to remove the CNF and to obtain a clear solution. This step is important for avoiding the

protonated groups from the CNF surface to react with 0.1 N HCl. Moreover, it has been proved that NaOH solution neutralizes acidic groups like carboxyl, lactone or phenolic [108]. From each solution, 2 mL aliquot was sampled, further diluted with 20 mL with distilled water, mixed with 2 drops of phenolphthalein and titrated with HCl solution until full neutralization. The operation was repeated 5 times for each specimen and the average value was further used for calculations. As the NaOH solution was prepared from solid pellets, the obtained solution needs a standardization procedure using 0.1 N HCl commercial acid solution, to avoid errors in calculation. The factor of the NaOH solution was calculated (using Eq. 4.1) after repeated titrations with standardized 0.1 N HCl.

$$C_{\text{CNF}} = \frac{C_{\text{NaOH}} \cdot V_{\text{NaOH},i} \cdot f_{\text{NaOH}} - C_{\text{HCl}} \cdot V_{\text{HCl},T}}{m_{\text{CNF}}} 10^{-3} \quad \text{Eq. 4.1}$$

where C_{NaOH} , V_{NaOH} , f_{NaOH} are the concentration [mol L^{-1}], volume [mL] and factor of NaOH solution, C_{HCl} , V_{HCl} , T is the volume [mL] of HCl necessary to neutralize 2 mL NaOH solution mixed with functionalized CNF, C_{CNF} denotes the concentration of functional groups [mol L^{-1}] on the CNF surface that reacts with the NaOH solution during the mixing step, m_{CNF} is the amount of CNF [g].

The functional groups concentration is strongly related to the specific surface area of the carbon material and depends on the treatment method. As the values from Table 4.3 present, a higher concentration of functional groups was achieved by applying a power of 80 W for 1800 s. Similar studies using CNF with a smaller BET surface ($45 \text{ m}^2 \text{ g}^{-1}$) have presented a concentration of 1.8 mmol g^{-1} for similar functionalization parameters (80 W, 1800 s) [77].

Table 4.3. Concentration of the acid functionalization groups

Sample	Concentration Acidic groups [$10^{-3} \text{ mol g}^{-1} \text{ CNF}$]
CNF untreated	0.4
CNF 80	4.4
CNF 100	3.6
CNF 120	1.2

4.1.2 CNF thermal behaviour

Thermogravimetric measurements were performed for untreated/treated CNF with each of the previous mentioned parameters to evaluate the thermal behavior of carbon structures in normal atmosphere. The measurements were carried out using a Netzsch STA 449 F1 instrument. An amount of 20 mg of each CNF sample was fixed in an Al_2O_3 crucible and heated with a constant rate of 20 K min^{-1} from 30°C up to 1200°C in synthetic air atmosphere. When the maximum temperature was reached, the system was maintained in isothermal conditions for 30 min to assure a complete burning of the flammable components. In Figure 4.3, TGA measurements of the CNF samples without and with previous plasma treatment are presented. TGA investigations offer important information regarding the thermal stability, decomposition or combustion onset temperature of the material and the effect of surface functionalization on the combustion temperature of CNF. Untreated CNF are thermally stable in the testing conditions below 650°C and no phase change can be

observed. The combustion of CNF occurs once the 650°C temperature is reached, taking place in one single step and the maximum rate of combustion is achieved at 850°C.

Insignificant weight losses below 150°C are assigned to water evaporation. By further heating up to 1200°C, the fibers are completely burned and the small amount of rest mass (less than 0.1%) corresponds to residual catalytic metal particles from the CNF production process. Plasma treated CNF present a lower combustion temperature in comparison to untreated CNF, around 550°C due to the defects generated during the functionalization treatment by breaking off the carbon double bond (C=C).

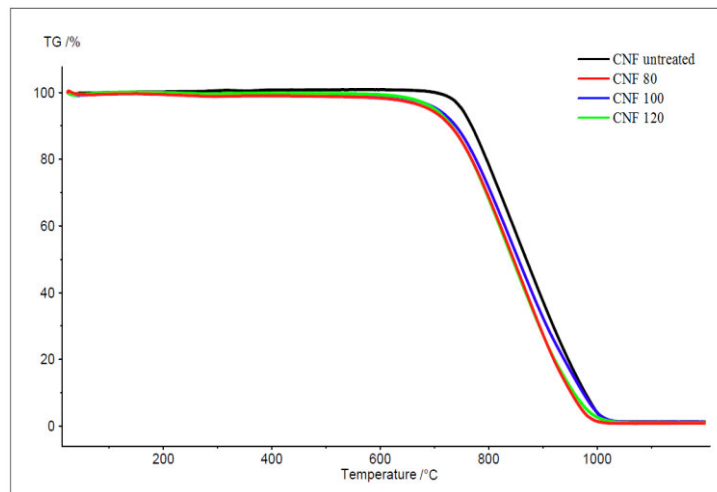


Figure 4.3. TGA measurements on CNF without and with oxygen plasma treatment

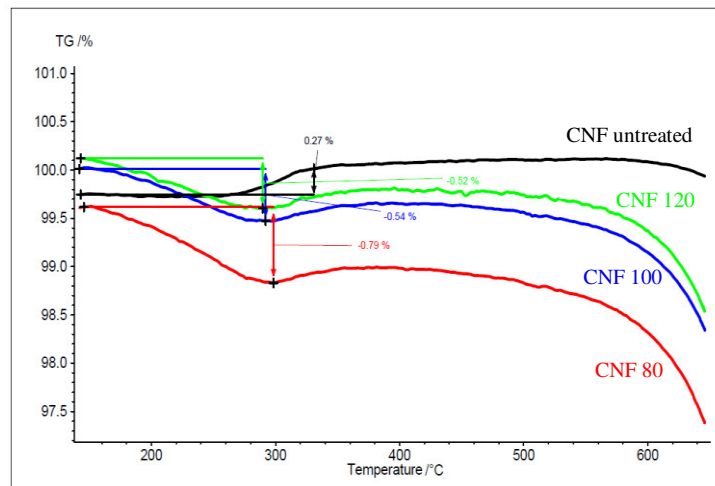


Figure 4.2. TGA measurements on CNF without and with oxygen plasma treatment

Between 150°C and 350°C, a minor weight loss can be observed on TGA curves performed on treated CNF samples (Figure 4.2), which varies in the range of 0.52% - 0.79%, depending on the applied parameters for the functionalization treatment. This mass loss is assigned to decomposition of functional groups formed onto CNF surface. In the case of untreated samples, a slight weight increase (0.27%) appears between 280°C and 340°C, being associated with the oxidation of the CNF surface. Similar behaviour was reported for MWCNT modified with sulphuric and nitric acid [108]. Moreover, defects created on the carbon surface during functionalization due to breaking down the carbon double layer may lead to reduction of thermal decomposition temperature.

The Gas Diffusion Layer (GDL), employed as support material in this study, was a commercial available product (H2315 I2C6 from Freudenberg, Germany). This material is suitable for PEMFC applications due to its porous structure, which assures the electrical conductivity essential for the electrons transfer process, a proper humidity and facilitates the gas diffusion inside the fuel cell. Furthermore, GDL presents a microporous layer, a hydrophobic surface, and a thickness of 250 μm . Characteristics of the material provided by the producer are presented in Table 4.4.

Table 4.4. Properties of the GDL material

Properties	Unit	Values
Thickness	μm	250
Area/weight	g m^{-2}	135
Electrical resistance	Ω	0,7
Contains	Carbon, CB, fluoropolymers	

Moreover, it has been reported [109] that this type of GDL presents a more hydrophilic surface (contact angle $\theta = 84^\circ$) in comparison to other commercial materials and lower surface roughness. The surface morphology of the GDL support material can be observed in Figure 4.4.

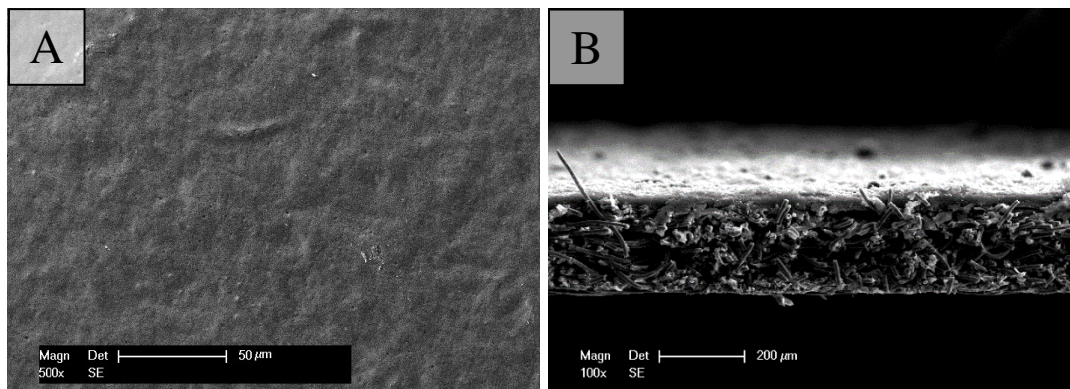


Figure 4.4. SEM micrographs of the GDL: A – surface; B – cross-section

Thermal behaviour of GDL was also investigated, performing TGA measurements in the same working conditions as for the CNF. The results are presented in Figure 4.5.

Unlike the CNF, GDL weight loss proceeds in two steps, the first one, a minor weight loss, around 7%, starts at 500°C and is attributed to the organic compounds and amorphous carbon existent on the material surface [110] and the second one, the main weight loss, around 92.5%, begins at higher temperatures around 650°C, being assigned to carbon combustion from the GDL structure (Figure 4.5). The rest mass of around 0.1% is associated with the non-flammable compounds existent on the GDL surface. Further TGA measurements performed in this study were corrected with the above-mentioned value.

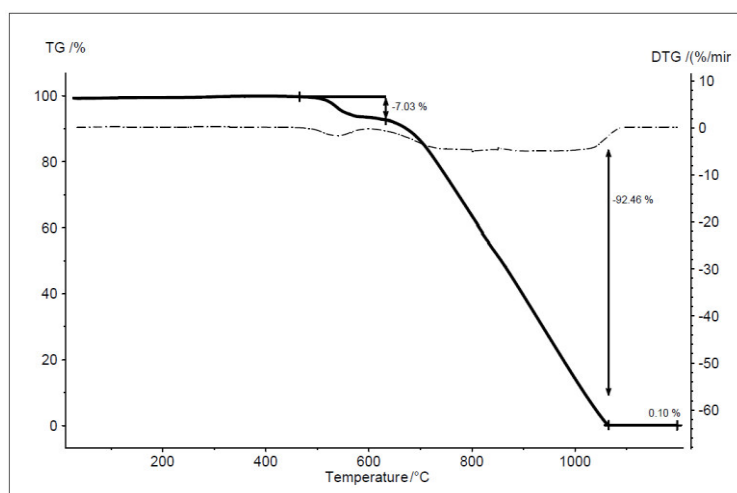


Figure 4.5. TGA measurements of the GDL material

4.1.3 CNF corrosion investigations

After the functionalization treatment, CNF were mixed with a suitable solvent to facilitate the spraying process onto the GDL surface. Several solvents (ethanol, water, isopropanol) have been previously tested in order to achieve a stable and homogeneous CNF ink formulation. The most stable dispersion was found to be the one prepared with isopropanol, which remained settled for a longer time and in addition, the evaporation process of the solvent is shorter, leaving near zero oil traces. Consequently, dispersions with isopropanol were prepared by mixing 5 mg CNF treated with each of the previous mentioned parameters and 50 mL solvent, then ultrasonicated for 20 minutes. The CNF ink was further manually sprayed on the GDL surface (25 cm²) with the aim to obtain a uniform CNF interlayer, with 5 μm thickness and a loading of about 0.2 mg cm⁻². The samples were dried for 15 minutes in oven at 80°C, to remove faster the solvent.

For electrochemical investigations, as well as for catalyst deposition, the GDL electrodes were cut into disks with 15 mm diameter using an automatized cutting machine. Figure 4.6 presents the morphology of the GDL coated with CNF. Realizing an analogy with the surface of the GDL material before applying the CNF interlayer, a

higher available surface area of the support electrode is produced, creating new more available sites for the catalyst deposition.

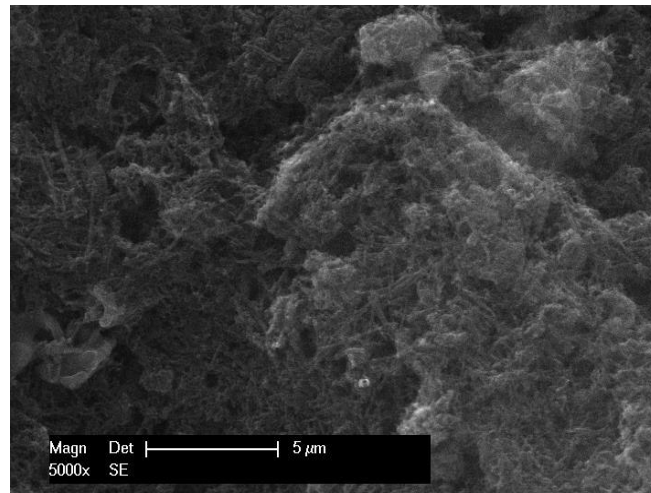


Figure 4.6. SEM micrograph of the CNF surface deposited onto the GDL material

The corrosion resistance of the support material mainly influences catalyst stability and durability. Electrochemical carbon corrosion is a major factor, which contributes to performance mitigation during the fuel cell operation. Furthermore, the carbon degradation leads to significant loss of catalyst particles and consequently, a decrease of catalytic activity of the electrode arises. Carbon black is more susceptible to corrosion than other carbon structures like CNF or CNT. Moreover, it has been shown that corrosion resistance of carbon is strongly related to the graphitic structure. An improved stability can be attributed to a lower amount of defect sites existent on the carbon surface, where the oxidation process occurs [111].

Hence, the obtained structures were further examined in respect to their corrosion behavior by electrochemical polarization in 0.5 M H_2SO_4 solution, in order to investigate the effect of functionalization treatment on the corrosion resistance of the fibers. The polarization curves were plotted using a Potentiostat/Galvanostat Ivium Technologies Vertex, in a three-electrode cell configuration, having as reference electrode a saturated calomel electrode (SCE) and a platinum disk with 1 cm^2 as counter electrode. The working electrode consisted in freshly prepared GDL disks (1 cm^2 exposed surface area) covered with CNF plasma untreated/treated with different parameters. Each measurement was carried out at constant scan rate of 1 mV s^{-1} , in the potential range of -1.0 V to 1.5 V. Polarization curves are presented in Figure 4.7.

The corrosion resistance of the carbon structures depends on several parameters like specific surface area, surface composition, morphology, or porosity [112]. The concentration of oxygen containing groups attached on the CNF outer surface during the plasma functionalization treatment plays an important role regarding the corrosion behaviour of CNF. Hydrophobicity of carbon surface is considered a significant factor, which improves the corrosion resistance of the material [93]. Defect sites created during functionalization treatment can corrode easily and may further cause and promote the oxidation.

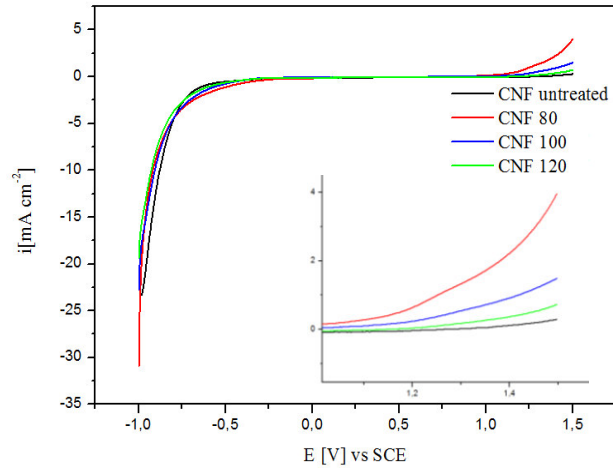


Figure 4.7. Polarization behaviour for GDE prepared with differently activated CNF

As the hydrophobicity of CNF changes during the functionalization treatment, the reactivity of the CNF active surface increases. As it can be observed (inset Figure 4.7), the onset for OER is enhanced for functionalized CNF in comparison to untreated fibers; the highest current density value (at 1.5 V vs. SCE) is achieved for sample CNF 80, which exhibits the most active surface area, as Boehm titration already confirmed it. The increased active surface of CNF after the functionalization treatment can create susceptibility to corrosion especially during the OER, at higher potential values (> 1.5 V vs. SCE) [113].

The corrosion current (i_{corr}) and corrosion potential (E_{corr}) are determined using Tafel slope method applied to the polarisation curves shown in Figure 4.8.

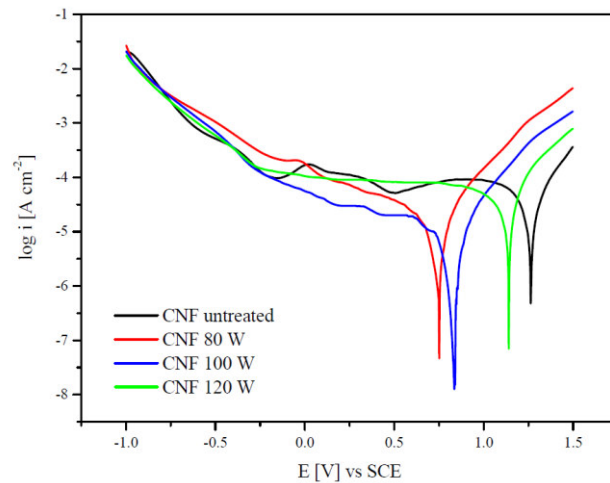


Figure 4.8. Polarization behaviour ($\log i - E$ representation) for corrosion behaviour of CNF differently functionalized samples in 0.5 M H_2SO_4 solution

Functionalized samples exhibit slightly lower corrosion current densities in comparison to the untreated fibers and this fact may be attributed to the presence of oxygen containing groups, which create a protective layer that can prevent the further oxidation of carbon. Moreover, the E_{corr} is shifted to more negative values, since the reactivity of the activated CNF increases. The values of i_{corr} and E_{corr} corresponding to the analyzed samples are presented in Table 4.5. Smaller current density values were found for CNF 80 and CNF 100 samples, being correlated with a higher corrosion resistance of the material.

Table 4.5. Corrosion current and potential for CNF samples

Sample	CNF untreated	CNF 80	CNF 100	CNF 120
i_{corr} [A m^{-2}]	$3.6 \cdot 10^{-5}$	$1.1 \cdot 10^{-5}$	$0.56 \cdot 10^{-5}$	$2.8 \cdot 10^{-5}$
E_{corr} [V/SCE]	1.26	0.74	0.81	1.13

As the corrosion process is always initiated at the defect sites in the carbon structure, the electrochemical degradation of carbon is lowered by a reduced graphitisation degree of the material. A high graphitisation degree assures a defect free crystalline material which is favourable for PEMFC electrodes production [114]. Furthermore, during the functionalization treatment, C=C bonds are broken, giving rise to structural defects. Thus, to investigate the influence of functionalization treatment on the CNF characteristics, XRD measurements have been performed. The measurements were carried out scanning the samples (CNF mixed with Si) under a 2θ angle varying from 20° to 60° with a scan rate of 5° min^{-1} at 45 kV and 40 mA. The graphitization degree (G_p) of the untreated/treated CNF can be calculated from the XRD patterns, using the d (002) value of the interlayer spacing corresponding to the measured sample, according to Eq. 4.2:

$$G_p = \frac{d_{002 \text{ TG}} - d_{002}}{d_{002 \text{ TG}} - d_{002 \text{ HOPG}}} \quad \text{Eq. 4.2}$$

where $d_{002 \text{ HOPG}} = 0.3544 \text{ nm}$ is the interlayer spacing of highly oriented pyrolytic graphite (HOPG), $d_{002 \text{ TG}} = 0.344$ is the interlayer spacing for turbostratic graphite and d_{002} is the interlayer spacing of the measured sample. The XRD patterns are shown in Figure 4.9 and the graphitization degrees calculated from the XRD patterns are presented in Table 4.6.

After the functionalization treatment, all carbon peaks are still visible in the XRD patterns, at same 2θ values as for untreated CNF. The height of the C (002) corresponding peak significantly decreased as the applied functionalization power was higher. This fact may be attributed to the etching character of the plasma treatment when a high power is used, even if the exposure time was reduced. The number of defect sites is considerably increased and the graphitization degree consequently decreased from 99.6% to 78.8%. The smallest change in graphitization degree was observed for CNF 80 (94.8 %), value which is in good agreement with the corrosion resistance evaluation.

Table 4.6. Graphitization degree of CNF before and after the functionalization treatment

Sample	d 002 (sample)	d 002 (Si)	Graphitization degree [%]
CNF untreated	3.361	3.142	99.6
CNF 80	3.364	3.141	94.8
CNF 100	3.356	3.127	87.1
CNF 120	3.368	3.131	78.8

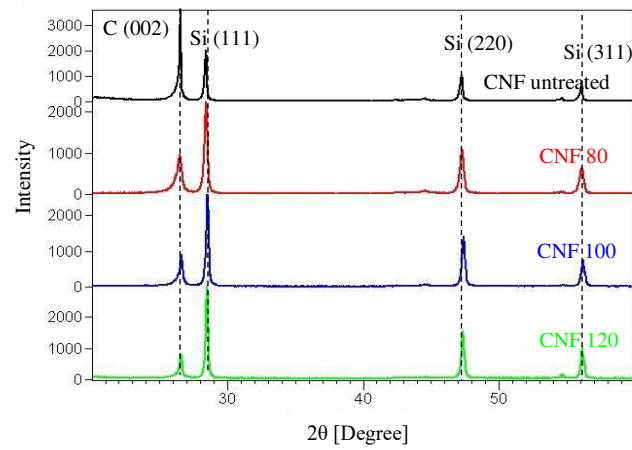


Figure 4.9. XRD patterns of the CNF untreated and treated in oxygen plasma

4.2 Synthesis of platinum based catalysts

Platinum catalyst particles deposition onto support material surface was performed using an electrochemical method. The deposition was carried out with the aid of a Potentiostat/Galvanostat Ivium Technologies Vertex in a three-electrode cell, with a SCE as reference and a platinum disk as counter electrode (Figure 4.10).

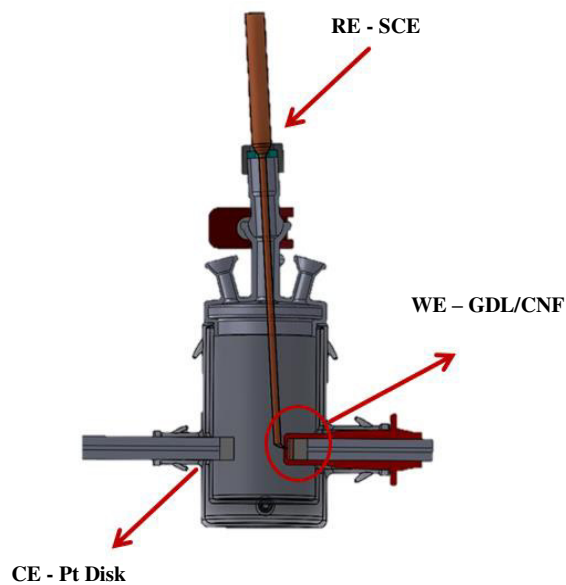


Figure 4.10. Electrochemical cell configuration

The working electrode consisted in GDL samples cut in 15 mm diameter disks covered with CNF without and with previous functionalization treatment, having an exposed surface area of 1 cm².

For platinum electrodeposition process, an acidic solution was developed, containing K₂PtCl₄ as source for platinum ions, KCl which assures an optimum electrical conductivity of the electrolyte and H₃BO₃ for stabilizing the pH value. As during the metal electrodeposition from aqueous solutions, parallel processes can occur, the morphology and structure of the deposit may be strongly influenced. Water electrolysis increases the pH value at the electrode surface, due to the HER effect and hydroxide ions formation. HER affects considerably the nucleation rate of the metal. To avoid pH variation, it is commonly to add boric acid in the electrolyte, to inhibit the hydroxide species formation. The chemicals were dissolved in freshly distilled water without further purification. The concentration of the electrolyte components is presented in Table 4.7.

Table 4.7. Chemical composition of the electrolyte

Electrolyte	K ₂ PtCl ₄ [M]	KCl [M]	H ₃ BO ₃ [M]
Bath 1	0.005	1	0.5

For examining the electrochemical behaviour of the deposition process, for understanding the deposition mechanism and for choosing the optimal deposition parameters, cathodic linear voltammetry and cyclic voltammetry measurements were plotted in the previous described electrolyte, on each of the aforementioned CNF samples. The effect of functionalization treatment of the carbon support material as well as deposition current density, duty cycle and number of cycles on the morphology of the obtained electrodes was additionally studied.

Regarding the linear voltammetry measurements, potential was varied in the cathodic direction, between 0.2 V and -0.7 V vs. SCE, with a constant scan rate of 5 mV s⁻¹. The platinum deposition process from the described electrolyte takes place according to Eq. 4.3. Linear polarization curves shown in Figure 4.11 correspond to platinum deposition process on CNF.

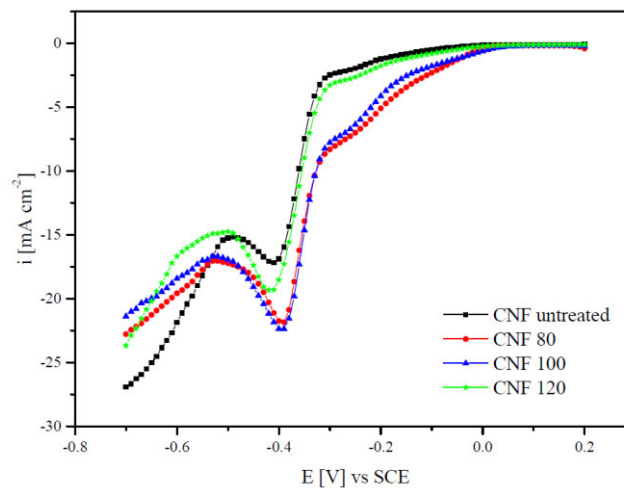
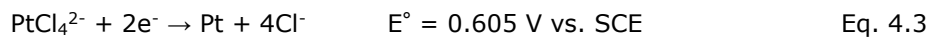


Figure 4.11. Cathodic linear voltammetry measurements for platinum deposition on untreated and treated CNF

For untreated CNF support material, platinum deposition starts when the -0.2 V vs. SCE potential is reached, with a high overpotential. As the scan continues in the negative direction, the Pt (II) reduction reaction proceeds forward and the current density considerably increases. At more negative potential values, around -0.4 V vs. SCE, a limitation of the current density is observed. The current density starts to decrease since the platinum concentration in the diffusion layer is significantly lowered. From that point further, platinum ions diffuse to the working electrode from a higher distance and the current density becomes a function of the platinum diffusion

process. In this region, the diffusion step controls the platinum deposition process. Beyond this peak, when the potential reaches -0.5 V, the current density starts to increase again, the deposition process taking place simultaneously with HER. In this region, the Pt ions concentration at the electrode/electrolyte interface is decreased and HER affects considerably the nucleation rate and the growth of platinum particles.

The hydrogen evolution creates two negative effects on the platinum deposition process. Firstly, the intense formation of hydrogen molecules may destroy the CNF layer, leading to detachment of the fibers from the GDL support and secondly, hydrogen atoms may adsorb on the already deposited platinum particles, blocking the active nucleation sites. Due to these facts, a proper understanding of the platinum deposition mechanism is strongly necessary to choose the right parameters and to overcome the above mentioned inconvenient.

For treated CNF, the shape of the polarization plots remains unchanged, the deposition process is intensified and diffusion limit current densities are higher due to the increased active surface area of the fibers achieved during the functionalization treatment. The functional groups act like an anchor for platinum cations, favouring the nucleation process.

Kinetic parameters for the platinum deposition process were obtained using Tafel equation (Eq.4.4):

$$\eta = \frac{2.3RT}{n(1-\alpha)F} \log \frac{i_0}{i} \quad \text{Eq. 4.4}$$

where η ($E(i)-E(0)$) is the overpotential, (the difference between the actual potential and open circuit potential), R is the ideal gas constant, T is the thermodynamic temperature, n is the number of exchanged electrons (usually $n=1$), $1-\alpha$ is the symmetry factor or cathodic charge transfer coefficient, F is Faraday's constant and i and i_0 are the current density and the exchange current density. Tafel extrapolation plots are shown in Figure 4.12.

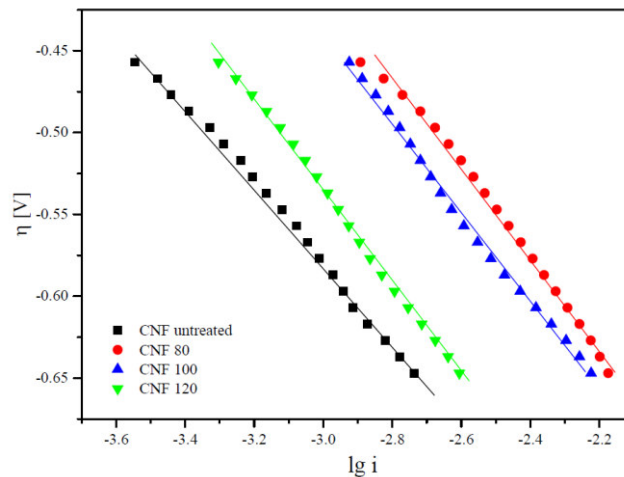


Figure 4.12. Tafel plots for Pt deposition on differently activated CNF

Table 4.8 emphasizes that the exchange current density is significantly increased in the case of plasma treated samples in comparison to those prepared using untreated fibers. A higher exchange current density correlated with a cathodic charge coefficient of 0.22 is obtained for sample CNF 80.

The cathodic charge coefficient $1 - \alpha$ slightly decreased for samples prepared with functionalized CNF since their surface is more active and the reaction plane (inner Helmholtz surface of the double layer) is shifted to the electrolyte solution. Moreover, the activation energy for electrons transfer process decreased [115].

Table 4.8. Tafel parameters for Pt deposition on untreated and treated CNF

Sample	A	B	B [mV dec ⁻¹]	1- α	lg i_0	$i_0 \cdot 10^6$ [A m ⁻²]
CNF untreated	-1.31	-0.244	244	0.24	-5.69	2.04
CNF 80	-1.23	-0.273	273	0.22	-4.51	30.9
CNF 100	-1.25	-0.272	272	0.22	-4.61	24.54
CNF 120	-1.38	-0.283	283	0.21	-4.89	12.88

The influence of the potential scan rate (ν) on the platinum deposition is shown in Figure 4.13. The data reveals that by increasing the sweep scan rate, peak current densities increase and peak potentials are slightly shifted to more negative values [116].

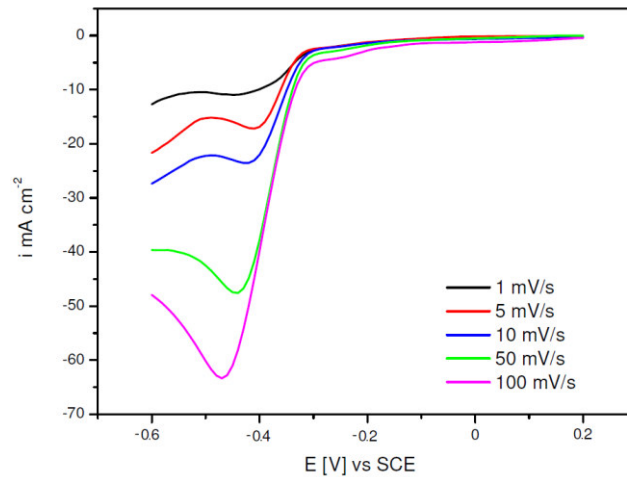


Figure 4.13. The influence of potential scan rate on the platinum deposition process on CNF 80

The relation between the current density peak (i_{pic}) and the square root of the scan rate ($\nu^{1/2}$) is illustrated in Figure 4.14. The linearity of this dependence indicates that the reduction process of the platinum ions occurs in this region under diffusion step control.

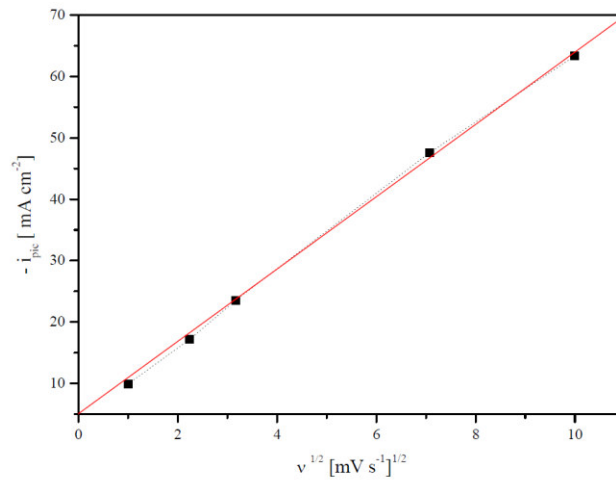


Figure 4.14. Variation of i_{pit} with $v^{1/2}$ for the platinum deposition process

Moreover, the CV measurement carried out on treated CNF (80 W) in the same electrolyte, applying a scan rate of 5 mV s^{-1} (Figure 4.15), shows that by positively sweeping the potential electrode towards 1 V, the oxidation process of the previously adsorbed hydrogen can be observed around -0.25 V vs. SCE.

Further, at more positive potentials, around 0.6 V, the platinum oxidation process takes place. The reduction of the platinum oxide can be noticed on the cathodic branch starting at the same potential value.

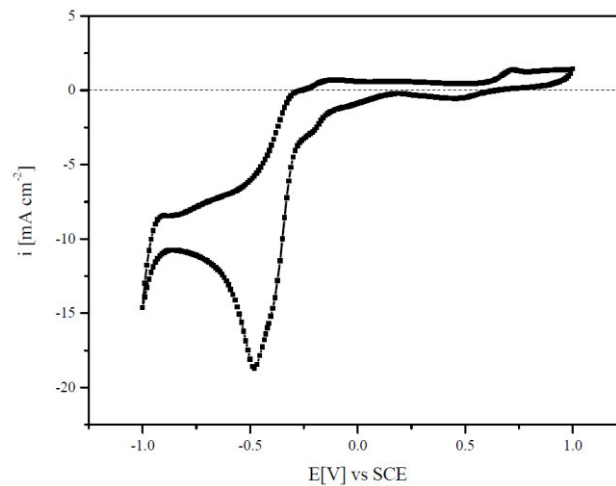


Figure 4.15. CV measurement for Pt deposition process on CNF 80 plasma treated

4.2.1 Pulsed current deposition of Pt nanoparticles on CNF support material

The electrochemical deposition of platinum catalysts was carried out using a pulse plating method. Pulse electrodeposition has many advantages as controlled particle sizes, improved adhesion, and uniform distribution. As the main variables, which describe this type of electrodeposition are t_{on} , t_{off} , and i , this study focused on varying these parameters to obtain the desired characteristics. The properties of the deposit are influenced by t_{on} and i regarding the nucleation and growth of the catalyst particles, meanwhile during the t_{off} , the concentration of metal ions at the interface is replenished and desorption of previously adsorbed ions takes place. Multiple current densities, deposition time t_{on} and t_{off} and number of cycles were changed to control the size and loading degree of the platinum particles, creating also a uniform distribution onto the CNF support. The current density was varied from $i = 25 \text{ mA cm}^{-2}$ to 100 mA cm^{-2} , t_{on} was changed from 1 ms to 50 ms, t_{off} from 5 ms to 100 ms and the number of cycles from 500 to 5000. During the t_{off} , the applied current density was 0. The schematic representation of the applied pulsed form is presented in Figure 4.16.

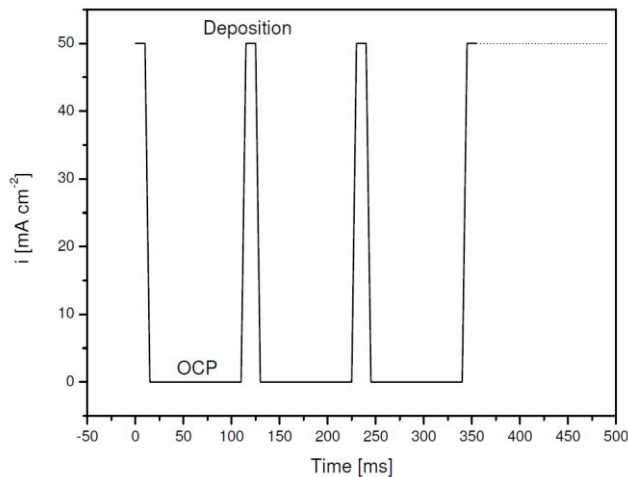


Figure 4.16. Schematic representation of i - t plots for platinum deposition process

The morphology and catalyst particles size and distribution of the obtained electrodes was investigated using SEM. Moreover, after the deposition process of Pt particles onto the CNF surface, the average crystallite sizes were determined by XRD.

A typical SEM micrograph of a Pt decorated CNF electrode, functionalized with 80 W is presented in Figure 4.17. The platinum particles agglomerated in nanoclusters are uniform positioned onto the CNF surface and the size distribution is constant. EDX spectrum confirms the presence of metallic platinum.

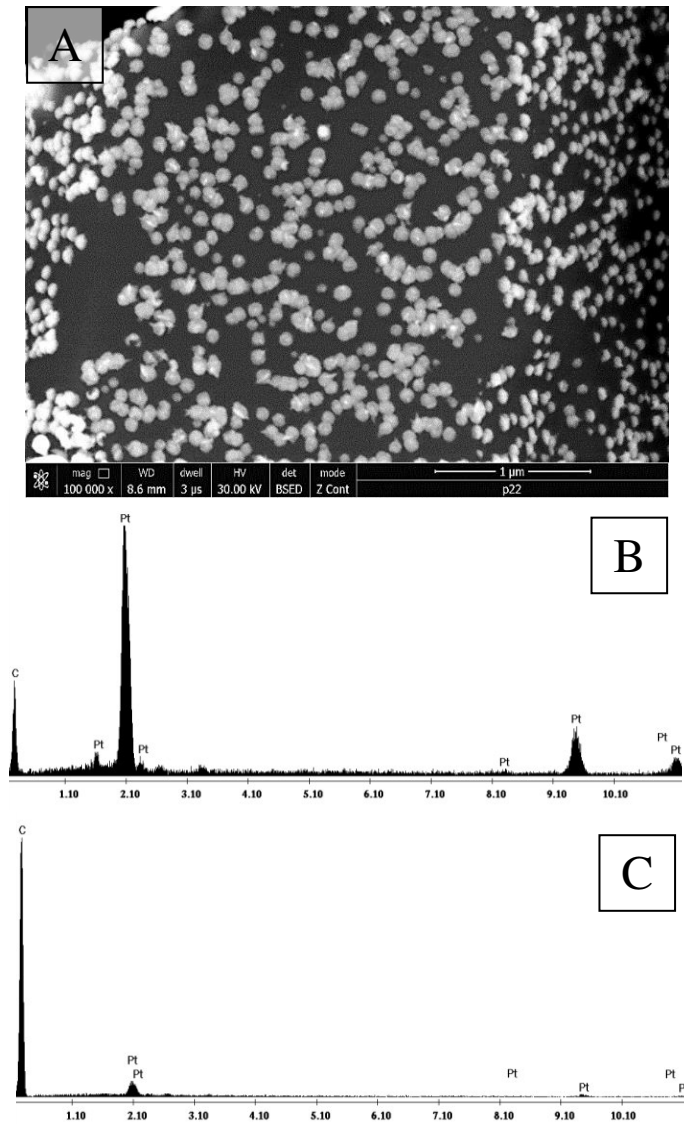


Figure 4.17. – SEM micrograph – A and EDX spectra corresponding to B – the white spots; C – dark grey areas.

The XRD measurements are based on the crystalline or polycrystalline structure of the materials, being conducted with the aid of an X-Ray Diffractometer. Applying this method, it was possible to identify and determine the average crystallite sizes of deposited Pt particles.

The data was acquired by scanning the sample at a 2θ angle in the range of 20° and 100° , with a scan rate of 5° min^{-1} at 45 kV and 40 mA. Figure 4.18 shows a

typical XRD pattern of the GDL material and of the platinum catalyst electrode. Platinum crystalline characteristic peaks are observed on the Pt/CNF XRD pattern.

The average size of platinum crystallites was calculated from the Debye-Scherrer equation (Eq. 4.5), using the full width at half maximum of the Pt (111) reflection.

$$d = 0.9 \frac{\lambda}{B \cos\theta} \quad \text{Eq. 4.5}$$

where d represents the average crystallite size, λ is the X-ray wavelength, B is the broadening at half the maximum intensity and θ denotes the Bragg angle.

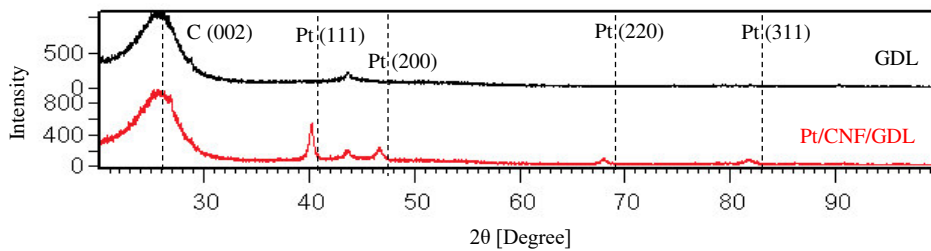


Figure 4.18. XRD patterns for GDL material and CNF decorated with Pt nanoparticles

Furthermore, the amount of deposited catalyst was determined by thermogravimetric measurements, carried out in the same conditions as for CNF (Section 4.1.1). The samples fixed in an Al_2O_3 crucible were heated up to 1200°C in synthetic air atmosphere. The rest mass corresponds to the metallic catalyst particles, after subtracting the residual amount from the GDL material.

4.2.1.1 Influence of the functionalization on the Pt/CNF morphology

A good dispersion of the catalyst particles on the CNF support material is the main condition for attaining an improved electrocatalytic activity. Moreover, small particles are required to create a larger active surface area of the catalyst. Choosing the right deposition parameters, these conditions can be easily fulfilled. It is strongly necessary to correlate the modification of each deposition parameter with a rigorous control of the morphology quality.

For studying the influence of the CNF functionalization treatment on the morphology of platinum catalysts, samples have been prepared using pulsed current plating method, applying a current density of 25 mA cm^2 , t_{on} of 10 ms and t_{off} of 100 ms for 5000 cycles. The SEM micrographs of the obtained electrodes are presented in Figure 4.19. The distribution of the platinum particles was considerably improved during the functionalization process of the CNF. In the case of untreated fibers, the particles tend to agglomerate due to the low surface energy and the poor contact with the electrolyte caused by the hydrophobic character of the CNF surface. Moreover, it can be observed that particle sizes increase when a higher power for functionalization treatment is applied. It can be highlighted that a greater functionalization degree is achieved on the CNF 80, which provides more active sites for platinum particles, furthermore favouring the nucleation rate.

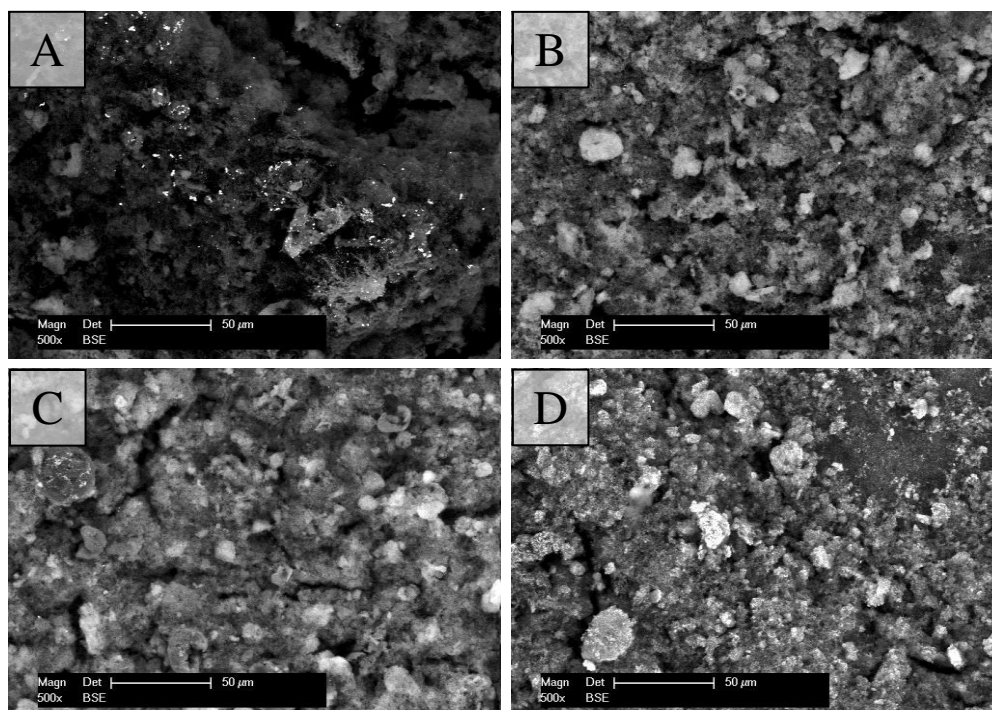


Figure 4.19. SEM micrographs of the CNF without and with plasma treatment decorated with Pt particles: A-CNF untreated, B – CNF 80, C – CNF 100, D – CNF 120

4.2.1.2 Influence of the current density on the Pt/CNF morphology

As a better particle distribution was observed when CNF treated with 80 W and 1800 s are used, further investigations are performed using these functionalization parameters for the support material. CNF decorated with Pt particles by applying different current densities are prepared, in order to detect the optimum values to achieve smaller platinum particles, a higher surface area and an increased sensitivity of the catalyst material.

Four current density values were applied, 25 mA cm^{-2} , 50 mA cm^{-2} , 75 mA cm^{-2} and 100 mA cm^{-2} , the other parameters being maintained constant, as $t_{\text{on}} = 20 \text{ ms}$, $t_{\text{off}} = 100 \text{ ms}$ and number of cycles = 5000. The corresponding SEM micrographs are presented in Figure 4.20.

The current density influences the nucleation rate of the platinum particles. Although, when a high current density value is applied, HER takes place simultaneously with the platinum deposition, affecting considerably the nucleation process. Hydrogen produced during the deposition process adsorbs onto the already deposited platinum sites and moreover can destroy the CNF layer. At low current densities (25 mA cm^{-2}), the diffusion rate is higher than the charge transfer rate and metal ions have enough time to be attached to the existing crystals previously formed. By increasing the deposition current density to 50 mA cm^{-2} , insufficient time is provided for metal ions to diffuse across the electrode surface and to be incorporated in the already formed crystals. Consequently, new small nuclei are formed and the size of the particles is smaller.

By further increase in the deposition current density, surface diffusion becomes the rate-determining step and the limiting current density is achieved. In this region, dendrites start to be formed and crystal growth becomes the dominant process. During this process, the catalyst particles start to grow and due to this fact, the specific surface area is decreased [117]. As the micrographs from Figure 4.20 present, smaller current density (25 mA cm^{-2} and 50 mA cm^{-2}) values lead to small particle sizes correlated with an improved distribution.

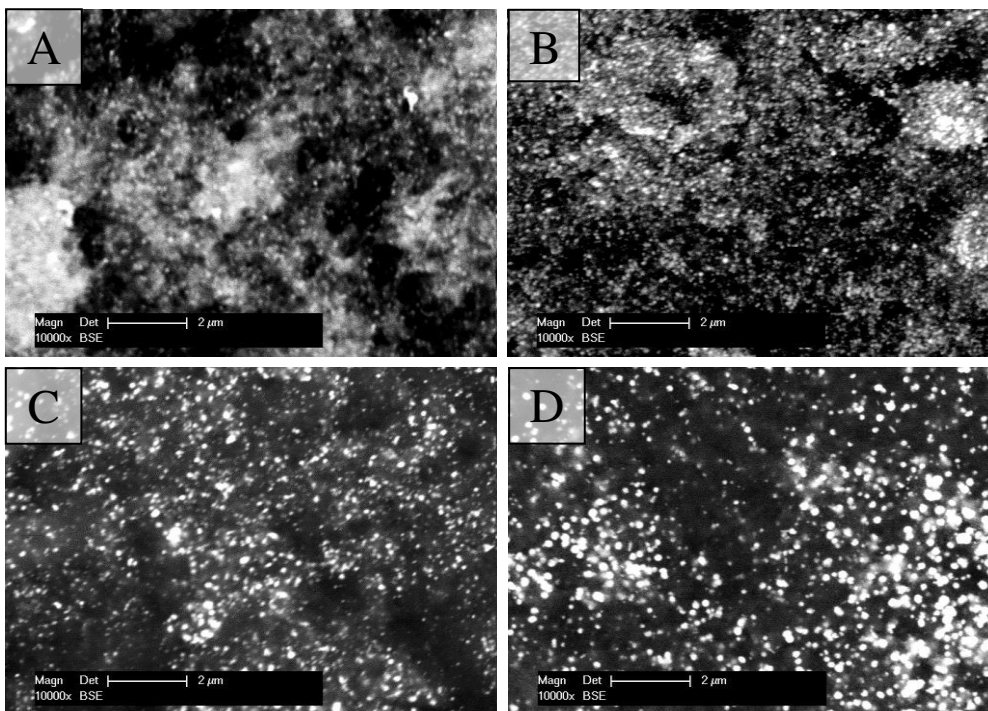


Figure 4.20. SEM micrographs of the CNF decorated with platinum particles at A - $i = 25 \text{ mA cm}^{-2}$, B - $i = 50 \text{ mA cm}^{-2}$, C - $i = 75 \text{ mA cm}^{-2}$, D - $i = 100 \text{ mA cm}^{-2}$

4.2.1.3 Influence of the duty cycle on the Pt/CNF morphology

SEM micrographs presented in Figure 4.21 reveal that duty cycle has an important effect on the platinum loading of the prepared electrodes. The depositions were carried out at constant current density $i = 50 \text{ mA cm}^{-2}$, $t_{\text{off}} = 100 \text{ ms}$ and number of cycles = 5000, varying only the t_{on} from 1 ms to 20 ms. By changing the deposition time (t_{on}), d.c varies from 1% to 17%. Analysing Figure 4.21, it can be observed that the platinum loading raises with the increase of the duty cycle since the corresponding t_{on} is higher, intensifying also the nucleation rate considerably.

The reason why a higher duty cycle leads to decreased particle sizes may be attributed to the fact that during a longer t_{on} period, the amount of hydrogen evolved on the electrode surface increases. The adsorption of hydrogen onto the active growth centres inhibits the crystal growth leading to formation of new active nucleation

sites [118]. Similar studies [119] have shown that by increasing the duty cycle over 25%, the deposited platinum particles tend to agglomerate in clusters. On the other hand, a duty cycle under 10%, correlated with a shorter t_{on} generates an insufficient time for a proper deposition, the nucleation rate is poor and platinum loading is modest.

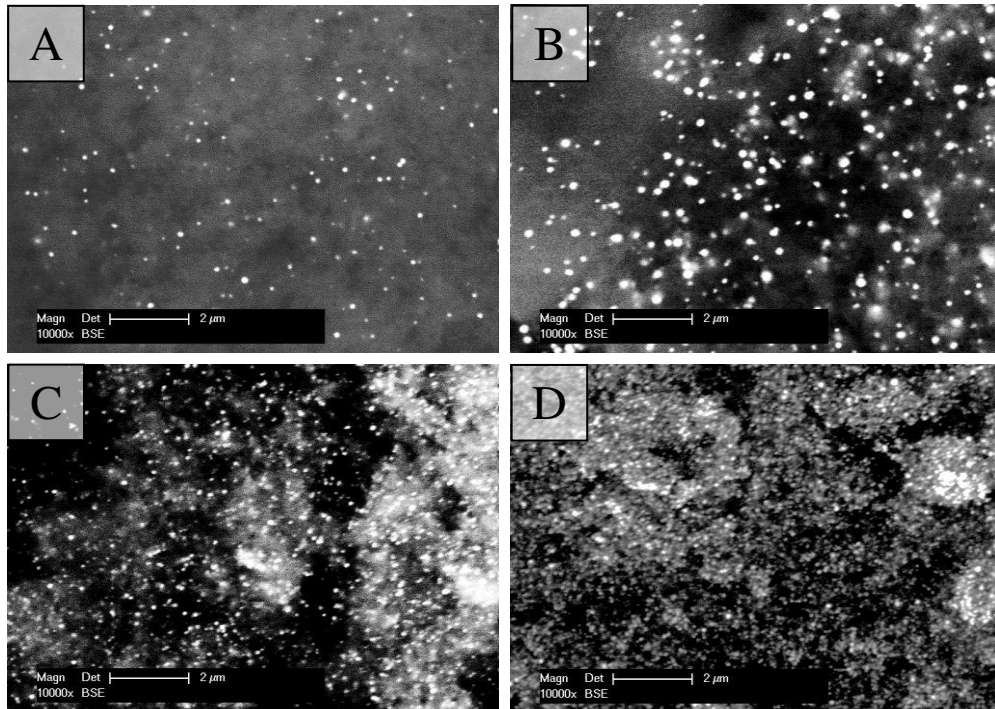


Figure 4.21. Effect of the duty cycle on the morphology of the catalysts deposited with 50 mA cm^{-2} and A - d.c = 1 %, B - d.c = 5 %, C - d.c = 9 %, D - d.c = 17 %

4.2.1.4 Influence of the number of cycles on the Pt/CNF morphology

The number of cycles influences only the platinum loading of the electrodes. To investigate the effect of number of cycles on the morphology of the catalysts, platinum deposition was carried out keeping the current density constant $i = 50 \text{ mA cm}^{-2}$, $t_{on} = 20 \text{ ms}$, $t_{off} = 100 \text{ ms}$, d.c = 17% and by varying the number of cycles from 500 to 5000. As Figure 4.22 presents, the platinum amount deposited on the electrodes surface increases by increasing the number of cycles. The nucleation and growth mechanism is not affected by the changing in the number of cycles and the particles size and distribution remain mostly constant. In some cases, agglomerations of platinum particles have been noticed.

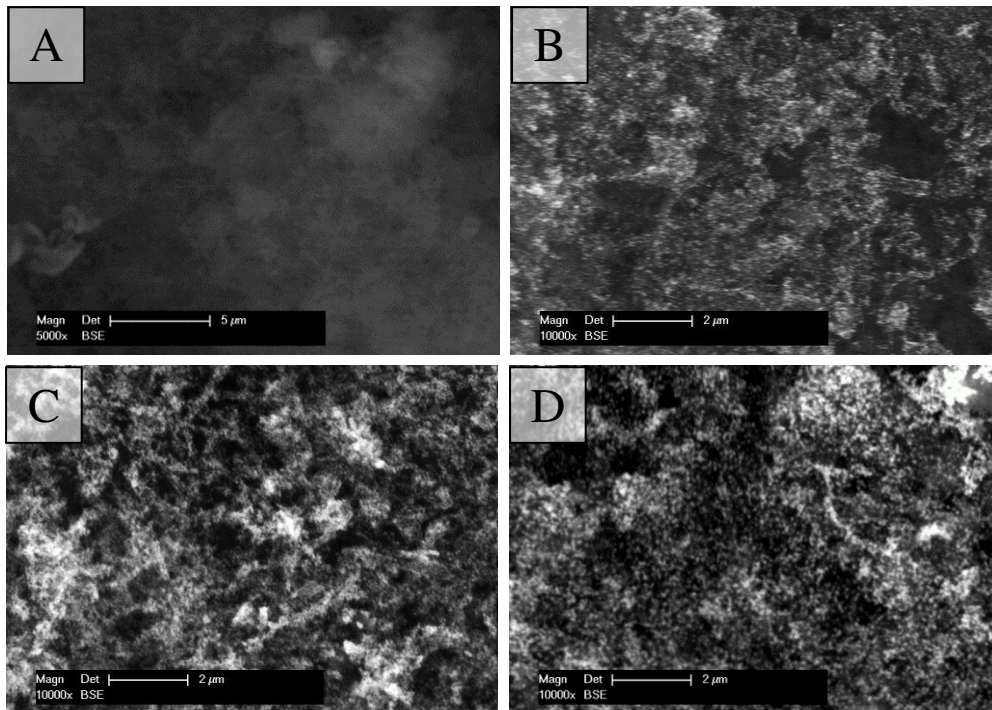


Figure 4.22. Effect of the number of cycles on the morphology and amount of platinum particles: A – CNF without catalyst; B – 500 cycles; C – 1000 cycles; D – 5000 cycles

4.2.2 Characterisation of the obtained platinum catalysts

Four of the previously investigated samples, decorated with platinum particles by applying $i = 50 \text{ mA cm}^{-2}$ deposition current density, duty cycle = 17%, for 5000 cycles, having as support material CNF functionalized with different parameters presented in Table 4.2, were further analysed regarding their, platinum loading, morphology, particle size as well as electrochemical surface area.

TGA measurements were performed on the selected samples in order to investigate the influence of CNF functionalization treatment on the platinum loading of the electrodes. By employing the same deposition parameters, a same amount of platinum catalyst is expected to be found on the electrodes surface.

Figure 4.23 presents the TGA measurements in synthetic air atmosphere for the electrodes obtained using differently functionalized CNF. The samples are stable until 500°C temperature is reached. The decomposition of electrodes takes place in two steps, as described in the previous section. The minor weight loss is assigned to GDL support material. The main weight loss occurs at 600°C associated to the carbon material and the rest mass found at the end of the measurement corresponds to the amount of catalyst particles. A higher amount of platinum loading is detected on samples produced with CNF 80, as they have been proven to have a more reactive surface, due to the presence of a higher number of functional groups. Platinum loading of the investigated samples is presented in Table 4.9. The values are significantly

smaller in comparison to other reported studies regarding similar platinum based catalyst materials for PEMFC applications [120, 121].

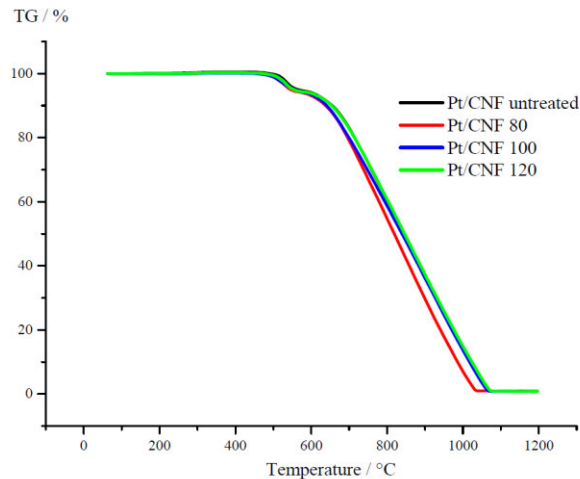


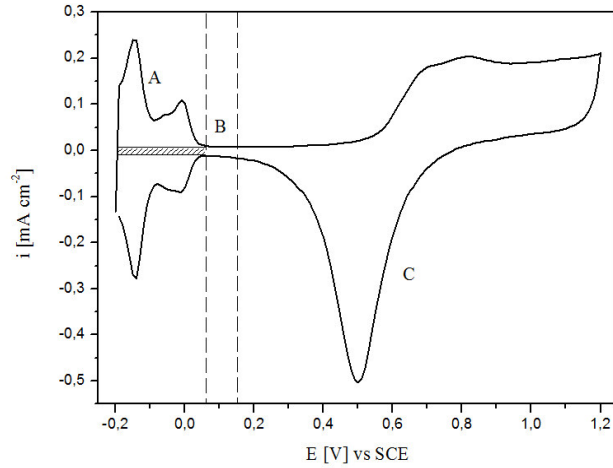
Figure 4.23. TGA measurements on differently functionalized CNF decorated with Pt particles

As one of the most important parameters in surface characterization of solid catalysts is the *ECSA*, CV measurements have been performed on the selected samples in 0.5 M H_2SO_4 solution. This analysis highlights the electrochemical activity of the catalysts associated with the corresponding *ECSA* values. *ECSA* was determined using the CV plots in N_2 saturated 0.5 M H_2SO_4 solution in a potential range of -0.2 V to +0.8 V vs. SCE on the catalyst samples. The measurements are recorded with a constant scan rate of 100 mV s^{-1} for 200 cycles. The *ECSA* values were calculated by integrating the charge related to hydrogen desorption reaction (region A, $i > 0$, Figure 4.24) after the subtraction of double layer capacity contribution.

Figure 4.24 presents a typical cyclic voltammetry curve performed on a polycrystalline platinum disk with 1 cm^2 geometrical surface area, plotted in 0.5 M H_2SO_4 . Region A represents the hydrogen adsorption ($i < 0$) and desorption ($i > 0$) zone, region B corresponds to the double layer capacity, and in region C, the platinum oxidation ($i > 0$) and reduction ($i < 0$) process occur [122].

In region A, the main peaks around -0.15 V and 0 V vs. SCE are assessed to adsorption/desorption of hydrogen on different crystallographic orientation of platinum Pt (110) and Pt (100). Changes in shape, height or width may be due to the presence of different other structures on the platinum surface.

The *ECSA* is calculated in the potential range -0.2 V to 0.1 V vs. SCE, after the double layer capacity subtraction (dashed region). It may be assumed that the platinum surface adsorbs a monoatomic hydrogen layer and the adsorption stoichiometry is 1:1.

Figure 4.24. Typical CV for polycrystalline platinum in 0.5 M H₂SO₄

The charge involved in the hydrogen desorption process is calculated using the following equation (Eq. 4.6):

$$Q_{\text{H}_{\text{des}}} = \int i(t)dt = \frac{1}{\nu} \int i(E)dE \quad \text{Eq. 4.6}$$

where $Q_{\text{H}_{\text{des}}}$ is, the charge related to integration of $i(t)$ for a certain amount of time t , which corresponds to current density value in the potential range, $i(E)$ divided to employed scan rate ν .

The amount of charge for the hydrogen desorption reaction was experimentally determined for three platinum surface structures and is widely used as reference:

- Pt (111) with an atom surface density of $1.5 \cdot 10^{15}$ atoms cm^{-2} , is associated with a charge of $225 \mu\text{C cm}^{-2}$;
- Pt (100) with an atom surface density of $4.6 \cdot 10^{14}$ atoms cm^{-2} , is associated with a charge of $147 \mu\text{C cm}^{-2}$;
- Pt (110) with an atom surface density of $1.5 \cdot 10^{15}$ atoms cm^{-2} , is associated with a charge of $240 \mu\text{C cm}^{-2}$ [122].

For adsorption of a hydrogen monolayer on a polycrystalline platinum surface, the global value for charge is $210 \mu\text{C cm}^{-2}$ (Q_{mono})

Using this value, the ECSA can be calculated using the Eq. 4.7.

$$ECSA = \frac{Q_{\text{H}_{\text{des}}}}{m_{\text{Pt}} \times Q_{\text{mono}}} = \frac{\frac{1}{\nu} \int i(E)dE}{m_{\text{Pt}} \times Q_{\text{mono}}} \quad \text{Eq. 4.7}$$

where $Q_{\text{H}_{\text{des}}}$ is the amount of charge necessary for the hydrogen desorption, calculated from the experimental, Q_{mono} is the amount of charge associated with the adsorption of a hydrogen monolayer on the surface of a polycrystalline platinum electrode ($210 \mu\text{C cm}^{-2}$), $i(E)$ is the current value recorded in the hydrogen desorption region [μA], E is the electrode potential (V vs. SCE), ν is the scan rate (V s^{-1}) and m_{Pt} is platinum amount (g). The CV measurements are performed by sweeping the potential from -0.2 V vs. SCE to 0.8 V vs. SCE with a scan rate of 100 mV s^{-1} .

Analysing Figure 4.25, CV features resemble very much to those obtained for a polycrystalline Pt electrode in the same electrolyte and working conditions (Figure 4.24). Hydrogen adsorption and desorption region appears in the potential range of -0.2 V vs. SCE and 0.1 V vs. SCE and platinum oxidation starts at around 0.6 V vs. SCE. Even if the voltammetric profiles are similar for all studied samples, significant differences in the evolved current densities can be observed.

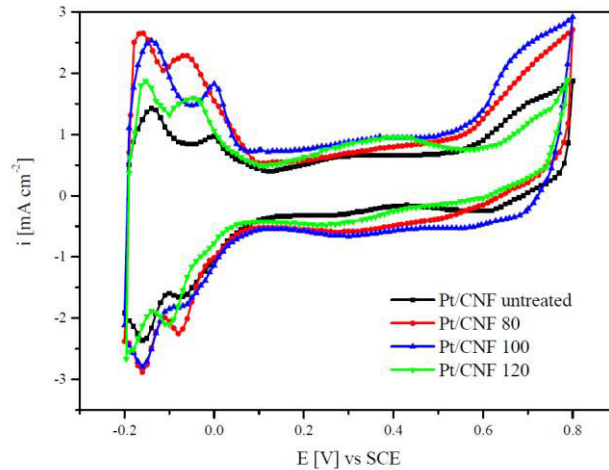


Figure 4.25. CV measurements on differently functionalized CNF decorated with Pt particles

Table 4.9 presents considerable higher *ECSA* for CNF 80 samples in comparison to untreated CNF supported catalysts. Due to the improved particles distribution achieved after functionalization treatment, observed in SEM micrographs (Figure 4.26) correlated with a higher electrochemical surface area obtained for CNF 80 samples, one can affirm that by applying a plasma functionalization treatment (80 W for 1800 s), the *ECSA* and catalytic activity is significantly increased. Moreover, the particles size considerably decreased due to the intensification of nucleation process promoted by the presence of functionalization groups. Making an analogy with the crystallite sizes from XRD measurements, it can be affirmed that particle sizes obtained by *ECSA* method (using Eq. 4.8) are larger. This can be attributed to the fact that platinum particles might be just partially electrochemical active and particles can be composed of more platinum crystallites agglomerated in a nanocluster.

$$d = \frac{6}{\rho \times ECSA} \quad \text{Eq. 4.8}$$

where d is the size of the catalyst particles, ρ denotes the density of the material and *ECSA* is the electrochemical surface area obtained from the CV measurements.

Figure 4.26 presents the morphology of the discussed samples. In comparison to untreated CNF, the functionalized samples present a good platinum distribution and smaller particles, which are directly linked with the increased *ECSA*.

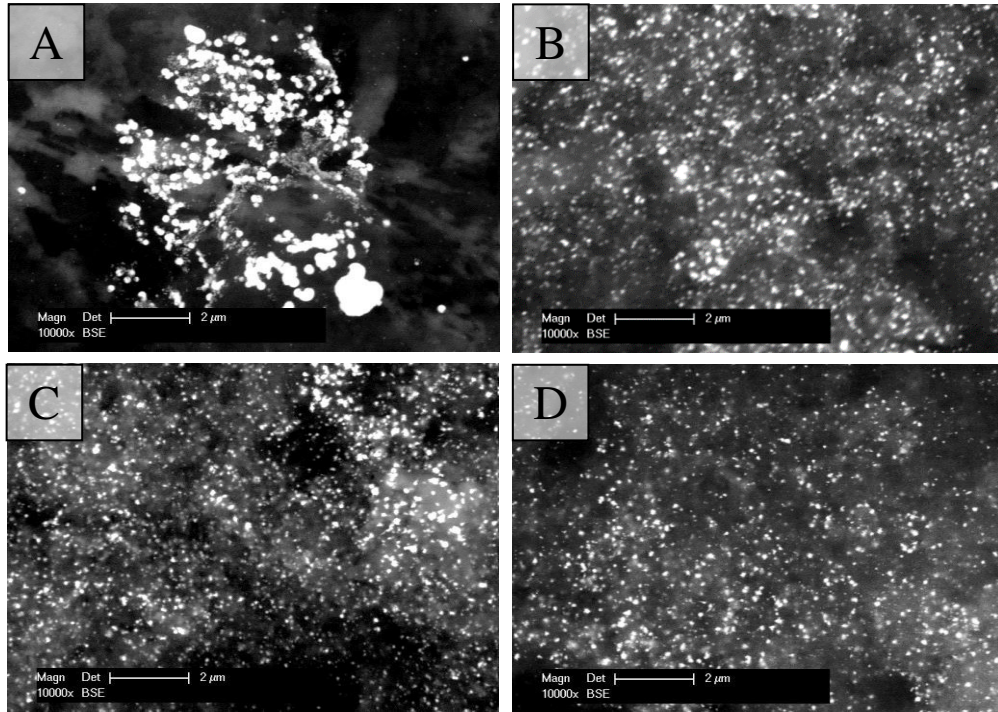


Figure 4.26. SEM micrographs of the CNF without and with plasma treatment decorated with Pt particles: A-CNF untreated, B – CNF 80, C – CNF 100, D – CNF 120

Table 4.9. Pt loading, particle sizes and ECSA of the selected electrodes

Sample	Pt loading [mg]	ECSA [m ² g ⁻¹]	Particle size[nm]	
			ECSA	XRD
CNF untreated	0.157 ± 0.005	3.9 ± 0.3	72	41
CNF 80 W	0.185 ± 0.007	9.1 ± 0.5	31	12
CNF 100 W	0.175 ± 0.003	6.8 ± 0.1	41	21
CNF 120 W	0.167 ± 0.004	4.5 ± 0.2	62	28

Figure 4.27 presents the morphology of the Pt/CNF 80 sample at higher magnifications, obtained by applying 50 mA cm⁻² current density, a duty cycle of 17% for 5000 cycles. The catalyst particles are well dispersed onto the CNF structure, having a uniform size distribution.

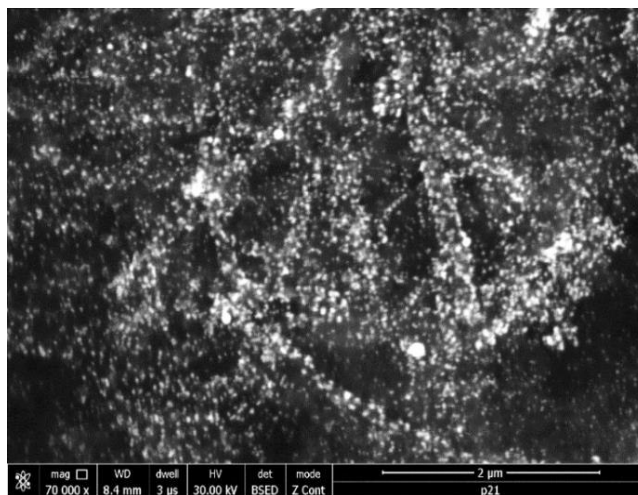


Figure 4.27. SEM micrograph of the Pt/CNF80 electrode obtained by applying 50 mA cm^{-2} deposition current density

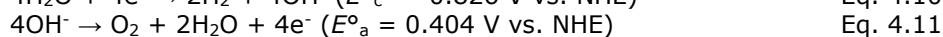
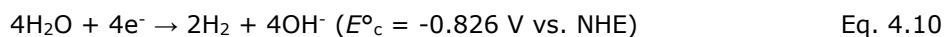
4.2.3 Applications of the Pt/CNF catalysts

4.2.3.1 HER on Pt/CNF electrodes

The HER is worldwide the most studied electrochemical reaction due to its great importance regarding the production of hydrogen using a clean and eco-friendly water splitting process. The overall water electrolysis can be described by the following equation (Eq. 4.9):



The process is composed of hydrogen evolution reaction (HER) on the cathodic side and oxygen evolution reaction (OER) on the anodic side of the electrolyzer. The pH value leads to different reaction mechanisms. Hence, in alkaline solutions (pH=14), the corresponding cathode and anode reactions are presented in Eq. 4.10 – Eq. 4.11:



where E°_{c} and E°_{a} are the equilibrium half-cell potentials at standard conditions.

In acid solutions (pH=0), the reactions are described by Eq. 4.12 and Eq. 4.13:



The catalytic activity for HER of the Pt/CNF electrodes has been investigated in $0.5 \text{ M H}_2\text{SO}_4$ solution (Figure 4.28). The linear cathodic polarization curves are plotted from 0 V vs. SCE to -0.4 V vs. SCE towards the cathodic region with a scan rate of

5 mV s⁻¹. HER in acidic medium can be further split into three reaction steps (Eq. 4.14 - Eq. 4.16):



It is difficult to assess experimentally which of the aforementioned steps dominate the process, particularly when more materials are involved in the system. Smaller Tafel slopes (40-50 mV dec⁻¹) indicate a Volmer-Tafel mechanism, meanwhile higher values (120-130 mV dec⁻¹) are characteristic to a Volmer-Heyrovsky step.

The improved catalytic activity of a material can be manifested by a reduced onset overpotential, particularly at high current densities region, either by changing the reaction mechanism (a different Tafel slope) or by maintaining the same reaction mechanism (same Tafel slope). When the reaction mechanism is changed, the charged transfer coefficient usually decreases, having as result lower overpotentials at higher current densities.

As it can be observed in Figure 4.28, the HER is significantly intensified and the onset potential decreases considerably for Pt/CNF functionalized samples. The HER depolarisation observed in the linear voltammetric plots is influenced by the amount of platinum onto the surface of the electrodes and by the *ECSA* consequently. Beyond the HER onset potential, the cathodic current densities are considerably higher for functionalized CNF based samples at the same overpotential value. Around -0.4 V vs. SCE, the cathodic current density for Pt/CNF 80 reaches much higher current densities than the untreated CNF samples. The enhanced HER activity can be attributed to the increased *ECSA*.

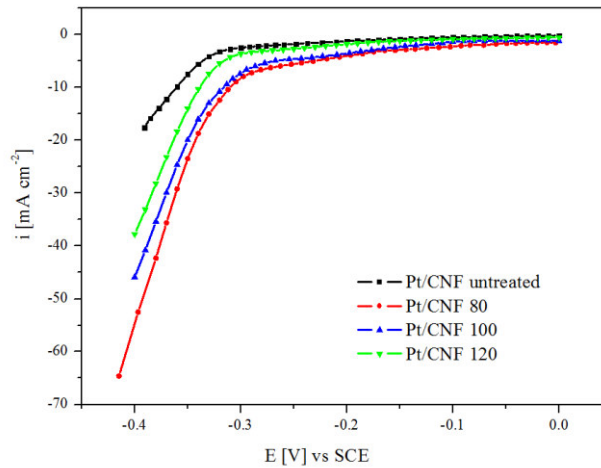


Figure 4.28. HER on selected Pt/CNF catalysts in 0.5 M H₂SO₄ solution

Based on the linear polarization curves, the exchange current densities for HER (*i*₀) are determined by fitting the HER kinetic current densities (*i*) to the Butler-Volmer equation, as a function of overpotential (*η*) [123] (Eq. 4.17):

$$i = i_0 \left[e^{\left(\frac{\alpha F}{RT}\right)\eta} - e^{\left[-\frac{(1-\alpha)F}{RT}\right]\eta} \right] \quad \text{Eq. 4.17}$$

where a is the transfer coefficient, F is Faraday's constant, R is the universal constant of gases, T is the absolute temperature.

Tafel plots, which describe the HER mechanism of the studied electrodes are presented in Figure 4.29. According to Table 4.10, the exchange current density increases considerably, more than 10 higher for samples prepared with plasma treated CNF compared to those prepared using untreated CNF as support. Additionally, comparing the exchange current densities of the treated CNF based samples, it can be observed that by applying a higher power during the functionalization treatment, a decrease in exchange current density values is obtained.

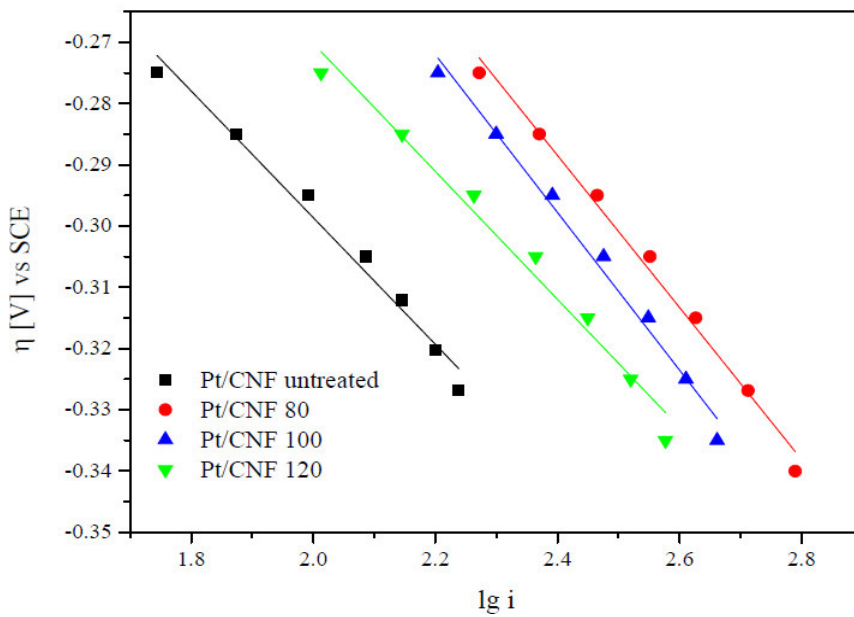


Figure 4.29. Tafel plots for HER in 0.5 M H₂SO₄ solution

Table 4.10 Tafel parameters for HER on untreated and treated CNF in 0.5 H₂SO₄

Sample	$-b$ [mV dec ⁻¹]	$1-a$	i_0 [A m ⁻²]
Pt/CNF untreated	103	0.57	0.13
Pt/CNF 80	135	0.44	1.88
Pt/CNF 100	105	0.56	1.22
Pt/CNF 120	129	0.46	0.26

The charge transfer coefficient, $1-\alpha$ slightly decreases from 0.57 for untreated CNF based electrodes to 0.44 for the sample functionalized with 80 W. As the $1-\alpha$ coefficient represents the fraction of the cathodic overpotential used for the enhancement of the electrode reaction, it can be stated the reaction plan is shifted to the electrolyte solution. This kinetically unfavourable effect is compensated by the exchange current density increase since the surface of CNF functionalized electrodes is more active in comparison to samples produced using untreated CNF. The exchange current density increase due to the high concentration of protons at the interface between electrode material and electrolyte [126].

The obtained kinetic parameters such as exchange current densities and Tafel slopes are in good agreement with the reported values for HER in similar studies on several electrodes [127, 125].

4.2.3.2 In situ PEMFC polarization curves on Pt/CNF catalysts

Plasma functionalized CNF with 80 W for 1800 s were further used as support material for PEMFC electrodes production. The geometry of the electrodes was 45 mm x 45 mm (20.25 cm²). The fibers were mixed with isopropanol and 2.5 wt. % Nafion solution, which was added to improve the binding between CNF and GDL material. The obtained ink was ultrasonicated for 30 minutes and was sprayed onto the GDL (Freudenberg H2315 I2C6) support material. The total loading of the CNF was set to 0.2 mg CNF cm⁻² and the platinum loading was around 0.1 mg Pt cm⁻² for A1, 0.15 mg Pt CNF cm⁻² for A2 and 0.2 mg Pt CNF cm⁻² for A3. The platinum deposition was performed electrochemically, using the previously described method, by varying the deposition current density (25 mA cm⁻² and 50 mA cm⁻²) and number of cycles (5000 and 10000 cycles). The resulted electrodes (Pt/CNF) were positioned onto the anodic side of the fuel cell and Pt/C electrodes with a total platinum loading of 0.35 mg Pt cm⁻² were employed as cathodes. Both electrodes were sprayed with 5 wt. % Nafion solution before the MEA production to improve the proton conductivity and the contact with the Nafion NR 212 membrane (for details see Appendix 3).

MEA was prepared by pressing the anode and cathode on both sides of a Nafion 212 membrane (0.050 mm thickness), assembled between two graphite pole plates designed with serpentine-type gas flow channels, in a single cell test bench, using hydraulic compression (up to 5 bar). Hydraulic compression is a unique feature for PEMFC test systems, which results in ideal operation conditions regarding cell compression and temperature distribution [128]. Hydrogen (99.9% purity) and air were fed to the anode and cathode respectively and the measurements were carried out at room temperature.

Polarisation curves of prepared MEA have been plotted in a PEMFC test bench with using an electronic load type Höcherl & Hackl type ZS1806NV. *U-i*-plots are obtained in constant current mode.

Table 4.11 presents the operation conditions and parameters of the fuel cell. Before recording the polarization curves, the electrodes were preconditioned for 50 minutes at different potential values (0.15 V, 0.4 V, 0.65 V) [129].

Table 4.11. Operation conditions in PEMFC

Parameters	Anode	Cathode
Temperature [°C]	25	25
Pressure [bar]	5	5
Gas Flow [mL min ⁻¹]	500	1000
Pt loading [mg cm ⁻²]	0.1 – 0.2	0.35

Figure 4.30 shows the polarization curves of MEA produced with the developed Pt/CNF electrodes, placed onto the anodic side of the fuel cell, where the HOR takes place. The polarization behavior, ($U-i$ dependence) represents the sum of three important phenomena, which take place during the cell operation: electrode kinetics, ohmic losses, and transport limitations. Typically, the reversible potential of electrochemical reactions in a fuel cell is 1.23 V measured in standard conditions, but the actual voltage of an operational fuel cell is lower than this value due to irreversible losses [121].

The activation polarization loss appears at low current density values and may be caused by slow rates of the electrochemical reactions, which take place at the electrode surface. Moreover, processes like adsorption of reactant species, transfer of electrons across the double layer, desorption of product species can also contribute to the activation polarization.

Ohmic losses may appear due to the resistance of the electrolyte membrane to the flow of protons, resistance of the electrode material to the flow of electrons or resistance which appears between different interfaces. The ohmic losses can be minimized by using either a thinner electrolyte membrane, combined with an optimal humidification, high electrically conductive materials, an improved design of the flow field or by reducing contact resistances at the interfaces [130].

The concentration polarization occurs at high current densities due to the mass transport limitation of the reactants and products from or towards the electroactive regions. The mass transport voltage losses can be mitigated by improving the gas distribution over the electrode surface, employing materials with a higher porosity as GDL and moreover, choosing a right combination of hydrophobic and hydrophilic materials for electrode layer to assure an efficient water removal [131].

It can be noticed that the open circuit voltage (OCV) for the investigated samples is higher than 1.0 V. The highest voltage drop appears at small current densities ($0 - 200 \text{ mA cm}^{-2} \text{ mg}^{-1} \text{ Pt}$) and is associated to activation energy barrier of the electrochemical reactions. The activation polarization loss is higher for sample A1 in comparison to the other studied samples and can be linked to the smaller platinum amount found on this sample. Starting from 0.8 V, the voltage drops nearly linear with increasing load current, according to membrane and electrode resistance. The ohmic drop remains constant for all the investigated samples, since the support material and other significant factors are the same.

Experimental results show a maximum power density of around $400 \text{ mW cm}^{-2} \text{ mg}^{-1} \text{ Pt}$ correlated with a developed current density of $800 \text{ mA cm}^{-2} \text{ mg}^{-1} \text{ Pt}$ achieved at a practical voltage of 0.5 V for anode A3, value comparable to other similar studies [120]. Electrodes A1 and A2 show inferior power and current density values, due to the lower platinum loading found on their surface. The differences can be attributed to the current density value and number of cycles applied during the platinum electrodeposition process, parameters which can provide a higher

catalyst amount and a better distribution when higher values are applied. The obtained power and current density values of the presented polarization curves are corrected with the platinum loading found on each of the investigated samples. It can be noticed that a higher platinum amount deposited onto the CNF support material leads to a 60 % increase in power output, improving the performance of the fuel cell. As the operation temperature inside the fuel cell is low, the gas diffusion and membrane conductivity is reduced, fact which is correlated with a decreased kinetic reaction, aspects which explain the lower current density values obtained for the studied samples in comparison to other reported studies.

Similar studies have presented a power density of $1250 \text{ mW cm}^{-2} \text{ mg}^{-1} \text{ Pt}$ (0.5 V voltage) at 80°C for anodes and cathodes prepared using a precipitation method. In this case, the improved performance is promoted by the increased temperature correlated with the increased specific surface area of the support carbonic material (from $250 \text{ m}^2 \text{ g}^{-1}$ to $1475 \text{ m}^2 \text{ g}^{-1}$) [132].

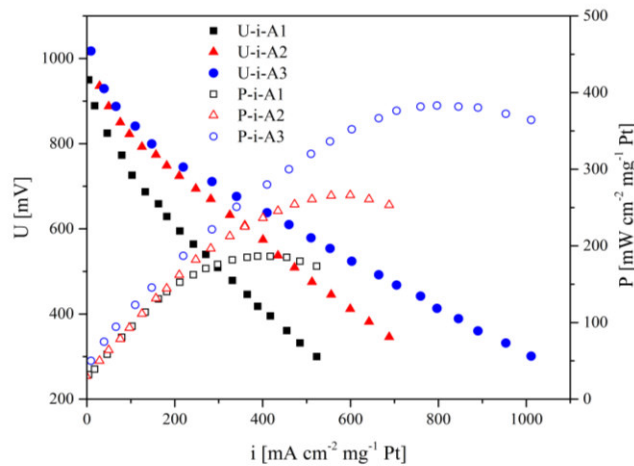


Figure 4.30. Polarization curves of MEA prepared with A1 – Pt/CNF 25 mA cm^{-2} , 10000 cycles; A2 - Pt/CNF 50 mA cm^{-2} , 5000 cycles; A3 - Pt/CNF 50 mA cm^{-2} , 10000 cycles

It has been shown that a higher specific surface area of the support material leads to significant improvement in the cell performance due to the increase in platinum loading and distribution. In the present study, the specific surface area of the investigated CNF is much lower ($115 \text{ m}^2 \text{ g}^{-1}$) in comparison to commercially available most commonly used carbon blacks Vulcan XC-72 ($> 250 \text{ m}^2 \text{ g}^{-1}$), fact which leads to a lower electrochemical surface area of the developed electrodes. Moreover, it was found that the functionalization treatment and the presence of oxygen containing groups contribute to an increase in the hydrophilicity degree of the CNF support, which may affect the water management inside the catalyst layer. The hydrophilic character leads to water absorption, enhancing the possibility of gas diffusion layer flooding. According to other studies [133], comparable behaviour was obtained for functionalized CNF, which showed decreased performance and activity in comparison to untreated CNF based catalysts. In the mentioned study, a maximum power density of $650 \text{ mW cm}^{-2} \text{ mg}^{-1} \text{ Pt}$ (500 mV voltage) at 70°C was obtained for Pt supported CNF catalysts obtained by a modified water-in-oil method.

4.3 Synthesis of platinum - cobalt based catalysts

As in the last period, a significant number of studies [134, 135] have proven that platinum alloyed with different transitional metals like Co, Fe, Cr, Ni, offers more increased catalytic activity towards the oxygen reduction reaction, even superior than pure platinum, the aim of this study is to obtain high surface area electrodes based on cobalt-platinum alloy for improving the activity for OER in alkaline mediums. The enhanced catalytic activity of Pt-Co alloys is attributed to several changes that occur in the electronic structure of platinum and furthermore due to the variations in the Pt-Pt interatomic distances [135].

Starting from platinum based catalysts developed in the previous subchapter, cobalt-platinum catalysts are prepared in a similar way, employing CNF 80 as support material, using the pulsed current plating method.

For studying cobalt deposition kinetics, pure cobalt deposition bath is prepared mixing $\text{CoCl}_2 \cdot 6\text{H}_2\text{O}$ with the same bulk electrolyte used for platinum solution (1 M KCl and 0.5 M H_3BO_3). For deposition of platinum-cobalt alloy, electrolytes containing platinum as well as cobalt cations have been developed, according to Table 4.12, varying the $\text{CoCl}_2 \cdot 6\text{H}_2\text{O}$ concentration and maintaining the same concentration for K_2PtCl_4 .

Table 4.12. Chemical composition of platinum and cobalt electrolytes

Electrolyte	K_2PtCl_4 [M]	$\text{CoCl}_2 \cdot 6 \text{H}_2\text{O}$ [M]
Bath 1	0.005	-
Bath 2	-	0.1
Bath 3	0.005	0.0025
Bath 4	0.005	0.005
Bath 5	0.005	0.025
Bath 6	0.005	0.05
Bath 7	0.005	0.1

By changing the CoCl_2 concentration in the electrolyte, the amount of cobalt in the obtained alloy structure is controlled. The molar ratio between Pt^{2+} and Co^{2+} is varied from 1:0.5 to 1:20, by increasing the cobalt concentration and maintaining the same platinum amount.

Firstly, the individual cobalt deposition is studied, by plotting the linear and cyclic voltammetric curves, from Bath 2, on the same CNF support material, CNF functionalized with oxygen plasma using a power of 80 W for 1800 s. The methodology for preparing the support material for catalyst deposition is presented in the previous chapter.

The linear voltammetry (Figure 4.31) is performed from 0 V vs. SCE towards the cathodic region to -2 V vs. SCE with different scan rates (5 mV s^{-1} , 10 mV s^{-1} and 50 mV s^{-1}) to investigate the Co deposition mechanism. Co deposition process takes place according to Eq. 4.18:



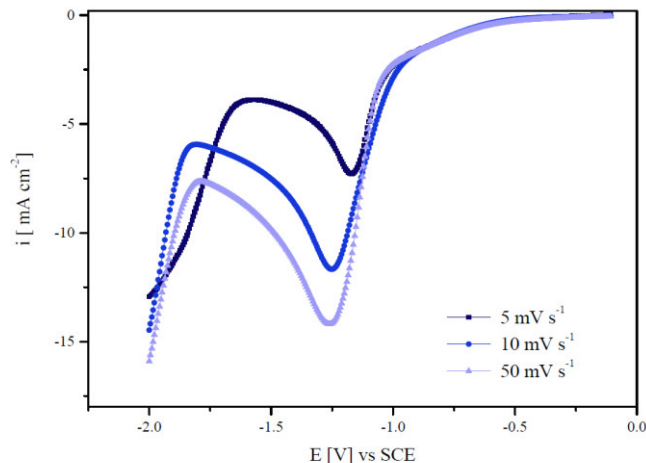


Figure 4.31. Cathodic linear voltammetry measurements for cobalt deposition from Bath 2 at different scan rates

Cobalt electrodeposition process starts around -0.5 V vs. SCE, simultaneously with the HER. When the potential reaches more negative values, (-0.9 V vs. SCE), a sharp increase in the current density value is observed. In this region, cobalt deposition is the predominant reaction, determined by the diffusion step. Around -1.25 V vs. SCE, a limitation in the current density value occurs, being associated with the cobalt reduction peak. A significant increase of the cathodic current is observed at more negative potentials (over 1.75 V vs. SCE), being associated with the proton reduction reaction. By increasing the scan rate, the electrochemical behaviour is similar and the diffusion limiting current density becomes higher. Concludent information is obtained from cyclic voltammograms realized for Pt (Bath 1), Co (Bath 2) and Pt-Co alloy (Bath 3) deposition (Figure 4.32), with 5 mV s^{-1} scan rate, for 10 cycles. The presented plots consist in the 10-th cycle from each of the tested samples. During the cathodic polarization, around -0.5 V vs. SCE, the cobalt deposition process sets in with a low overpotential. As the current density increases, the nucleation process occurs, since it is related to the increase in density of the nuclei and crystal growth. At more pronounced cathodic polarization, HER occurs simultaneously with Co deposition (Co^{2+}/Co , $E^\circ = -0.52$ V vs. SCE). Consequently, in the vicinity of the working electrode, the electrolyte solution is alkalinized, and Co^{2+} cations can precipitate to $\text{Co}(\text{OH})_2$. In these circumstances, Co deposition may occur through $\text{Co}(\text{OH})_2$ reduction ($\text{Co}(\text{OH})_2/\text{Co}$, $E^\circ = -0.97$ V vs. SCE) [136]. At anodic polarization, around -0.5 V vs. SCE, a high peak assigned to cobalt oxidation process can be observed. The same behaviour was previously reported by other studies [137].

The possibility of cobalt passivation can be as well taken into consideration, resulting species like CoOOH that come from CoOH or $\text{Co}(\text{OH})_2$ which could have been previously adsorbed onto the electrode surface [138]. Over $+0.75$ V vs. SCE, the oxygen evolution reaction takes place, simultaneously with the cobalt dissolution.

Platinum deposition starts once the -0.1 V vs. SCE potential is reached, towards the cathodic polarization. At more negative potentials, around -0.25 V vs. SCE, HER takes place simultaneously with the platinum reduction process. At -0.5 V vs. SCE, the current density is limited since the diffusion of Pt^{2+} ions from the bulk of the electrolyte solution to electrode becomes rate determining step. When the potential

is scanned in the anodic direction, around +0.6 V vs. SCE, the current density slightly increases due to the platinum oxidation process.

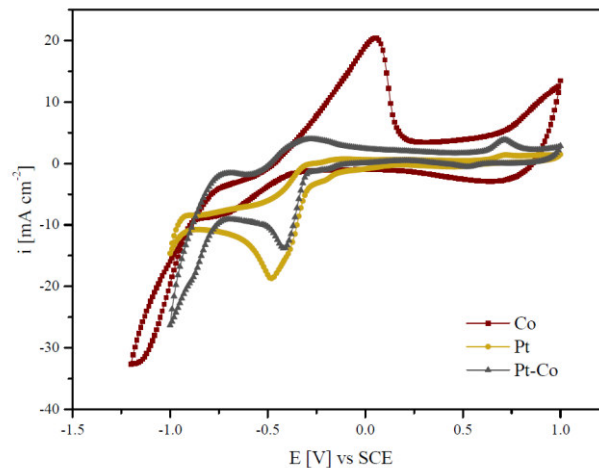


Figure 4.32. Cyclic voltammetry for Co, Pt and Pt-Co deposition process

For Pt and Co codeposition process, HER can be noticed in the cathodic region around 0.9 V vs. SCE, the reaction being catalysed by the freshly deposited platinum and cobalt particles. By scanning the potential in the cathodic direction, the current densities in the diffusion region are smaller in comparison with platinum deposition. The codeposition of Pt and Co is indicated by the presence of both cobalt oxidation peak, around -0.5 V vs. SCE and platinum oxidation around +0.6 V vs. SCE. In addition, CV polarization curves for Pt-Co alloy deposition are performed from different electrolytes prepared by varying the Pt-Co molar ratio in the solution: Pt-Co-1 – Bath 3, Pt-Co-2 – Bath 4, Pt-Co-3 – Bath 5, Pt-Co-4 – Bath 6, Pt-Co-5 – Bath 6, with 10 mV s^{-1} scan rate, for 10 cycles. The presented plots (Figure 4.33) correspond to the last cycle (10-th cycle).

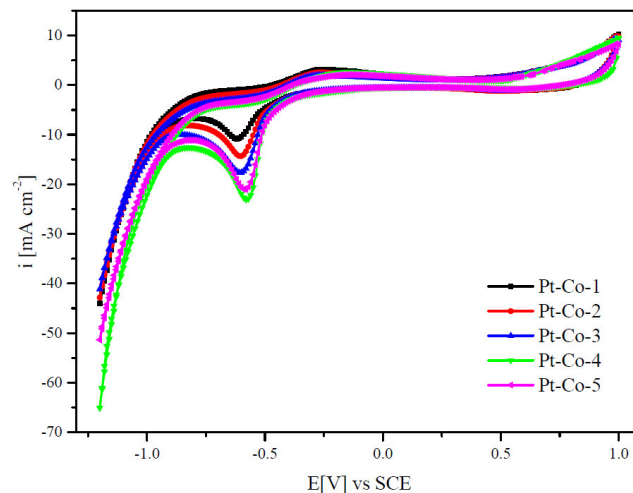


Figure 4.33. CV on CNF electrodes for Pt-Co deposition using different electrolytes

The electrochemical behaviour of cobalt deposition from different electrolytes is similar to the previous described plot; the main difference consists in the diffusion peak of platinum deposition. As a higher amount of Pt-Co alloy is formed on the surface of the working electrode, HER is consequently intensified. The highest cathodic current densities are achieved for the deposition performed from Bath 6, which contains a Pt^{2+} : Co^{2+} molar ratio of 1:10.

4.3.1 Pulsed current deposition of Pt-Co alloy on CNF support material

The electrochemical deposition of Pt-Co alloy catalyst was performed on CNF 80 support material, using the same configuration as described previously for Pt/CNF catalysts. The pulsed current deposition parameters like t_{on} , t_{off} , current density (i) were varied in order to obtain alloy catalyst particles with size distribution in the nanometric range. The choice of applied pulse parameters affects additionally the chemical composition of the deposited alloy. Moreover, five different deposition baths with various cobalt contents were prepared and tested for catalyst deposition.

4.3.1.1 Influence of the bath composition on the Pt-Co/CNF morphology

The deposition of Pt-Co catalysts is carried out from the electrolytes described in Table 4.12, with different Pt-Co ion ratios, in order to identify the proper composition bath which leads to CoPt_2 alloy phase formation. The deposition was made by applying 100 mA cm^{-2} current density, $t_{\text{on}} = 20 \text{ ms}$, d.c - 17%, for 5000 cycles. The morphology of the electrodes presented in Figure 4.34 is similar for all investigated deposition baths. Agglomerations of particles observed on the electrodes surface can be assigned to the irregularities of the CNF layer, as well as the functionalization degree of the support material.

The different chemical compositions of the deposition bath influence the alloy composition. As XRD measurements confirm, by increasing the Co ions concentration in the deposition bath, the Co content in the deposit structure increases, resulting in a higher amount of CoPt_3 alloy. Moreover, a higher concentration of cobalt in the electrolyte determines an increase of the nucleation rate. Consequently, smaller particle sizes are obtained for Pt-Co alloys deposited from the deposition bath with a higher cobalt concentration. The finer grained-structures are also confirmed by the XRD results. Similar behaviour is reported by Saejeng and team [139].

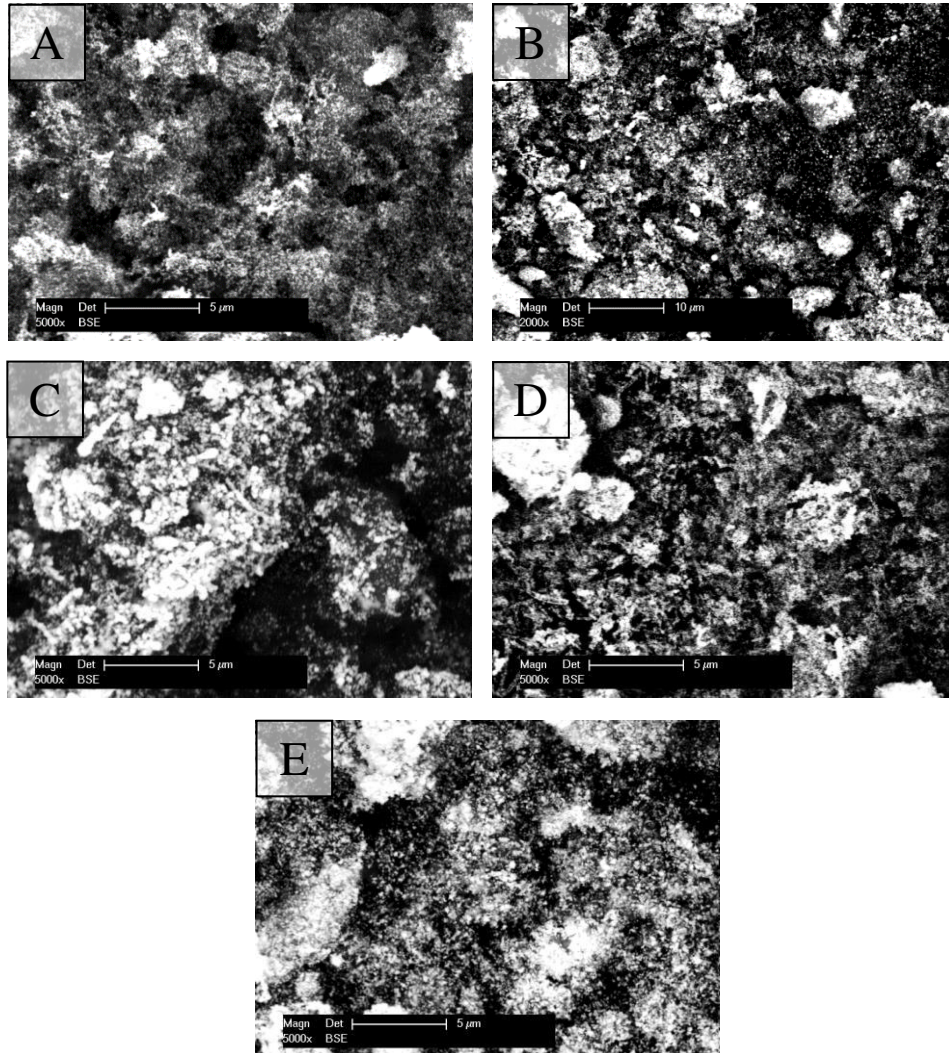


Figure 4.34. SEM micrographs of the Pt-Co catalysts prepared from different electrolytes: A – Bath 3; B - Bath 4; C – Bath 5; D – Bath 6; E – Bath 7

4.3.1.2 Influence of the current density on the Pt-Co/CNF morphology

The influence of the applied current density on morphology and chemical composition of the Pt-Co alloy has been investigated. Figure 4.35 presents the morphology of the Pt-Co catalysts deposited by applying different current densities. Four current densities were applied (50 mA cm^{-2} , 100 mA cm^{-2} , 200 mA cm^{-2} and 300 mA cm^{-2}), maintaining the other parameters constant, like bath deposition (Bath 6), $t_{\text{on}} = 20 \text{ ms}$, d.c = 17%, and number of cycles = 5000. The electrodeposition of Pt-Co alloy using a higher current density takes place under mass transfer limitations for

platinum and the excess current density is used for cobalt deposition, concomitantly with HER. As HER proceeds with a faster rate than cobalt deposition, a higher fraction of excess current is used towards the proton reduction reaction and consequently the composition of the Pt-Co alloys remains constant [140].

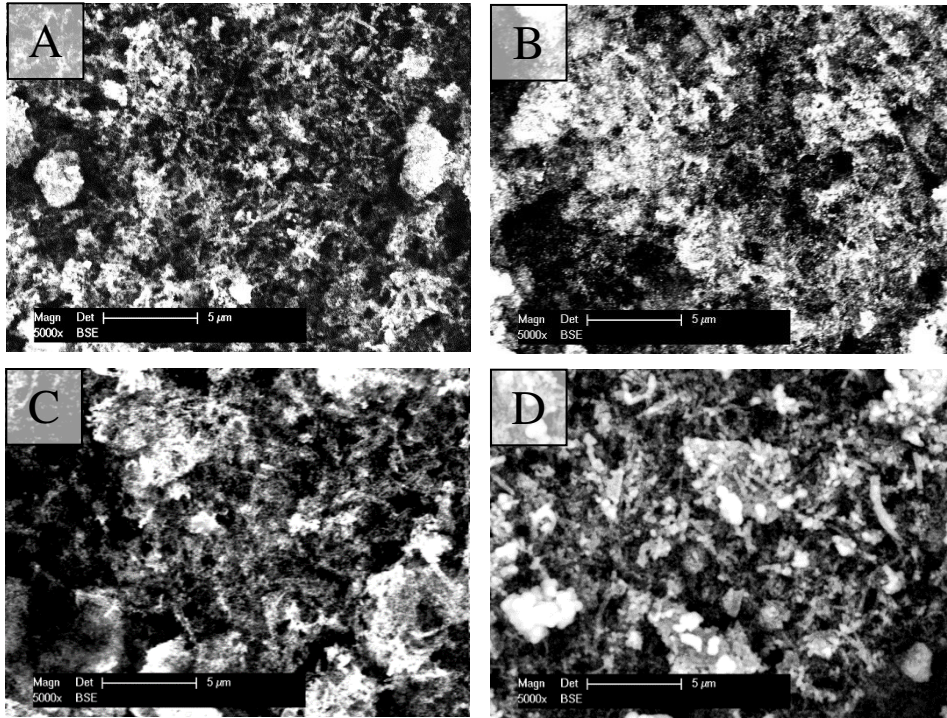


Figure 4.35. SEM micrographs of Pt-Co catalysts deposited using different current densities values A – 50 mA cm^{-2} ; B – 100 mA cm^{-2} ; C – 200 mA cm^{-2} ; D – 300 mA cm^{-2} from Bath 6

It has been reported previously that deposition current density has an insignificant effect on the composition of the Pt-Co alloys. As in the case of platinum catalysts, although the current density affects the nucleation process of the catalyst particles, an increase in the current density over 100 mA cm^{-2} intensifies the HER, favouring the particles growth mechanism by achieving the diffusion limiting current density. It is clearly observed that the Pt-Co alloy catalyst produced with a pulsed current density of 100 mA cm^{-2} consists of very small-grained particles. As can be observed in SEM micrographs (C) and (D), when applying a higher current density, the particles start to grow and dendrites start to form. As an optimum nucleation and size particle is obtained for a deposition conducted with 100 mA cm^{-2} , further depositions and investigations on Pt-Co catalysts are referred to this parameter.

4.3.1.3 Influence of number of cycles on the Pt-Co/CNF morphology

Number of cycles, as it was mentioned in the previous section has a strong influence on the catalyst loading of the electrodes. Figure 4.36 presents the micrographs of the Pt-Co catalysts obtained by applying 500, 1000 and 5000 cycles, using Bath 6, with 100 mA cm^{-2} deposition current density. It is necessary to mention that the alloy amount increases, since the deposition time is higher, according to Faraday's Law. TGA measurements confirm an increase in the amount of the metallic catalyst, proportional with the applied number of cycles. Regarding the morphology and chemical composition, no changes can be observed by increasing the number of applied cycles. The size of the particles remains constant and by increasing the number of cycles to 5000, particles start to agglomerate.

The cyclic voltammetry performed on the Pt-Co samples prepared by applying a different number of cycles highlights an increase in the *ECSA* of the electrodes (Figure 4.37). The shape of the cyclic voltammograms are similar for all studied samples. The higher active surface is obtained for electrode prepared with 5000 cycles associated with $13.5 \text{ m}^2 \text{ g}^{-1}$. The current densities achieve greater values in the hydrogen adsorption/desorption regions and moreover, the oxygen evolution reaction is also promoted.

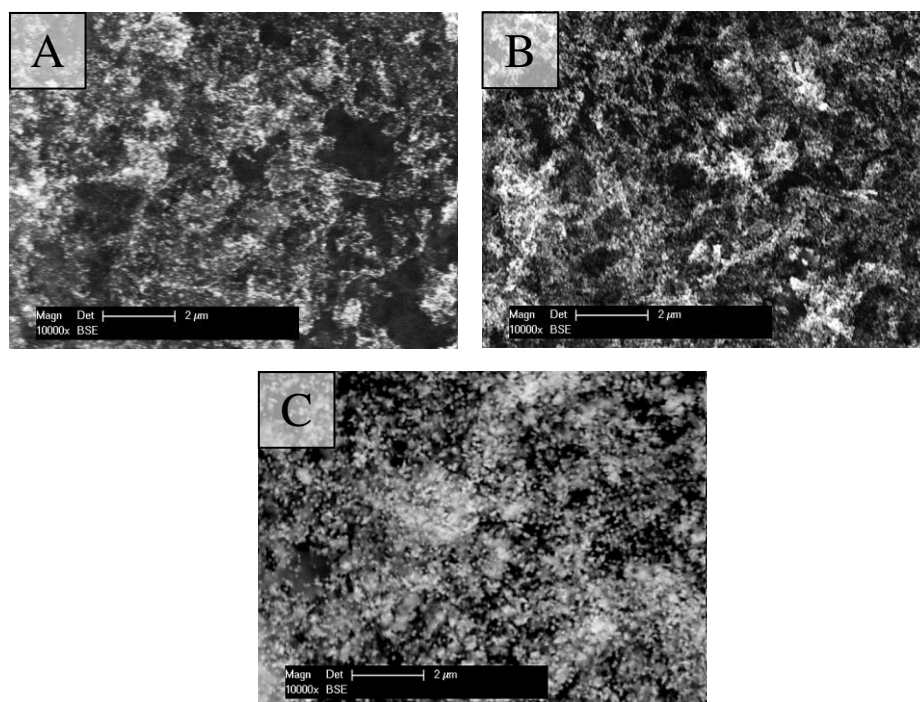


Figure 4.36. SEM micrographs on Pt-Co catalysts deposited from Bath 6, with 100 mA cm^{-2} current density, for A – 500 cycles; B – 1000 cycles; C - 5000 cycles

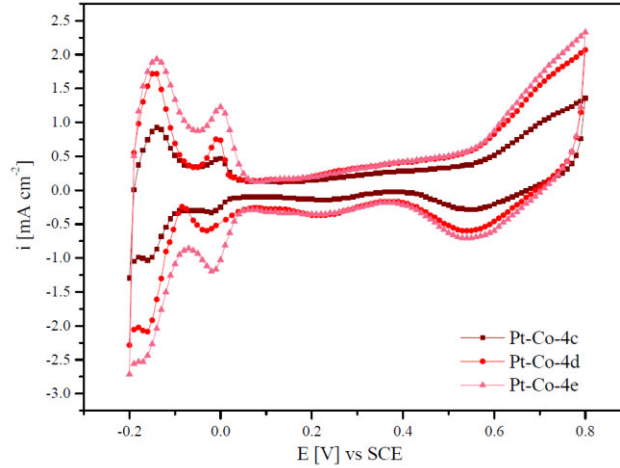


Figure 4.37. CV measurements on Pt-Co catalysts prepared and different cycles:
Pt-Co-4c – 500 cycles, Pt-Co-4c – 1000 cycles, Pt-Co-4c – 5000 cycles

4.3.1.4 Influence of the duty cycle on the Pt-Co/CNF morphology

In pulsed current electrodeposition, beside the applied current density and number of cycles, t_{on} and t_{off} are expected to play an important role. For pulsed current electrodeposition of a single metal, t_{on} and t_{off} are expected to influence only the structure of the catalyst and the nucleation and growth process of the crystals. For pulsed current deposition of a binary alloy, the effect of t_{on} and t_{off} is expected to be more complicated [139]. Beside the structure of the deposit, t_{on} and t_{off} may influence the chemical composition, since during the t_{off} period, the less noble metal can be selectively dissolved from the alloy by the more noble one, through a displacement reaction. In this case, the duration of the applied t_{on} and t_{off} can affect both the Pt-Co alloy catalyst structure and the Pt-Co chemical composition.

As Figure 4.39 presents, larger catalyst particles are obtained by applying a higher duty cycle (by increasing the t_{on} from 10 ms to 20 ms). This aspect can be explained by the fact that the limiting current density may decrease when the duty cycle increase. Since limiting current density is smaller than the applied current density (100 mA cm^{-2}), deposition favours the growth of the particles. When t_{off} is much longer than t_{on} (a lower applied duty cycle) the limiting current density becomes higher than the applied current density and in this case, a higher number of cycles is necessary to achieve the same platinum loading [84]. EDX spectra presented in Figure 4.38 highlight the increase in cobalt content of the Pt-Co alloy by increasing the applied t_{on} .

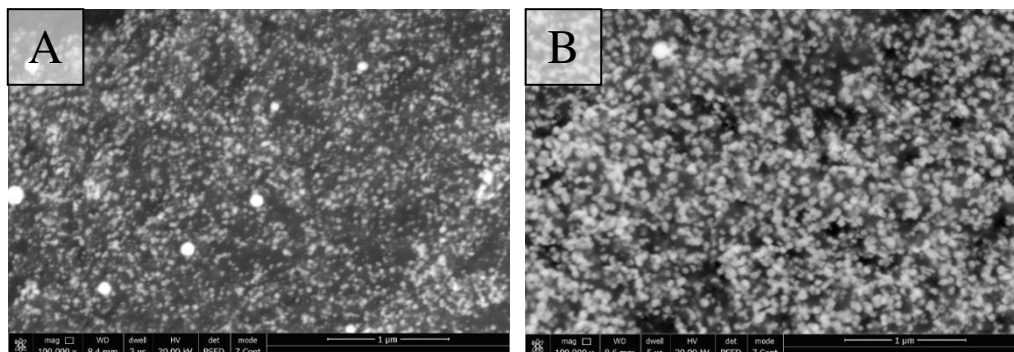


Figure 4.39. SEM micrographs of Pt-Co catalysts prepared with A - $t_{on} = 10$ ms (9 % duty cycle); B - $t_{on} = 20$ ms (17 % duty cycle) from Bath 6, 100 mA cm^{-2} , 5000 cycles

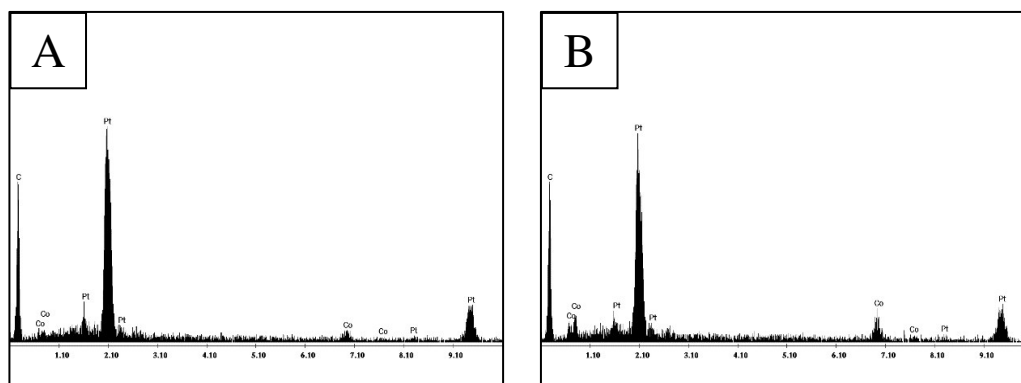


Figure 4.38. EDX spectra of the Pt-Co catalysts prepared with: A - $t_{on} = 10$ ms (9 % duty cycle); B - $t_{on} = 20$ ms (17 % duty cycle) from Bath 6, 100 mA cm^{-2} , 5000 cycles

4.3.2 Characterization of the obtained Pt-Co catalysts

Pt-Co catalysts obtained from deposition baths with different chemical compositions (variation in the Co concentration) are further investigated regarding the alloy phase composition, platinum loading, electrochemical surface area, particle sizes and catalytic activity. The deposition parameters are maintained constant, applied current density $i = 100 \text{ mA cm}^{-2}$, $t_{on} = 20$ ms, d.c = 17%, for 5000 cycles. Co concentration varied from 0.0025 M to 0.1 M and the platinum concentration was kept constant to 0.005 M.

XRD measurements (Figure 4.40) are performed to investigate the structural characteristics, in order to determine the alloy phase composition and moreover to detect the average crystallites sizes of the catalysts. Figure 4.40 shows the XRD patterns of the Pt-Co developed catalysts. The first peak observed on all patterns, at $2\theta = 26.5^\circ$, corresponds to the characteristic carbon peak C (002) from the support material. For all the Pt-Co samples, a single alloy phase - CoPt_3 - was detected, this

being present in different amounts from 45% to 60%, depending on the chemical composition of the deposition bath. Unalloyed platinum is also found on the electrode structure.

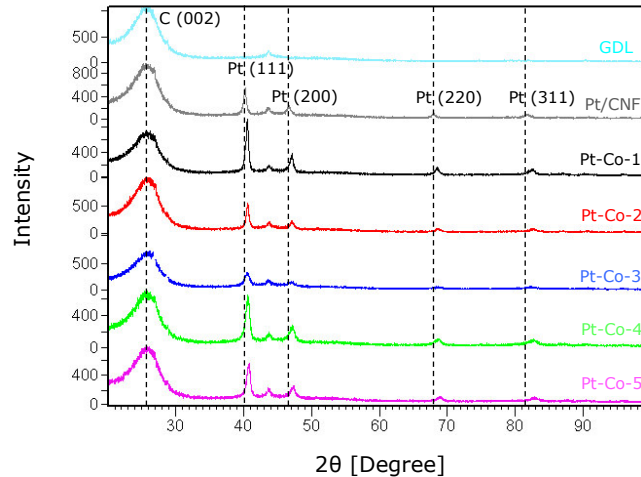


Figure 4.40. XRD of selected Pt-Co electrodes

The diffraction patterns of CoPt_3 alloy phase and pure Pt are very similar and no additional peaks are observed. No extra peaks for pure cobalt have been identified on the diffraction patterns of the studied electrodes. The characteristic peaks for Pt-Co alloy are slightly shifted to higher angles in comparison with pure Pt diffraction peaks, this aspect indicates a contraction in the lattice constant and a high alloying degree through incorporation of smaller cobalt atoms in the platinum structure [140]. The findings are in good agreement with those reported by other authors [135, 141].

Previous studies have revealed that by decreasing the Pt-Pt bond length, the binding energy is reduced and the catalytic activity is considerably increased [142]. In the Pt-Co alloy structure no pure cobalt could be identified, which implies that all the cobalt atoms are incorporated in the platinum structure, forming the CoPt_3 alloy. Moreover, due to incorporation of smaller cobalt atoms in the Pt lattice led to a decrease of the corresponding average crystallites sizes, estimated using Debye-Scherrer equation (listed in Table 4.13) in comparison to Pt/CNF samples.

The thermogravimetric measurements carried on Pt-Co catalyst samples are shown in Figure 4.41. When a temperature of 500°C is reached, a slight mass loss can be observed, the process being assigned to the combustion of organic compounds related to GDL material. The main mass loss corresponds to the burning process of the carbon from support material (CNF and GDL) and rest mass represents the Pt-Co alloy previously deposited onto the support material surface. The possibility of Pt-Co alloy oxidation may cause a deviation in weight percent. The amount of Pt-Co alloy is strongly influenced by deposition parameters, as well as by the amount of CNF and their functionalization degree.

Figure 4.42 shows the CV polarisation curves in $0.5\text{ M H}_2\text{SO}_4$ for the Pt-Co samples obtained from different deposition baths. Similar to pure platinum disk, two adsorption peaks can be identified at a potential value of 0.15 V (Pt 110) and 0 V (Pt

100), as well as an oxidation/reduction peak around 0.5 V. No peak for cobalt oxidation can be observed. It can be remarked that sample Pt-Co-4 presents the highest current density values, which lead to higher ECSA. The increased ECSA value is attributed to a higher percent of CoPt_3 alloy formed due to the higher available Co amount in the deposition bath. An estimation of the deposited catalyst particles size was realized, similar as for the Pt/CNF catalysts, using Eq. 4.8 presented in the previous subchapter.

As in the case of Pt/CNF samples, the particles size values obtained through this method are larger compared to those obtained through XRD method, as particles are composed of more agglomerated crystallites and the catalyst surface might be partially active for the electrochemical reactions.

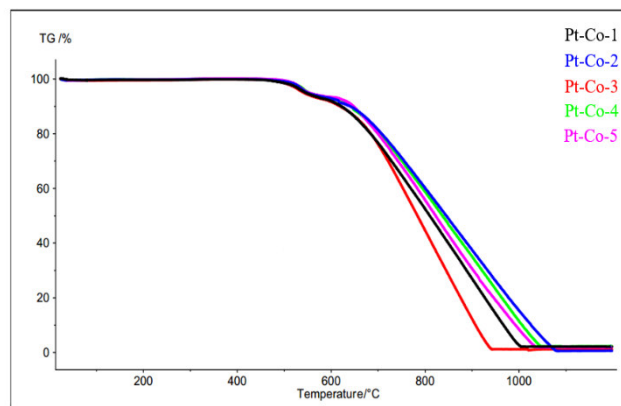


Figure 4.41. TGA measurements on Pt-Co catalysts prepared using deposition baths with different chemical compositions

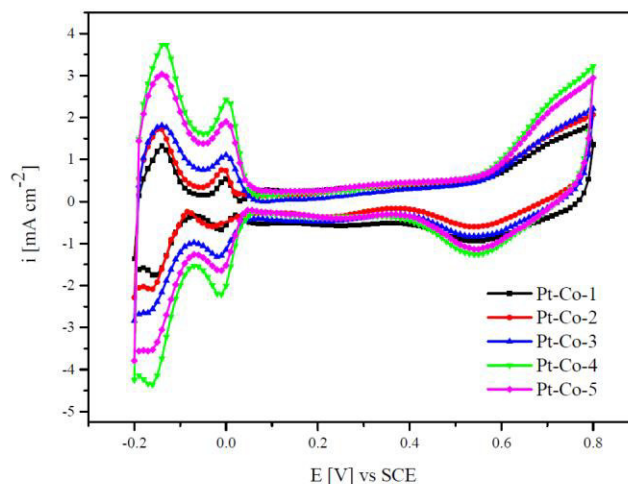


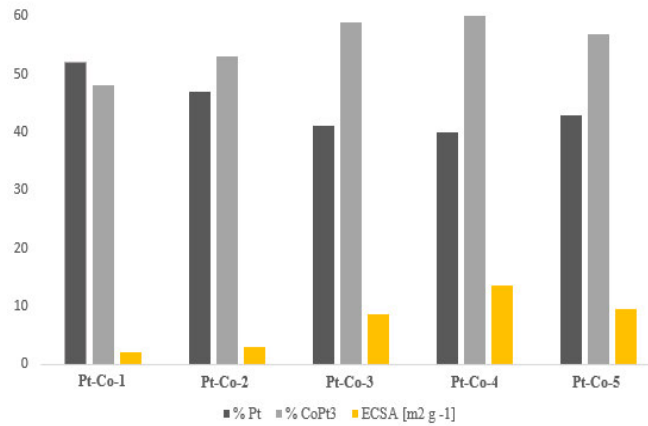
Figure 4.42. CV measurements on Pt-Co decorated CNF using different composition baths: Pt-Co-1 (Bath 1); Pt-Co-2 (Bath 2); Pt-Co-3 (Bath 3); Pt-Co-4 (Bath 4); Pt-Co-5 (Bath 5) deposited with 100 mA cm^{-2} for 5000 cycles

Table 4.13 presents the Pt-Co ratio in the alloy, catalyst loading and *ECSA* of the studied electrodes. Likewise, Figure 4.43 illustrates the differences in the chemical composition of Pt-Co /CNF samples as well as the corresponding *ECSA* calculated from the CV polarisation curves. Although the Co concentration in the deposition electrolyte was higher than the Pt concentration (in all the studied cases), nobler metal (Pt) tends to deposit faster. This aspect explains the higher amount of platinum as well as the rich Pt alloy phase found on all the investigated samples. An increased *ECSA* is observed when a higher CoPt_3 alloy is formed.

Table 4.13. Pt-Co ratio, rest mass and *ECSA* of the Pt-Co electrodes

Sample	Pt-Co ratio [%]				Rest mass [mg]	<i>ECSA</i> [$\text{m}^2 \text{g}^{-1}$]	Particles size [nm]	
	XRF		XRD				XRD	<i>ECSA</i>
	Pt	Co	Pt	Co				
Pt-Co-1	72	28	88	12	0.28	2.1	50	130
Pt-Co-2	69	31	87	13	0.23	2.9	32	96
Pt-Co-3	65	35	85	15	0.21	8.6	13	32
Pt-Co-4	61	39	84	16	0.18	13.5	12	20
Pt-Co-5	62	38	86	14	0.20	9.6	19	30

Figure 4.44 presents the SEM micrograph of a Pt-Co/CNF electrode produced with optimised deposition parameters, from Bath 6, 100 mA cm^{-2} current density, 5000 cycles. The alloy particles are well distributed onto the CNF surface and the size distribution is uniform.

Figure 4.43. *ECSA*, CoPt_3 % and Pt% of the studied Pt-Co catalysts

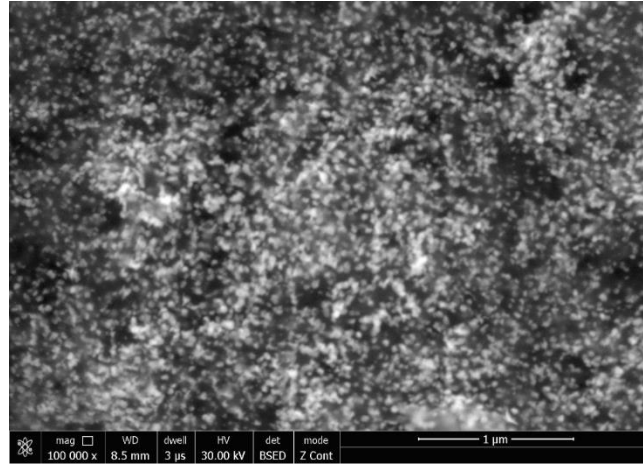


Figure 4.44. SEM micrograph of the Pt-Co catalyst deposited with the optimized parameters

To further understand the structure of the Pt-Co/CNF catalyst material as well as the alloying degree of the elements, Energy Dispersive X-Ray spectroscopy (EDX) mapping was used to collect the elemental composition and distribution and certain position of Pt and Co in the alloy structure. A representative EDX mapping, presented in Figure 4.45, reveals a high alloying degree of the obtained Pt-Co catalyst. Both elements are evenly distributed throughout the electrode surface and platinum presents a higher content in comparison to cobalt.

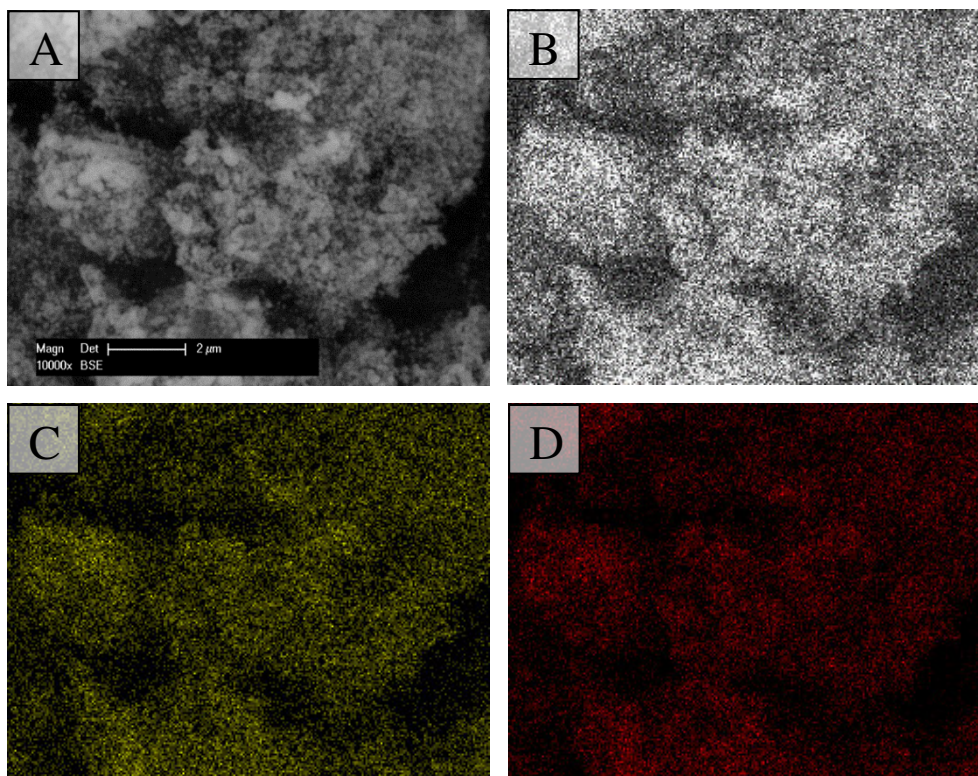


Figure 4.45. EDX mapping of the Pt-Co electrode obtained from Bath 6 (A-SEM micrograph; B-Pt-Co alloy; C-Pt; D-Co)

4.3.3 Applications of the Pt-Co/CNF catalysts

4.3.3.1 OER on Pt-Co/CNF electrodes

Finding a catalyst that is both stable and active for OER, has represented a major research focus in electrocatalysts. Although Pt is nearly ideal for ORR, it has shown poor OER activity. The lower rates have been attributed to reduced surface area and formation of a low electric conductivity PtO_x layer that resists to current flow under the normal OER conditions. These aspects may be overcome by using a bifunctional catalyst consisting of conventional Pt particles used for ORR and Co particles. As the most common electrolyser systems operate in alkaline mediums, the electrochemical activity for the OER of the selected Pt-Co electrodes is investigated in alkaline solution. OER is slower in the acidic medium due to catalyst surface oxidation and Co lower stability.

The evaluation of the catalytic properties of the developed electrodes is performed by linear sweep voltammetry in 1 M NaOH solution, by scanning the potential from 0 V vs. SCE to 0.7 V vs. SCE in the anodic direction with a scan rate of 5 mV s^{-1} . The obtained polarisation curves are shown in Figure 4.46.

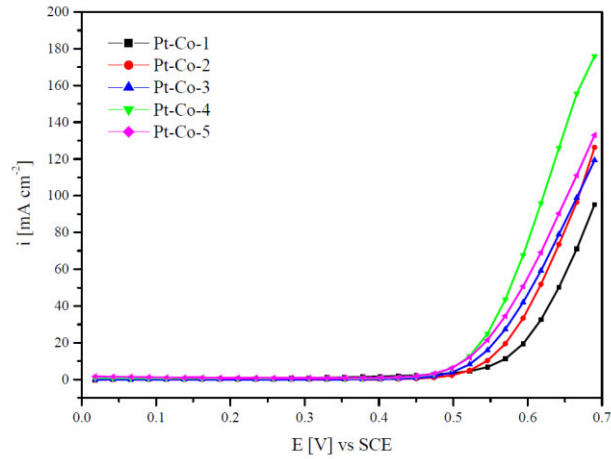


Figure 4.46. Linear voltammetry for OER in 1 M NaOH solution on selected Pt-Co electrodes

In addition, Tafel slopes, charge transfer coefficient and exchange current density were obtained from the Tafel plots presented in Figure 4.47. The corresponding values are shown in Table 4.14. Pt-Co 1 shows a sluggish OER process with an onset potential around 0.55 V vs. SCE and a Tafel slope of 137 mV dec^{-1} in comparison to other samples. The Pt-Co-4 exhibits the lowest onset potential, developing the highest current densities. The kinetics of the OER, on the studied electrodes are characterized by a Tafel slope in the range of 137 mV dec^{-1} to 227 mV dec^{-1} . Similar studies conducted on Pt-Co supported electrodes in alkaline aqueous solutions [143] revealed a comparable behaviour.

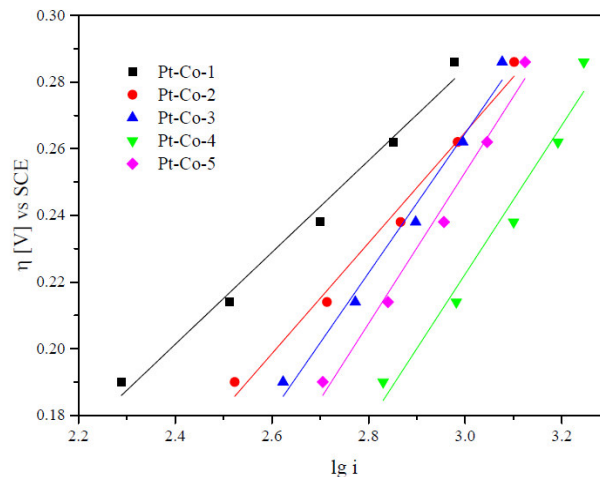


Figure 4.47. Tafel plots in 1 M NaOH solution on selected Pt-Co electrodes

Nevertheless, the enhancement of the OER can be ascribed to the presence of cobalt in the platinum structure, due to the structural changes caused by alloying (increase in d-band vacancy) and geometrical changes (decrease of the Pt-Pt bond distance) [40], providing more favorable sites for dissociative adsorption and desorption of oxygen. Similar studies have shown that by alloying platinum with metal elements which present smaller atomic size cause lattice contraction being more active, while the alloys with metals with larger atomic size lead to lattice expansion and are less active [144].

Table 4.14 Kinetic parameters for OER in 1 M NaOH solution

Sample	b [mV dec ⁻¹]	a	i_o [A m ⁻²]
Pt-Co-1	137	0.43	8.74
Pt-Co-2	166	0.36	25.32
Pt-Co-3	209	0.28	54.55
Pt-Co-4	223	0.26	101.03
Pt-Co-5	227	0.26	76.81

4.3.3.2 In situ PEMFC polarization curves on Pt-Co/CNF catalysts

Alloying platinum with transition metals increases the catalytic activity of Pt-based catalyst for the oxygen reduction reaction in polymer electrolyte membrane PEM fuel cells. The formation of a new electronic structure, by shortening the Pt-Pt distance favours the adsorption of oxygen molecules, changes the composition of the surface oxides and improves the corrosion resistance of Pt [145]. Starting from this statement, the prepared Pt-Co/CNF catalysts were tested for the ORR, in situ in a PEMFC test bench. Previous studies have indicated that by alloying Co with Pt in a ratio of 1:3 (CoPt₃) provides higher catalytic activity than any other 3d transition metal in different compositions with Pt.

The prepared Pt-Co electrodes obtained using the pulsed electrodeposition method (C1 – deposited with 50 mA cm⁻², for 5000 cycles, C2 – 100 mA cm⁻², for 5000 cycles, C3 – 100 mA cm⁻², for 10000 cycles) having as platinum-cobalt loadings 0.1 mg Pt cm⁻², 0.15 mg Pt cm⁻² and 0.2 mg Pt cm⁻² were used as cathodes, whereas a commercial Pt/C electrode (0.35 mg cm⁻² Pt) was used as an anode to fabricate the MEA. The cathodes were impregnated with PTFE solution (2.5 wt. % in isopropanol) prior to catalyst particles deposition to achieve the necessary hydrophobicity and to minimize the water flooding of the cathode. The electrodes were then sintered at 270°C in normal atmosphere for 30 min and at 370°C for another 30 min.

Both electrodes, the Pt-Co cathode and the commercial Pt/C electrode were sprayed with 5 wt. % Nafion solution before the MEA production to provide ionic transport between the membrane and the catalyst site. The MEA were prepared as described previously for Pt/CNF electrodes. The operation parameters are maintained constant. Before recording the polarization curves, the electrodes were preconditioned for 50 minutes at different potential values (0.45 V, 0.65 V, and 0.95 V).

The catalytic activity of the Pt-Co electrodes was investigated regarding the ORR in situ in a PEMFC test bench. MEA were produced as previously described for Pt/CNF electrodes testing. The polarization curves for Pt-Co electrodes employed as cathodes are presented in Figure 4.48.

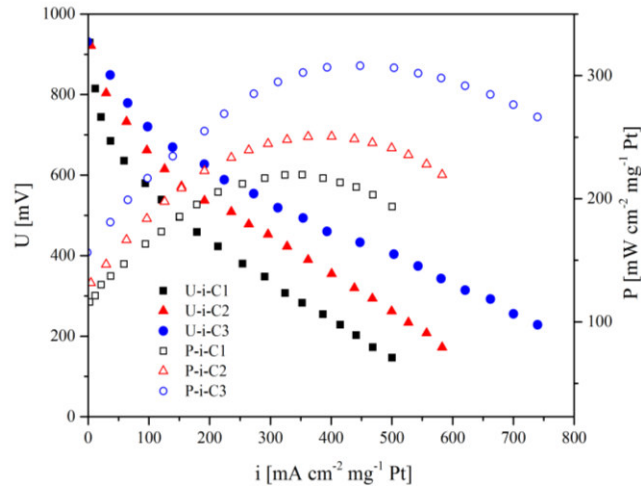


Figure 4.48. Polarization curves of MEA prepared with the same Pt/C anode and: C1 – Pt-Co/CNF 50 mA cm⁻², 5000 cycles; C2 – Pt-Co/CNF 100 mA cm⁻², 5000 cycles; C3 – Pt-Co/CNF 100 mA cm⁻², 10000 cycles

In this case, the OCV for the investigated samples is lower than 0.95 V. Likewise, the highest voltage drop occurs in the small current densities region (0 – 100 mA cm⁻² mg⁻¹ Pt) being correlated to the activation energy barrier. Sample C1 presents the higher activation polarization loss, which can be explained by the smaller platinum-cobalt loading in comparison to the other investigated samples. Polarisation curves display a maximum power density of 300 mW cm⁻² mg⁻¹ Pt associated with a current density of 500 mA cm⁻² mg⁻¹ Pt (at 0.5 V) for sample C3. Cathodes C1 and C2 show lower values due to the smaller catalyst amount. Likewise, differences in the polarisation behaviour are assigned to deposition parameters of the Pt-Co alloy catalyst which determine the catalyst loading.

5 Conclusions

The original research described in the present work consists in a theoretical study on available literature data regarding catalyst materials, fabrications methods and applications. The focus was directed to aspects concerning the production of novel catalyst materials suitable for PEMFC and water splitting electrolyzers and regarding the development of effective methods to improve the catalytic activity, stability and durability of the discussed electrodes respectively.

Considering that platinum is the most suitable catalyst material, (due to its highest activity, good stability and improved corrosion resistance), the main attention was focused on reducing the amount of this expensive metal, simultaneously preserving the superior characteristics. Practically, these directions can be accomplished either by depositing nano-sized platinum particles on a compatible support material that exhibits a large surface area, by choosing a suitable deposition method or by developing an appropriate platinum alloy with transitional metals, which exhibits catalytic activity for electrochemical reactions that take place in different electrochemical cells. Carbon blacks are the most employed electrocatalyst support materials for PEMFC technology due to their high surface area and increased electrical conductivity. However, during start-up and shut-down of the PEMFC, electrode materials are subjected to severe corrosion conditions, especially on the cathodic side. Hence, other important objective of the present thesis is to replace the carbon black with more corrosion resistant carbon based support materials. Alloying platinum with transition metals increases the catalytic activity of Pt-based catalysts for the oxygen reduction reaction in PEM fuel cells. The formation of a new electronic structure, by shortening the Pt-Pt distance, favours the adsorption of oxygen molecules, changes the composition of the surface oxides and improves the corrosion resistance of Pt.

The present work dealt with the development of catalyst materials based on carbon nanofibers using an **electrochemical method**. The CNF provide a high surface area for the catalyst particles, improving considerably the active surface area. The electrodeposition process has several advantages in comparison to other available methods, being more efficient at low operating costs, conferring also an easier control for the nucleation and growth of the metal particles and providing a higher utilisation degree of the catalyst particles. Moreover, this technique provides a simple fabrication way for the electrodes and guarantees that the ions from the plating bath, pass through the electrolyte towards the support material and are deposited on the areas where protonic and electronic conduction coexist. This condition is mandatory for developing fuel cell catalyst materials due to the essential demand of three-phase zones existence. In addition, this method proved to be an efficient way to synthesize catalyst nanoparticles with high density of atoms and clean surfaces, since this process does not require the addition of stabilizers which may be adsorbed onto the electrode surface, poisoning the active area of the catalyst. Furthermore, applying this method, the control of the microstructure and thickness or chemical composition in case of an alloy deposition is facilitated. The pulsed current deposition technique has also several advantages in comparison to direct current electrodeposition, as it can provide a better current distribution and controlled mass transfer step. Additionally, the deposition is more uniform and the porosity is reduced.

Furthermore, it is strongly necessary to correlate the deposition technique with an appropriate functionalization treatment to achieve improved catalysts materials with low platinum loading. In this regard, a chemical-physical process based on oxygen plasma was applied on the CNF support material, generating functional acidic groups directly onto their outer surface. **Plasma functionalization** produces covalent chemical bonds between oxygen and carbon atoms facilitating the further interactions between the treated material and other substances or environment due to their polarity. Such chemical bonds are stable over time and there is no degradation under normal storage conditions. This treatment is based on an efficient and rapid process, providing a high functionalization degree onto the exposed material. In addition, no by-products are released during the operation and the process can last a few minutes in comparison with other available functionalization methods.

The main topic of the present thesis is well correlated with the actual major problems encountered in the development catalyst materials with low platinum loading and moreover, this work aims to contribute to several research questions related to the state of the art in the field of PEMFC.

This study focused on the development of two types of catalyst materials suitable for electrochemical applications, based on carbon nanofibers decorated with **platinum nanoparticles** and **platinum-cobalt alloy nanoparticles** respectively. As state of the art in the PEMFC indicates, the platinum based catalysts are produced for the anodic side of a fuel cell, where the hydrogen oxidation reaction takes place. On the other hand, the cathodic reaction is considered more complicated than the anodic one, because it can consist in two distinct routes and the major voltage losses in a PEMFC system are caused by the high oxygen reduction overpotential. Moreover, the catalyst material needs to be very resistant for the increased corrosive conditions that occur on the cathodic side of the fuel cell. Consequently, the cathode needs either a higher platinum loading than the anode or a suitable platinum alloy, to overcome the afore mentioned difficulties. In the actual state of the art it is mentioned that platinum alloyed with transitional metals significantly improves the catalytic activity for the cathodic reaction, reducing the dissolution and migrations phenomena of platinum particles and increasing the catalyst durability respectively. Concerning these aspects, a platinum – cobalt alloy catalyst was developed for the OER as well as for the cathodic side of the fuel cell. The obtained electrode materials were characterized using various techniques such as SEM, EDX, XRD, XRF, TGA, LV and CV. Moreover, the behaviour of the obtained electrodes as catalysts for PEMFC was investigated plotting in situ polarization curves.

Finding a catalyst material that is both stable and active for HER/OER and HOR/ORR respectively has represented a major research focus in the field of electrocatalysts. Although Pt is nearly ideal for HER, HOR and ORR, it has shown poor OER activity due to the reduced surface area and formation of a platinum oxide layer that behaves as an electrical insulator. These aspects may be overcome by using a catalyst consisting of conventional Pt and Co particles.

The original contributions of this study refer to:

- possibility of combining the **oxygen plasma functionalization treatment** with the **electrochemical deposition method**, to develop low platinum loading catalysts for the most important electrochemical reactions;
- investigations on the **degradation mechanism** (including corrosion resistance, thermal stability, graphitization degree) of the CNF support material, particularly **after the functionalization treatment**;
- studies on the deposition mechanisms of platinum and platinum-cobalt

codeposition respectively from a **self-developed electrolyte**, as well as investigations on the influence of the significant deposition parameters on the structure and morphology of the electrodes;

- evaluation of the **dual catalytic effect** of the developed electrodes by determination of the kinetical parameters for HER and OER, respectively and catalytic performance of the electrodes for the electrochemical reactions that occur inside a PEMFC.

In this regard, several aspects can be highlighted:

- CNF with an increased specific surface area ($>100 \text{ m}^2 \text{ g}^{-1}$) and a high graphitization degree ($\approx 100 \%$) were used as support material for catalyst particles deposition; CNF have been treated in oxygen plasma and during this step, functional acidic groups were generated onto their surface;
- The initial hydrophobicity of CNF changed during the functionalization treatment and the reactivity of the CNF active surface area increased due to the presence of oxygen-carrying polar functional groups;
- The functional groups concentration was determined using an acidic titration method; the functionalization degree is strongly related to the specific surface area of the carbon material;
- The surface energy of the fibers was significantly improved and this positive effect was reflected on the catalyst distribution and loading; a higher concentration of functional groups was achieved applying a power of 80 W for 1800 s;
- Thermal stability of the CNF investigated using TGA measurements showed that defects created on the carbon surface during functionalization, due to breaking down the C=C, lead to reduction of thermal decomposition temperature; the decomposition of functional groups takes place between 150°C and 350°C;
- The concentration of oxygen containing groups attached on the CNF surface during the plasma functionalization treatment plays an important role regarding the corrosion behaviour of CNF; functionalized samples exhibited slightly lower corrosion current density in comparison to untreated fibers, this fact being attributed to the presence of oxygen containing groups, which create a protective layer that can prevent the further oxidation of carbon.
- Corrosion process of the CNF is initiated at the defect sites in the carbon structure and consequently the electrochemical degradation of carbon is lowered by a higher graphitisation degree of the material;
- The distribution of the catalyst particles was considerably improved through the functionalization process of the CNF support material; in the case of untreated CNF, the particles tend to agglomerate due to the low surface energy and the poor contact with the electrolyte caused by the hydrophobic character of the fibers;
- Particle sizes increase when a higher power for functionalization treatment is applied; particle sizes for Pt/CNF samples ranged between 12 nm and 40 nm;
- Due to the higher functionalisation degree of CNF 80 sample, more active sites for platinum particles were provided, which favoured the nucleation rate;
- The current density significantly influenced the nucleation rate of the platinum/platinum cobalt particles; by changing the number of cycles applied during the deposition process, the nucleation and growth mechanism

was not affected, the particle size and distribution remained mostly constant and the catalyst amount increased;

- Due to the improved particles distribution achieved through the functionalization treatment, correlated with a higher electrochemical surface area obtained for CNF 80 samples, it can be affirmed that plasma functionalization treatment (80 W for 1800 s) led to highest ECSA values and increased catalytic activity;
- Prepared Pt/CNF electrodes exhibited superior catalytic activity regarding the HER; the process was significantly intensified (onset potential decreased) for Pt/CNF functionalized samples;
- The Tafel slopes were estimated in the range of 103 mV dec⁻¹ to 135 mV dec⁻¹, describing a Volmer-Heyrovsky rate-determining step for HER;
- In-situ polarisation curves (PEMFC) showed a maximum power density of around 400 mW cm⁻² mg⁻¹ Pt correlated with a developed current density of 800 mA cm⁻² mg⁻¹ Pt achieved at a practical voltage of 500 mV for a Pt/CNF prepared anode; a higher platinum amount deposited onto the CNF support material led to 60 % increase in power output;
- For Pt-Co alloy deposition, the molar ratio between Pt²⁺ and Co²⁺ was varied from 1:0.5 to 1:20, by changing the cobalt concentration and maintaining the same platinum amount; increasing the Co amount, the alloy composition was consequently influenced.
- XRD measurements confirmed a higher amount of CoPt₃ alloy in the deposit for samples obtained from an electrolyte with a higher Co content; a high alloying degree was achieved, both elements were evenly distributed on electrode surface and platinum presented a higher content in comparison to Co;
- Particle sizes for Pt/CNF samples ranged between 12 nm and 50 nm; the increased surface area, as well as the chemical composition (CoPt₃ alloy) contributed to an improved catalytic activity;
- The activity of Pt-Co catalysts for OER was significantly improved when a higher Co content was added in the deposition electrolyte; the enhancement of the OER was ascribed to the presence of cobalt in the platinum structure, due to the structural changes caused by alloying (increase in d-band vacancy) and geometrical changes (decrease of the Pt-Pt bond distance);
- In situ PEMFC polarisation curves displayed a maximum power density of 300 mW cm⁻² mg⁻¹ Pt associated with a current density of 500 mA cm⁻² mg⁻¹ Pt (at 500 mV) for a Pt-Co/CNF sample placed at the cathodic side;

Using the described method, low platinum loading electrocatalysts have been synthesized. The activity of the electrodes is attributed to the higher electrochemical surface area achieved by applying platinum nanoparticles. Moreover, the support material played a significant role for increasing the active surface area, by providing a higher available surface. The high utilisation degree of the deposited platinum particles achieved by applying an electrochemical method had also a significant influence on the catalyst activity.

The obtained electrodes present a dual character. Pt/CNF electrodes are suitable as catalyst materials either for HER in acidic environments, as well as for HOR inside a PEMFC. Likewise, Pt-Co/CNF catalysts have been proven to catalyse the OER in alkaline mediums and moreover, the catalytic behaviour as cathodes inside a PEMFC was also noticed.

Outlook

Carbon based structures supported platinum nanoparticles present a great interest as electrocatalysts for electrochemical cell applications. The increased surface area of the carbon nanostructures can provide a suitable support for the catalyst particles improving consequently the catalytic activity and diminishing the platinum consumption. Moreover, carbon nanofibers/nanotubes present interest in many other research areas due to their unique properties such as electrical and thermal conductivity, strength, corrosion resistance, good interaction with metal and polymer materials. Among the current challenges, the development of new effective processes to extend the surface chemistry and reactivity, to enlarge the potential range of applications is a priority. Regarding the functionalization methods, a low temperature nitrogen plasma treatment can be a suitable alternative to oxygen plasma process presented in this study, to raise the surface energy of the carbon support material. Nitrogen functionalities have been shown to possess good catalytic activity for oxygen reduction reaction and are regarded as a metal free alternative to noble catalyst like platinum.

Undoubtedly, numerous possibilities can be adopted and explored regarding the development of new catalyst materials. As platinum still represents the better option for electrocatalytic reactions, the possibility to obtain alloys with a low platinum content that exhibit increased catalytic activity has lately attracted a great interest. Binary and ternary alloys of platinum with transitional metals can represent a future alternative in the field of electrocatalysts. Even if the currently developed platinum alloys present improved results regarding the catalytic activity, the durability and stability of these materials still represent a problem. By improving the chemical composition of the platinum based alloys, more stable and durable catalyst materials can be obtained.

The possibility of combining the carbon-based materials that possess an increased surface area, high graphitisation degree and good corrosion resistance with active and stable platinum alloys may lead to superior catalytic materials with increased sensitivity and longer lifetime.

References

- [1] A. Lavacchi, H. Miller and F. Vizza, *Nanotechnology in Electrocatalysis for Energy*, New York: Springer, 2013.
- [2] J. Larminie and A. Dicks, *Fuel Cell Systems Explained*, England: 2nd Edition Wiley, 2003.
- [3] J. G. Martinez, *Nanotechnology for the energy challenge*, Germany: 2nd Edition Wiley-VCH, 2013.
- [4] J. H. Hirschenhofer, D. B. Stauffer, R. Engleman and M. G. Klett, *Fuel Cell Handbook*, USA: Parsons Corporation, 1998.
- [5] S. Curtin and J. Gangi, "2013 Fuel Cell Technologies Market Report," U.S Department of Energy, Washington DC, 2014.
- [6] D. P. Wilkinson, J. Zhang, R. Hui, J. Fergus and X. Li, *Proton Exchange Membrane Fuel Cell*, USA: Taylor & Francis Group, 2010.
- [7] F. Barbir, *PEM Fuel Cells Theory and Practice*, 2nd Edition, Waltham: Academic Press, 2013.
- [8] J. Zhang, *PEM Fuel Cell Electrocatalysts and Catalyst Layers*, Canada: Springer, 2008.
- [9] M. Gangeri, G. Centi, A. L. Malfa, S. Perathoner, R. Vieira, C. Pham-Huu and M. J. Ledoux, "Electrocatalytic performances of nanostructured platinum-carbon materials," *Catalysis Today*, Vols. 102-103, pp. 50-57, 2005.
- [10] V. Meille, "Review on methods to deposit catalysts on structured surfaces," *Applied Catalysis. A: General*, vol. 315, pp. 1-17, 2006.
- [11] E. Furimsky, *Carbons and Carbon-Supported Catalysts in Hydroprocessing*, USA: RSC Catalysis Series, 2008.
- [12] D. Steinborn, *Fundamentals of Organometallic Catalysis*, Weinheim, Germany: Wiley-VCH, 2012.
- [13] J. Hagen, *Industrial Catalysis: A Practical Approach*, 2nd Edition, Weinheim, Germany: Wiley-VCH, 2006.
- [14] E. Farnetti, R. D. Monte and J. Kaspar, "Homogeneous and Heterogeneous Catalysis" *Inorganic and Bio-Inorganic Chemistry*, vol. II.
- [15] M. G. Zidan, *Some of General Types of Catalysts*, New York, USA: Pearson Prentice Hall, 2007.
- [16] R. Sheldon, I. Arends and U. Hanefeld, *Green Chemistry and Catalysis*, Weinheim: Wiley-VCH, 2007.
- [17] C. Wang, M. Waje, X. Wang, J. Tang and Y. Y. R. C. Haddon, "Proton Exchange Membrane Fuel with Carbon Nanotube Based Electrodes," *Nano Letters*, vol. 4, no. 2, pp. 345-348, 2004.
- [18] F. Gao, B. Blunier and A. Miraoui, *Proton Exchange Membrane Fuel Cell Modeling*, New York: Wiley, 2012.

- [19] "Fuel Cells, Multi Year Research, Development and Demonstration Plan," 2012.
- [20] T. Maiyalagan and S. Pasupathi, "Components of PEMFC, An Overview," *Materials Science Forum*, vol. 657, pp. 143-149, 2010.
- [21] V. Ramoni, "Fuel Cells," *The Electrochemical Society Interface*, pp. 41-44, 2006.
- [22] S. Litster and G. McLean, "PEM fuel cell electrodes," *Journal of Power Sources*, vol. 130, pp. 61-76, 2004.
- [23] R. Othman, A. L. Dicks and Z. Zhu, "Non-precious metal catalysts for the PEM fuel cell cathode," *Hydrogen Energy*, vol. 37, pp. 357-372, 2012.
- [24] L. Gan, C. Cui, S. Rudi and P. Strasser, "Core-Shell and Nanoporous Particle Architecture and Their Effect on the Activity and Stability of Pt ORR Electrocatalysts," *Springer*, 2013.
- [25] A. J. J. Kadjo, P. Brault, A. Caillard, C. Coutanceau, J. P. Garneir and S. Martemianov, "Improvement of proton exchange membrane fuel cell electrical performance by optimization of operating parameters and electrodes preparation," *Journal of Power Sources*, vol. 172, pp. 613-622, 2007.
- [26] L. A. Dobrzanski, M. Pawlyta, A. Krzton, B. Liszka and K. Labisz, "Synthesis and characterisation of carbon nanotubes decorated with platinum nanoparticles," *Journal of Achievements in Materials and Manufacturing Engineering*, vol. 39, no. 2, pp. 184-189, 2010.
- [27] O. T. Holton and J. W. Stevenson, "The role of platinum in Proton Exchange Membrane Fuel Cells," *Platinum Metals Review*, vol. 57, no. 4, pp. 259-271, 2013.
- [28] J. X. Wang, T. E. Springer and R. R. Adzic, "Dual-Pathway Kinetic Equation for Hydrogen Oxidation Reaction on Pt Electrodes," *Journal of Electrochemical Society*, vol. 153, no. 9, pp. 1732-1740, 2006.
- [29] W. Sheng, H. A. Gasteiger and Y. S. Horn, "Hydrogen Oxidation and Evolution Reaction Kinetics on Platinum: Acid vs Alkaline Electrolytes," *Journal of The Electrochemical Society*, vol. 157, no. 11, pp. 1529-1536, 2010.
- [30] C. He, S. Desai, G. Brown and S. Bollepalli, "PEM Fuel Cell Catalysts: Cost, Performance, and Durability," *The Electrochemical Society Interface*, pp. 41-44, 2005.
- [31] S. Woo, I. Kim, J. K. Lee, S. Bong, J. Lee and H. Kim, "Preparation of cost effective Pt-Co electrodes by pulse electrodeposition for PEMFC electrocatalysts," *Electrochimica Acta*, vol. 56, pp. 3036-3041, 2011.
- [32] S. Mukerjee, "Particle size and structural effect in platinum electrocatalysis," *Journal of applied electrochemistry*, vol. 20, pp. 537-548, 1990.
- [33] J. Y. Kim, T. K. Oh, Y. Shin, J. Bonnet and K. S. Weil, "A novel non-platinum group electrocatalyst for PEM fuel cell application," *International Journal of Hydrogen Energy*, pp. 1-8, 2010.
- [34] L. Liu, H. Kim, J. W. Lee and B. N. Popov, "Development of Ruthenium-Based Catalysts for Oxygen Reduction Reaction," *Journal of Electrochemical Society*, vol. 154, no. 2, pp. 123-128, 2007.

- [35] A. A. Kandari, H. A. Kandari, A. M. Mohamed, F. A. Kharafi and A. Katrib, "Catalytic Active Sites in Molybdenum Based Catalysts," *Modern Research in Catalysis*, vol. 2, pp. 1-7, 2013.
- [36] S. Grigoriev, E. Lyutikova, S. Martemianov, V. Fateev, C. Lebouin and P. Millet, "Palladium-based electrocatalysts for PEM applications," in *WHEC 16*, Lyon France, 2006.
- [37] V. M. Nikolic, I. M. Perovic, N. M. Gavrilov, I. A. Pasti, A. B. Saponjic, P. J. Vulic, S. D. Karic, B. M. Babic and M. P. M. Kaninski, "On tungsten carbide synthesis for PEM fuel cell application - Problems, challenges and advantages," *International Journal of Hydrogen Energy*, vol. 39, pp. 11175-11185, 2014.
- [38] P. H. Matter, E. J. Biddinger and U. S. Ozkan, "Non-precious metal oxygen reduction catalysts for PEM fuel cells," *Catalysis*, vol. 20, pp. 338-366, 2007.
- [39] H. Zhong, H. Zhang, G. Liu, Y. Liang, J. Hu and B. Yi, "A novel non-noble electrocatalyst for PEM fuel cell based on molybdenum nitride," *Electrochemistry Communications*, vol. 8, pp. 707-712, 2006.
- [40] M. Yaldagard, N. Seghatoleslami and M. Jahanshahi, "Preparation of Pt-Co nanoparticles by galvanostatic pulse electrochemical codeposition on in situ electrochemical reduced graphene nanoplates based carbon paper electrode for oxygen reduction reaction in proton exchange membrane fuel cell," *Applied Surface Science*, vol. 315, pp. 222-234, 2014.
- [41] N. Todoroki, T. Kato, T. Hayashi, S. Takahashi and T. Wadayama, "Pt-Ni Nanoparticle-Stacking Thin Film: Highly Active Electrocatalysts for Oxygen Reduction Reaction," *American Chemical Society*, vol. 5, pp. 2209-2212, 2015.
- [42] H. Yang, N. A. Vante, J. M. Leger and C. Lamy, "Tailoring, Structure, and Activity of Carbon Supported Nanosized Pt-Cr Alloy Electrocatalysts for Oxygen Reduction in Pure and Methanol Containing Electrolytes," *The Journal of Physical Chemistry*, vol. 108, no. 6, pp. 1938-1947, 2004.
- [43] C. Xu, Y. Su, L. Tan, Z. Liu, J. Zhang, S. Chen and S. P. Jiang, "Electrodeposited PtCo and PtMn electrocatalysts for methanol and ethanol electrooxidation of direct alcohol fuel cells," *Electrochimica Acta*, vol. 54, no. 26, pp. 6322-6326, 2009.
- [44] H. Duan, Q. Hao and C. Xu, "Nanoporous PtFe alloys as highly active and durable electrocatalysts for oxygen reduction reaction," *Journal of Power Sources*, vol. 296, pp. 589-596, 2014.
- [45] E. Ding, K. L. More and T. He, "Preparation and characterisation of carbon-supported PtTi alloy electrocatalysts," *Journal of Power Sources*, vol. 175, no. 2, pp. 794-799, 2008.
- [46] A. O. Neto, J. Gonzalez, P. R. and E. A. Ticianelli, "Platinum/Cobalt electrocatalysts dispersed on high surface area carbon. Study of the oxygen reduction reaction," *Journal of New Materials for Electrochemical Systems*, vol. 2, pp. 189-195, 1999.
- [47] B. Li and S. H. Chan, "PtFeNi tri-metallic alloy nanoparticles as electrocatalyst for oxygen reduction reaction in proton exchange membrane fuel cells with ultra-low Pt loading," *Hydrogen Energy*, vol. 38, no. 8, pp. 3338-3345, 2013.

- [48] S. J. Y. S. J. Hwang, S. Jang, T. H. Lim, S. A. Hong and S. K. Kim, "Ternary PtFeCo Alloy Electrocatalysts Prepared by Electrodeposition: Elucidating the Roles of Fe and Co in the Oxygen Reduction Reaction," *The Journal of Physical Chemistry*, vol. 115, pp. 2483-2488, 2011.
- [49] M. R. Tarasevich, V. A. Bogdanovskaya and V. N. Andreev, "PtCoCr/C Electrocatalysts for Proton-Conducting Polymer Electrolyte Fuel Cells," *Catalysis in Industry*, vol. 6, no. 3, pp. 159-169, 2014.
- [50] S. Grau, M. Montiel, E. Gomez and E. Valles, "Ternary PtCoNi functional film prepared by electrodeposition: Magnetic and electrocatalytic properties," *Electrochimica Acta*, vol. 109, pp. 187-194, 2013.
- [51] C. R. K. Rao and D. C. Trivedi, "Chemical and electrochemical depositions of platinum group metals and their applications," *Coordination Chemistry Reviews*, vol. 249, pp. 613-631, 2005.
- [52] S. M. Ayyadurai, Y. S. Choi, P. Ganesan, S. P. Kumaraguru and B. N. Popov, "Novel PEMFC Cathodes Prepared by pulsed Deposition," *Journal of The Electrochemical Society*, vol. 154, pp. 1063-1073, 2007.
- [53] M. L. Toebes, Carbon Nanofibers as Catalyst Support for Noble Metals, Utrecht, 2004.
- [54] M. Yaldagard, M. Jahanshahi and N. Seghatoleslami, "Carbonaceous Nanostructured Support Materials for Low Temperature Fuel Cell Electrocatalysts - A review," *World Journal of Nano Science Engineering*, vol. 3, pp. 121-153, 2013.
- [55] Y. Shao, J. Liu, Y. Wang and Y. Lin, "Novel catalyst support materials for PEM fuel cells: current status and future prospects," *Journal of Materials Chemistry*, vol. 19, pp. 46-59, 2009.
- [56] Y. Zhang and C. Erkey, "Preparation of Platinum-Nafion-Carbon Black Nanocomposites via Supercritical Fluid Route as Electrocatalysts for Proton Exchange Membrane Fuel Cells," *Industrial and Engineering Chemistry Research*, vol. 44, pp. 5312-5317, 2005.
- [57] W. Li, C. Liang, J. Qiu, W. Zhou, H. Han, Z. Wei, G. Sun and Q. Xin, "Carbon nanotubes as support for cathode catalyst of a direct methanol fuel cell," *Carbon*, vol. 40, pp. 787-803, 2002.
- [58] A. Guha, W. Lu, T. A. Zawodzinski and D. A. Schiraldi, "Surface-modified carbons as platinum catalysts support for PEM fuel cells," *Carbon*, vol. 45, pp. 1506-1617, 2007.
- [59] Y. Yao, Q. Fu, Z. Zhang, H. Zhang, T. Ma, D. Tan and X. Bao, "Structure control of Pt-Sn bimetallic catalysts supported on highly oriented pyrolytic graphite (HOPG)," *Applied Surface Science*, vol. 254, pp. 3808-3812, 2008.
- [60] F. Pagnanelli, P. Altimari, M. Bellagamba and G. Granata, "Pulsed electrodeposition of cobalt nanoparticles on copper: influence of the operating parameters on size distribution and morphology," *Electrochimica Acta*, vol. 155, pp. 228-235, 2015.
- [61] J. v. Drunen, B. K. Pilapil, Y. Makonnen, D. Beauchemin, B. D. Gates and G. Jerkiewicz, "Electrochemically active nickel foams as support materials for nanoscopic platinum electrocatalysts," *Applied Mater Interfaces*, vol. 13, no. 15, pp. 12046-12061, 2014.

- [62] C. R. K. Rao and M. Pushpavanam, "Electroless deposition of platinum on titanium substrates," *Materials Chemistry and Physics*, vol. 68, pp. 62-65, 2001.
- [63] S. Bagheri, N. M. Julkapli and S. B. A. Hamid, "Titanium Dioxide as a Catalyst Support in Heterogeneous Catalysis," *The Scientific World Journal*, vol. 2014, p. 21 pages, 2014.
- [64] T. Matsui, K. Fujiwara, T. Okanishi, R. Kikuchi, T. Takeguki, K. Eguchi, "Electrochemical oxidation of CO over tin oxide supported platinum catalysts," *Journal of Power Sources*, vol. 155, pp. 152-156, 2006.
- [65] A. Guha, W. Lu, T. A. Zawodzinski and D. A. Schiraldi, "Surface-modified carbons as platinum catalyst support for PEM fuel cells," *Carbon*, vol. 45, pp. 1507-1517, 2007.
- [66] P. Trogadas, T. F. Fuller and P. Strasser, "Carbon as Catalyst and Support for Electrochemical Energy Conversion," *Carbon*, 2014.
- [67] E. Antolini, "Carbon supports for low-temperature fuel cell catalysts," *Applied Catalysis B: Environmental*, vol. 88, pp. 1-24, 2009.
- [68] K. L. Klein, A. V. Melechko, T. E. McKnight, S. T. Rack, P. D. Retterer, J. D. Fowlkes, D. C. Joy and M.-L. Simpson, "Surface characterization and functionalization of carbon nanofibers," *Journal of Applied Physics*, vol. 103, no. 061301, pp. 1-26, 2008.
- [69] I. Salame and T. J. Bandosz, "Surface Chemistry of Activated Carbons: Combining the Results of Temperature-Programmed Desorption, Boehm and Potentiometric Titrations," *Journal of Colloid and Interface Science*, vol. 240, pp. 252-258, 2001.
- [70] F. Aviles, J. Cauich-Rodriguez, L. Moo-Tah and R. Vargas-Coronado, "Evaluation of mild acid oxidation treatments for MWCNT functionalization," *Carbon*, vol. 47, pp. 2970-2975, 2009.
- [71] L. Chen, H. Xie and W. Yu, "Functionalization Methods of Carbon Nanotubes and its Applications," in *Carbon Nanotubes Applications on Electro Devices*, China, In Tech, 2011, pp. 213-232.
- [72] V. Mittal, "Surface Modification of Nanotube Fillers," *Wiley-VCH Verlag, GmbH*, 2011.
- [73] N. T. Hung, N. M. Tuong and E. G. Rakov, "Acid Functionalization of Carbon Nanofibers," *Inorganic Materials*, vol. 46, pp. 1077-1083, 2010.
- [74] R. Chetty, K. K. Maniam, W. Schuchmann and M. Muhler, "Oxygen-Plasma-Functionalized Carbon Nanotubes as Supports for Platinum-Ruthenium Catalysts Applied in Electrochemical Methanol Oxidation," *ChemPlusChem*, pp. 1-7, 2014.
- [75] T. Zhang, M. B. Nix, B.-Y. Yoo, M. A. Deshusses and N. V. Myung, "Electrochemically Functionalized Single-Walled Carbon Nanotube Gas Sensor," *Electroanalysis*, vol. 18, pp. 1153-1158, 2006.
- [76] V. Chirila, G. Marginean and W. Brandl, "Effect of the oxygen plasma treatment parameters on the carbon nanotubes surface properties," *Surface and Coatings Technology*, vol. 200, pp. 548-551, 2005.
- [77] W. Brandl and G. Marginean, "Functionalization of the carbon nanofibres by plasma treatment," *Thin Solid Films*, vol. 447, pp. 181-186, 2004.

- [78] C. R. K. Rao and D. Trivedi, "Chemical and electrochemical deposition of platinum group metals and their applications," *Coordination Chemistry Reviews*, vol. 249, pp. 613-631, 2004.
- [79] Z. Kaidanovych, Y. Kalishyn and P. Strizhak, "Deposition of Monodisperse Platinum Nanoparticles of Controlled Size on Different Supports," *Scientific Research*, vol. 2, pp. 32-38, 2013.
- [80] N. Job, M. Pereira, S. Lambert, A. Cabiac, G. Delahay, J.-F. Colomer, J. Marien, J. L. Figueiredo and J.-P. Pirard, "Highly dispersed platinum catalysts prepared by impregnation of texture-tailored carbon xerogels," *Journal of Catalysis*, vol. 240, pp. 160-171, 2006.
- [81] L. Giorgi, L. Pilloni, R. Giorgi and M. Pasquali, "Electrodeposition and Sputter Deposition of Platinum Nanoparticles on Gas Diffusion Electrodes," in *3rd European Forum on PEFC*, Switzerland, 2005.
- [82] U. Mohanty, "Electrodeposition: a versatile and inexpensive tool for the synthesis of nanoparticles, nanorods, nanowires, and nanoclusters of metals," *Journal of Applied Electrochemistry*, vol. 41, no. 3, pp. 257-270, 2011.
- [83] M. D. Argyle and C. H. Bartholomew, "Heterogeneous Catalyst Deactivation and Regeneration: A review," *Catalysts*, vol. 5, pp. 145-269, 2015.
- [84] H. Kim, N. P. Subramanian and B. N. Popov, "Preparation of PEM fuel cell electrodes using pulse electrodeposition," *Journal of Power Sources*, vol. 138, pp. 14-24, 2004.
- [85] M. Pushpavanam, "Pulse and pulse reverse plating - Conceptual, advantages and applications," *Electrochimica Acta*, vol. 53, pp. 3313-3322, 2008.
- [86] M. M. E. Duarte, A. S. Pilla, J. M. Sieben and C. E. Mayer, "Platinum particles electrodeposition on carbon substrates," *Electrochemistry Communications*, vol. 8, pp. 159-164, 2006.
- [87] S. D. Thompson, L. R. Jordan and M. Forsyth, "Platinum electrodeposition for polymer electrolyte membrane fuel cells," *Electrochimica Acta*, vol. 46, pp. 1657-1663, 2001.
- [88] A. Brenner, *Electrodeposition of Alloys: Principles and Practice*, London: Academic Press, 1963.
- [89] S. S. Djokic and P. L. Cavallotti, "Electroless Deposition: Theory and Applications," in *Modern Aspects of Electrochemistry*, Springer, 2010, pp. 251-289.
- [90] A. Islam, M. A. K. Bhuiya and M. S. Islam, "A Review on Chemical Synthesis Process of Platinum Nanoparticles," *Asia Pacific Journal of Energy and Environment*, vol. 1, no. 2, pp. 107-120, 2014.
- [91] P. B. P-12, *Nafion, Ion exchange Materials*, 2016.
- [92] H. Tang, S. Peikang, S. P. Jiang, F. Wang and M. Pan, "A degradation study of Nafion Proton Exchange Membrane of PEM Fuel Cells," *Journal of Power Sources*, vol. 170, pp. 85-92, 2007.
- [93] H. S. Oh, K. H. Lim, B. Roh, I. Hwang and H. Kim, "Corrosion resistance and sintering effect of carbon supports in polymer electrolyte membrane fuel cells," *Electrochimica Acta*, vol. 54, pp. 6515-6521, 2009.

- [94] *Technical Manual and Operating Instructions - Scanning Electron Microscope XL 30 ESEM TMP*, FEI Company, 1999.
- [95] J. Goldstein, D. Newbury, D. Joy and C. Lyman, *Scanning Electron Microscopy and X-Ray Microanalysis*, 3rd Edition: Springer, 2013.
- [96] P. W. Hawkes, *Scanning Electron Microscopy: Physics of Image Formation and Microanalysis*, Springer, 2013.
- [97] FEI, *An Introduction to electron Microscopy*, ISBN 978-0-578-06276-1, 2010.
- [98] J. J. Friel, *X-Ray and Image Analysis in Electron Microscopy*, Princeton Gamma Tech, 2003.
- [99] *X'Pert - MPD Service Manual 940501*, The Netherlands: Philips Analytical X-Ray, 1994.
- [100] M. Birkholz, *Thin Film Analysis by X-Ray Scattering*, Weinheim: WILEY-VCH Verlag GmbH&Co KGaA, 2006.
- [101] T. Hatakeyama and F. X. Quinn, *Thermal Analysis: Fundamentals and Applications to Polymer Science*, 2nd Edition, March 1999.
- [102] "Brochure Technical specifications," [Online]. Available: www.netzsch-thermal-analysis.com. [Accessed 24 September 2016].
- [103] "<http://www.spectro.com>," [Online].
- [104] "http://archaeometry.missouri.edu/xrf_overview.html," [Online].
- [105] H. P. Boehm, E. Diehl, W. Heck and R. Sappok, "Surface Oxides of Carbon," *Angewandte Chemie International Edition*, vol. 3, no. 10, pp. 669-677, 1964.
- [106] I. I. Salame and T. J. Bandosz, "Surface Chemistry of Activated Carbons: Combining the results of Temperature-Programmed Desorption, Boehm and Potentiometric Titrations," *Journal of Colloid and Interface Science*, vol. 240, pp. 252-258, 2001.
- [107] F. Aviles, J. V. Cauich-Rodriguez, L. Moo-Tah, A. May-Pat and R. Vargas-Coronado, "Evaluation of mild acid oxidation treatments for MWCNT functionalization," *Carbon*, vol. 47, pp. 2970-2975, 2009.
- [108] R. Yudianti, H. Onggo, Y. Saito, T. Iwata and J. Azuma, "Analysis of Functional Group Sited on Multi-Wall Carbon Nanotube Surface," *The Open Materials Science Journal*, vol. 5, pp. 242-247, 2011.
- [109] A. El-kharouf, T. J. Mason, D. J. L. Brett and B. G. Pollet, "Ex-situ characterisation of gas diffusion layers for proton exchange membrane fuel cells," *Journal of Power Sources*, vol. 218, pp. 393-404, 2012.
- [110] A. Mahajan, A. Kingon, A. Kukovecz, Z. Konya and P. M. Vilarinho, "Studies on the thermal decomposition of multiwall carbon nanotubes under different atmospheres," *Materials Letters*, vol. 90, pp. 165-168, 2013.
- [111] S. V. Selvaganesh, G. Selvarani, P. Sridhar, S. Pitchumani and A. K. Shukla, "Graphitic Carbon as Durable Cathode-Catalyst Support for PEFCs," *Fuel Cells*, vol. 11, no. 3, pp. 372-384, 2011.
- [112] V. A. Golovin, E. N. Gribov, A. G. Okunev, I. N. Voropaev, A. N. Kuznetsov and A. V. Romanenko, "Development of Carbon Supports with Increased Corrosion Resistance for Pt/C Catalysts for Oxygen

- Electroreduction," *Kinetics and Catalysis*, vol. 56, no. 4, pp. 509-514, 2015.
- [113] Y. Yi, J. Tornow, E. Willinger, M. G. Willinger, C. Ranjan and R. Schlögl, "Electrochemical Degradation of Multiwall Carbon Nanotubes at High Anodic Potential for Oxygen Evolution in Acidic Media," *ChemElectroChem*, vol. 2, no. 12, pp. 1929-1937, 2015.
- [114] U. Rost, R. Muntean, G. Marginean, C. Merino, R. Diez, N. Vasilcsin and M. Brodmann, "Effect of Process Parameters for Oxygen Plasma Activation of Carbon Nanofibers on the Characteristics of Deposited Platinum Nanoparticles as Electrocatalyst in Proton Exchange Membrane Fuel Cell," *International Journal of Electrochemical Science*, vol. 11, pp. 9110-9122, 2016.
- [115] J. O. Bockris, "Modern electrochemistry," New York, Plenum Press, 1970, p. 917.
- [116] R. Muntean, U. Rost, G. Marginean and N. Vasilcsin, "Optimisation of the Electrodeposition Parameters for Platinum Nanoparticles on Carbon Nanofibers Support," *Solid State Phenomena*, vol. 254, pp. 153-158, 2016.
- [117] S. Karimi, "Pulse Current Electrodeposition of Nanocatalysts Using Different Waveforms for Use in PEMFCs," *ECS Trans*, vol. 53, no. 11, pp. 59-67, 2013.
- [118] H. N. Vatan, M. M. Shafiee, A. Khanfekr, M. Laleh, H. Kaffashan and K. Jafarzadeh, "Optimisation of experimental conditions for pulse electrodeposition of nanostructured platinum," *Surface Engineering*, vol. 30, no. 2, pp. 89-96, 2014.
- [119] G. Adilbish, J.-W. Kim, H.-G. Lee and Y.-T. Yu, "Effect of the deposition time on the electrocatalytic activity of Pt/C catalyst electrodes prepared by pulse electrophoresis deposition method," *International Journal of Hydrogen Energy*, vol. 38, pp. 3606-3613, 2013.
- [120] Y. Wang, J. Jin, S. Yang, G. Li and J. Qiao, "Highly active and stable platinum catalyst supported on porous carbon nanofibers for improved performance of PEMFC," *Electrochimica Acta*, vol. 177, pp. 181-189, 2015.
- [121] M. Gangeri, G. Centi, A. L. Malfa, S. Perathoner, R. Vieira, C. Pham-Huu and M. J. Ledoux, "Electrocatalytic performances of nanostructured platinum-carbon materials," *Catalysis Today*, Vols. 102-103, pp. 50-57, 2005.
- [122] C. Coutanceau, S. Baranton and T. W. Napporn, "Platinum Fuel Cell Nanoparticle Syntheses: Effect on Morphology, Structure and Electrocatalytic Behaviour," in *The Delivery of nanoparticles*, Rijeka, Intech, 2012, pp. 403-426.
- [123] W. Sheng, H. A. Gasteiger and Y. Shao-Horn, "Hydrogen Oxidation and Evolution Reaction Kinetics on Platinum: Acid vs Alkaline Electrolytes," *Journal of Electrochemical Society*, vol. 157, no. 11, pp. 1529-1536, 2010.
- [124] D. Hou, W. Zhou, X. Liu, K. Zhou, J. Xie and G. Li, "Pt nanoparticles/MoS₂ nanosheets/carbon fibers as efficient catalyst for the hydrogen evolution reaction," *Electrochimica Acta*, vol. 166, pp. 26-31, 2015.

- [125] M. A. Dominguez-Crespo, E. Ramirez-Meneses, A. M. Torres-Huerta, V. Garibay-Febles and K. Philippot, "Kinetics of hydrogen evolution reaction on stabilized Ni, Pt, and Ni-Pt nanoparticles obtained by organometallic approach," *International Journal of Hydrogen Energy*, vol. 37, pp. 4798-4811, 2012.
- [126] C. C. Vaduva, N. Vaszilcsin and A. Kellenberger, "Aromatic amine as proton carriers for catalytic enhancement of hydrogen evolution reaction on copper in acid solutions," *International Journal of Hydrogen Energy*, vol. 37, pp. 12089-12096, 2012.
- [127] M. Tavares, S. A. S. Machado and L. H. Mazo, "Study of hydrogen evolution reaction in acid medium on Pt microelectrodes," *Electrochimica Acta*, vol. 46, pp. 4359-4369, 2001.
- [128] U. Rost, R. Muntean, P. Podleschny, G. Marginean, M. Brodmann and V. A. Şerban, "Influence of the Graphitisation Degree of Carbon Nano Fibres Serving as Support Material for Noble Metal Electro Catalysts on the Performance of PEM Fuel Cells," *Solid State Phenomena*, vol. 254, pp. 27-32, 2016.
- [129] U. Rost, G. Mărginean, R. Muntean, P. Podleschny and M. Bradmann, "A cost-effective PEM fuel cell test system based on hydraulic compression with optimised platinum catalyst loading," *IEEE Xplore*, vol. DOI:10.1109/IESC.2016.7569500, 2016.
- [130] M. Perez-Page and V. Perez-Herranz, "Effect of the Operation and Humidification Temperatures on the Performance of a Pem Fuel Cell Stack on Dead-End Mode," *International Journal of Electrochemical Science*, vol. 6, pp. 492-505, 2011.
- [131] C. M. Bautista-Rodriguez, A. Rosas-Paleta, A. Rodriguez-Castellanos, J. A. Riviera-Marquez, O. Solorza, J. A. Guevara-Garcia and J. I., "Study of the Flow Fluids and Design Engineering Under PEM Fuel Cell Working Conditions," *International Journal of Electrochemical Science*, vol. 2, pp. 820-831, 2007.
- [132] M. Kim, J. Park, H. Kim, S. Song and W. H. Lee, "The preparation of Pt/C catalysts using various carbon materials for the cathode of PEMFC," *Journal of Power Sources*, vol. 163, pp. 93-97, 2006.
- [133] G. Alvarez, F. Alcaide, P. L. Cabot, M. J. Lazaro, E. Pastor and J. Solla-Gullon, "Electrochemical performance of low temperature PEMFC with surface tailored carbon nanofibers as catalyst support," *International Journal of Hydrogen Energy*, vol. 37, pp. 393-404, 2012.
- [134] N. Chaisubanan, K. Pruksathorn, H. Vergnes, F. Senocq and M. Hunsom, "Stability of TiO₂ Promoted Pt-Co/C Catalyst for Oxygen Reduction Reaction," *International Journal of Electrochemical Science*, vol. 11, pp. 1012-1028, 2016.
- [135] D. Morales-Acosta, D. Fuente, L. G. Lopez de la Arriaga, G. V. Gutierrez and F. J. R. Varela, "Electrochemical Investigation of Pt-Co/MWCNT as an Alcohol-Tolerant ORR Catalyst for Direct Oxidation Fuel Cells," *International Journal of Electrochemical Science*, vol. 6, pp. 1835-1854, 2011.
- [136] J. Santos, F. Trivinho-Strixino and E. C. Pereira, "Investigation of Co(OH)₂ formation during cobalt electrodeposition using a chemometric

- procedure," *Surface & Coatings Technology*, vol. 205, p. 2585, 2010.
- [137] J. S. Santos, R. Matos, F. Trivinho-Strixino and E. C. Pereira, "Effect of temperature on Co electrodeposition in the presence of boric acid," *Electrochimica Acta*, vol. 53, pp. 644-649, 2007.
- [138] W. A. Badawy, F. M. Al-Kharafi and J. R. Al-Ajmi, "Electrochemical behaviour of cobalt in aqueous solutions of different pH," *Journal of Applied Electrochemistry*, vol. 30, pp. 693-704, 2000.
- [139] Y. Saejeng and N. Tantavichet, "Preparation of Pt-Co alloy catalysts by electrodeposition for oxygen reduction in PEMFC," *Journal of Applied Electrochemistry*, vol. 39, pp. 123-134, 2009.
- [140] N. Chaisubanan and N. Tantavichet, "Pulse reverse electrodeposition of Pt-Co alloys onto carbon cloth electrodes," *Journal of Alloys and Compounds*, vol. 559, pp. 69-75, 2013.
- [141] K. Hosoiri, F. Wang, S. Doi and T. Watanabe, "Preparation and Characterization of Electrodeposited Co-Pt Binary Alloy Film," *Materials Transactions*, vol. 44, no. 4, pp. 653-656, 2003.
- [142] Z. Yan, M. Wang, B. Huang, R. Liu and J. Zhao, "Graphene Supported Pt-Co Alloy Nanoparticles as Cathode Catalyst for Microbial Fuel Cells," *International Journal of Electrochemical Science*, vol. 8, pp. 149-158, 2013.
- [143] A. E. Stoyanova, E. D. Lefterova, V. I. Nikolova, P. T. Iliev, I. D. Dragieva and E. P. Slavcheva, "Water splitting in PEM electrolysis with Ebonex supported catalysts," *Bulgarian Chemical Communications*, vol. 42, no. 1, pp. 167-173, 2010.
- [144] M. Min, J. Cho, K. Cho and H. Kim, "Particle size and alloying effects of Pt-based alloys catalysts for fuel cell applications," *Electrochimica Acta*, vol. 45, pp. 4211-4217, 2000.
- [145] B. P. Vinayan, R. I. Jafri, R. Nagar, N. Rajalakshmi, K. Sethupathi and S. Ramaprabhu, "Catalytic activity of platinum-cobalt alloy nanoparticles decorated functionalized multiwalled carbon nanotubes for oxygen reduction reaction in PEMFC," *International Journal of Hydrogen Energy*, vol. 37, pp. 412-421, 2011.
- [146] D. Zhao, B. L. Yi, H. M. Zhang and M. Liu, "The effect of platinum in a Nafion membrane on the durability of the membrane under fuel cell conditions," *Journal of Power Sources*, vol. 195, pp. 4606-4612, 2010.
- [147] M. S. Chandrasekar and M. Pushpavanam, "Pulse and pulse reverse plating- Conceptual, advantages and applications," *Electrochimica Acta*, vol. 53, pp. 3313-3322, 2008.
- [148] R. Brukh, O. Sae-Khow and S. Mitra, "Stabilizing single-walled carbon nanotubes by removal of residual metal catalysts," *Chemical Physics Letters*, vol. 459, p. 149, 2008.
- [149] J. O. Bockris, *Modern electrochemistry*, p.917, New York: Plenum Press, 1970.
- [150] Available: <http://pubs.usgs.gov/of/2001/of01-041/htmldocs/xrpd.htm>. [Accessed 24 September 2016].

APPENDIX 1

GANF TECHNICAL DATA SHEET

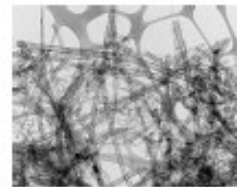
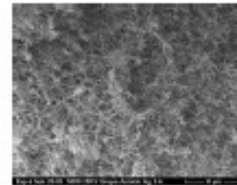
GRUPO ANTOLIN CARBON NANOFIBRES : GANF



Grupo Antolin Carbon Nanofibres (GANFs) are s-VGCF, (sub-micron Vapour Grown Carbon Fibres) with very small diameter, excellent aspect ratio and highly graphitic structure (graphitization degree about 70%). They are characterised by outstanding mechanical and transport properties (exceptionally high electric and thermal conductivity). Owing to their very small diameter and high aspect ratio, GANFs are able of making up a very effective conductive network in polymer or other matrices at very low loading content. Furthermore, conductive parts fabricated with GANFs added thermoplastic compounds present smoother surface finish than parts fabricated with alternative conductive additives such as carbon black or carbon fibres.

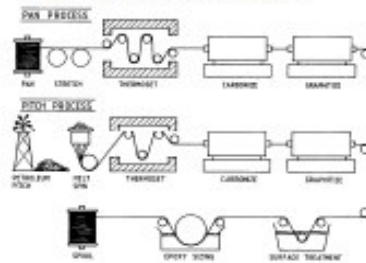
Other properties that set GANFs as an extraordinary product to be used in several industrial applications are:

- > Low coefficient of thermal expansion
- > Recyclable composite parts
- > Anticorrosive properties
- > Tribological properties
- > High specific surface area
- > Mechanical properties improvement

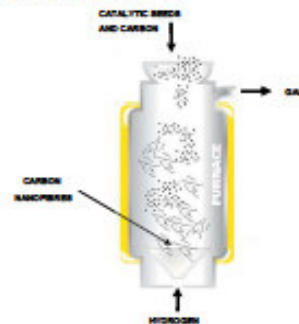


COMPARISON BETWEEN CARBON FIBRES AND GANF

Standard continuous carbon fibres are obtained through different thermal treatments of precursor fibre material. The precursor material is typically a polymer yarn such as rayon or polyacrylonitrile (PAN) or can also be melted and spun pitch.



Grupo Antolin Carbon Nanofibres (GANF) are continuously produced in a single step from the thermal decomposition of hydrocarbons in presence of metallic catalyst particles by the floating catalyst technique at about 1100°C.



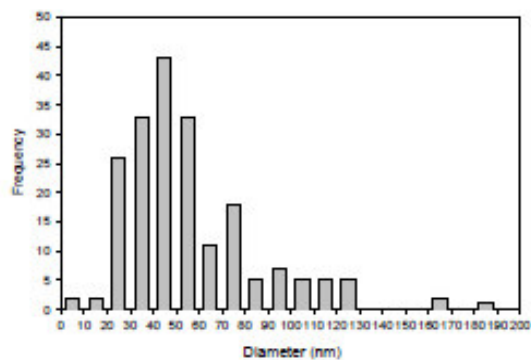
APPENDIX 2

GANF TECHNICAL DATA SHEET



GRUPO ANTOLIN CARBON NANOFIBRES PROPERTIES:

MEASURED PROPERTY	UNIT	GANF	GANF graphitized
FIBRE DIAMETER (TEM)	nm	20 - 80	20-80
FIBRE LENGTH (SEM)	μm	>30	>30
BULK DENSITY	g/cc	>1,97	<2.1
APPARENT DENSITY	g/cc	0.060	0.085
SURFACE ENERGY	mJ/m^2	≈ 100	-
SPECIFIC SURFACE AREA BET (N_2)	m^2/g	150-200	105-115
GRAPHITIZATION DEGREE	%	≈ 70	≈ 100
ELECTRICAL RESISTIVITY	$\text{Ohm}\cdot\text{m}$	$1\cdot 10^{-3}$	$1\cdot 10^{-4}$
METALLIC PARTICLES CONTENT	%	6-8	0.1 - 0.2

DIAMETER DISTRIBUTION GANF NANOFIBRES
TEM (Transmisión Electron Microscopy)



FREUDENBERG FCCT SE & CO. KG

**FREUDENBERG GAS DIFFUSION LAYERS
FOR PEMFC AND DMFC**

TECHNICAL DATA

PRODUCT NAME	H23	H24	H15	H14	H15	H2316	H23C2	H23C4	H23C9	H23C6	H23C7	H23C8	H23C3	H23C5	H14C7	H14C9	H15C9
	H2315 H2415	H2316 H2416	H1511 H1411	H1410 H1510	H1511 H1411	H231610 H241610	H231512 H241512	H231514 H241514	H231514C2 H241514C2	H231512C6 H241512C6	H231512C7 H241512C7	H231512C8 H241512C8	H231512C3 H241512C3	H231512C5 H241512C5	H141012C7 H151012C7	H141014C9 H151014C9	H151014C9 H141014C9
HYDROPHOBIC TREATMENT																	
MICROPOROUS LAYER																	
Thickness @ 0.025 MPa (internal*) in µm	210	150	155	150	155	210	255	255	250	250	250	230	250	270	175	180	185
Thickness @ 1 MPa (internal*) in µm	170	115	120	115	120	175	215	215	210	210	210	200	230	215	145	150	150
Area weight (DIN EN ISO 29073-1) in g/m ²	95	65	65	65	65	115	135	135	135	135	135	135	150	130	100	100	95
Compression Set @ 1 MPa (internal*) in µm	2	1.5	4	1.5	4	3	8	8	8	8	9	3	25	15	8	7	8
TP electrical resistance @ 1 MPa (internal*) in mΩ·cm ²	4.5	4	5.5	7	10	8	8	8	8	7	8	9	9	9	6	7	7.5
IP electrical resistance (internal*) in Ω	0.8	1.1	1.2	0.8	0.8	0.8	0.8	0.8	0.7	0.7	0.7	0.8	0.8	0.7	1.0	1.0	1.1
TP air permeability** (DIN EN ISO 9237) in l / m ² ·s	400	570	800	160	160	160	-	-	-	-	-	-	-	-	-	-	-
TP air permeability acc. to Gurler (ISO 9696-3) in s	-	-	-	-	-	-	70	50	30	70	50	50	35	40	50	30	40
IP air permeability @ 1 MPa (internal*) in µm ²	4.2	4.0	7.0	1.7	2.5	2.5	2.5	2.0	1.8	1.9	1.5	1.5	1.5	2.5	1.0	1.5	3.5
Tensile strength (DIN EN ISO 29073-3) in N/50mm	25	20	20	80	80	80	60	70	70	70	70	70	110	70	70	70	70

* Freudenberg internal measurement standard
 ** at 200Pa pressure drop
 TP = transporance, IP = impaire
 (Rev. 03 - 22.12.2014)

CONTACT
FREUDENBERG FCCT SE & CO. KG Hoehnenweg 2-4, 69465 Weinheim, Germany, www.freudenbergfcct.com
 FAX +49 6201 88 4489 E-MAIL fuelcell@freudenberg.de

APPENDIX 4

Properties of Nafion® PFSA Membrane

A. Thickness and Basis Weight Properties¹

Membrane Type	Typical Thickness (microns)	Basis Weight (g/m ²)
NR211	25.4	50
NR212	50.8	100

B. Physical Properties

Property ²	Typical Values				Test Method
	NR211		NR212		
	MD	TD	MD	TD	
Physical Properties					
- measured at 50% RH, 23 °C					
Tensile Strength, max., MPa	23	28	32	32	ASTM D 882
Non-Std Modulus, MPa	288	281	266	251	ASTM D 882
Elongation to Break, %	252	311	343	352	ASTM D 882

C. Other Properties

Property	NR 211	NR 212	Test Method
Specific Gravity ¹	1.97	1.97	DuPont
Available Acid Capacity ³ meq/g	0.92 min.	0.92 min.	DuPont NAE305
Total Acid Capacity ⁴ meq/g	0.95 to 1.01	0.95 to 1.01	DuPont NAE305
Hydrogen Crossover ⁵ , (ml/min-cm ²)	< 0.020	< 0.010	DuPont

D. Hydrolytic Properties

Property	Typical Value	Test Method
Hydrolytic Properties		
Water content, % water ⁶	5.0 ± 3.0%	ASTM D 570
Water uptake, % water ⁷	50.0 ± 5.0%	ASTM D 570
Linear expansion, % increase ⁸		
from 50% RH, 23 °C to water soaked, 23 °C	10	ASTM D 756
from 50% RH, 23 °C to water soaked, 100 °C	15	ASTM D 756

¹ Measurements taken with membrane conditioned to 23 °C, 50% RH.

² Where specified, MD - machine direction, TD - transverse direction. Condition state of membrane given.

³ A base titration procedure measures the equivalents of sulfonic acid in the polymer, and used the measurements to calculate the available acid capacity of the membrane (acid form).

⁴ A base titration procedure measures the equivalents of sulfonic acid in the polymer, and used the measurements to calculate the total acid capacity or equivalent weight of the membrane (acid form).

⁵ Hydrogen crossover measured at 22 °C, 100% RH and 50-psi delta pressure. This is not a routine test.

⁶ Water content of membrane conditioned to 23 °C and 50% RH (dry weight basis).

⁷ Water uptake from dry membrane to conditioned in water at 100 °C for 1 hour (dry weight basis).

⁸ Average of MD and TD. MD expansion is similar to TD expansion for NR membranes.

LIST OF PUBLICATIONS AND CONFERENCE PRESENTATIONS

- *R. Muntean, U. Rost, G. Mărginean, N. Vaszilcsin* - **Optimization of the electrodeposition parameters for platinum nanoparticles on carbon nanofibers support**, Solid State Phenomena, Trans Tech Publications, Switzerland, ISSN:1662-9779, Vol. 254, p. 153-158, 2016.
- *U. Rost, R. Muntean, P. Podleschny, G. Mărginean, M. Brodmann, V. A. Șerban* - **Influence of Graphitization Degree of Carbon Nano Fibers Serving as Support Material for Noble Metal Electro Catalysts on the Performance of PEM Fuel Cells**, Solid State Phenomena, Trans Tech Publications, Switzerland 2016, ISSN: 1662-9779, p. 27-32, 2016.
- *U. Rost, R. Muntean, G. Mărginean, C. Merino, R. Diez, N. Vaszilcsin, M. Brodmann* - **Effect of Process Parameters for Oxygen Plasma Activation of Carbon Nanofibres on the Characteristics of Deposited Platinum Catalyst Nanoparticles as Electrocatalyst in Proton Exchange Membrane Fuel Cells**, International Journal of Electrochemical Science, Vol 11, 2016, 9110-9122, doi: 10.20964/2016.11.55.
- *R. Muntean, D. Pascal, G. Mărginean, N. Vaszilcsin* - **Carbon nanofibers decorated with Pt-Co nanoparticles as catalysts for electrochemical cell applications. I. Synthesis and structural characterization** – International Journal of Electrochemical Science – In press.
- *U. Rost, G. Mărginean, R. Muntean, Pit Podleschny, M. Brodmann* - **A cost-effective PEM fuel cell test system based on hydraulic compression with optimized platinum catalyst loading** – Energy and Sustainability Conference, 2016, 30. 06. 2016 – 01. 07. 2016, IEEE Xplore, September 2016, DOI: 10.1109/IESC.2016.7569500.
- *R. Muntean, U. Rost, D. Pascal, G. Mărginean, N. Vaszilcsin* - **Determination of the electrochemical surface area for CNF/Pt electrocatalyst using cyclic voltammetry**, Chemical Bulletin of "Politehnica" University of Timișoara, Romania, Vol. 61 (75) 2, 2016.
- *R. Muntean, U. Rost, G. Mărginean, N. Vaszilcsin* - Studies on electrodeposition of platinum nanoparticles as a function of differently activated carbon nanofibers, Carbon 2015, 12 – 17 July, Dresden, Germany, 2015.
- *U. Rost, R. Muntean, G. Mărginean, N. Vaszilcsin, M. Brodmann* - Effect of the parameters for oxygen plasma activation of carbon nanofibers on the characteristics of deposited platinum catalyst nanoparticles, Carbon 2015, 12 – 17 July, Dresden, Germany, 2015.
- *R. Muntean, U. Rost, G. Mărginean, N. Vaszilcsin* - Determination of the electrochemical surface area for CNFs electrocatalyst using cyclic voltammetry, BraMat 2015, 5 – 7 March, Brasov, Romania, 2015.
- *R. Muntean, U. Rost, G. Mărginean, N. Vaszilcsin* - Optimization of the electrodeposition parameters for platinum nanoparticles on carbon nanofibers support, AMS 2015, 16 – 17 October, Timisoara, Romania, 2015.
- *U. Rost, R. Muntean, P. Podleschny, G. Mărginean, M. Brodmann, V. A. Șerban* - Investigation of the influence of graphitization degree of carbon nano fibers serving

- as catalysts support material for noble electro catalysts on the performance of PEM fuel cells, AMS 2015, 16 – 17 October, Timisoara, Romania, 2015.
- *R. Muntean, I. Secoșan, G. Mărginean, W. Brandl* - Influence of the morphology and structure of different protective Al – based coatings on their corrosion behavior in aqueous NaCl 3.5% solution, Junior Euromat 2014, The Federation of European Materials Societies, 21-25 July, Lausanne, Switzerland, 2014.
 - *P. C. Vălean, G. Mărginean, R. Muntean, N. Kazamer* - Characteristics of NiCrBSi thermal sprayed coatings remelted by an electromagnetic induction process, Junior Euromat 2016, The Federation of European Materials Societies, 10-14 July, Lausanne, Switzerland, 2016.
 - *D.T. Pascal, R. Muntean, N. Kazamer, G. Mărginean, W. Brandl, V. A. Serban*, Characteristics of High Temperature Vacuum Brazed WC-Co-NiCrBSi Functional Composite Coatings, 8th International Conference on Nanomaterials Research & Application, 19 – 21 October, Brno, Czech Republic.
 - *M. Kiryc, R. Muntean, A. Enache, D. Pascal, N. Kazamer, P. Vălean, G. Mărginean* - Electrodeposition and characterization of Zn-GO thin coatings, ZENIT Science Conference between North Rhine-Westphalia and the Russian Federation, 26 April, Münster, Germany, 2016.
 - *R. Muntean, U. Rost, G. Mărginean, W. Brandl* - Bestimmungen der elektrochemischen Oberfläche für CNFs – Pt – Electrocatalyst mit Cyclovoltammetrie, KoopKaffee Workshop, 6 Mai, Gelsenkirchen, Deutschland, 2015.
 - *R. Muntean, U. Rost, G. Mărginean* - Optimierung der Parameter für die elektrochemische Abscheidung von Platinnanopartikeln auf Kohlenstoffnanofasern, KoopKaffee Workshop, 27 April, Gelsenkirchen.
 - *R. Muntean, I. Secoșan, G. Mărginean, W. Brandl* - Einfluss der Morphologie und der Struktur verschiedener Al-basis-Schutzschichten auf das Korrosionsverhalten in wässrigen 3.5% NaCl – Lösungen, KoopKaffee Workshop, 24 April, Gelsenkirchen, Germany 2014.
 - *D.T. Pascal, R. Muntean, N. Kazamer, G. Mărginean, W. Brandl, V. A. Șerban*, Characteristics of High Temperature Vacuum Brazed WC-Co-NiCrBSi Functional Composite Coatings, NANOCON 2016, 19 – 21 October, Brno, Czech Republic.

CURRICULUM VITAE

PERSONAL INFORMATION:

Name: Roxana Muntean
Nationality: Romanian
Date of Birth: 04. July 1988
Email: roxana.muntean@upt.ro;
roxana.muntean@w-hs.de

EDUCATION:

October 2013 – present: PhD Student

- Faculty of Industrial Chemistry and Environmental Engineering – Politehnica University of Timișoara, Romania;
- Materials Science Department – Westphalian University of Applied Sciences, Gelsenkirchen, Germany;
- Research activities in the field of corrosion, metal electrodeposition, materials characterisation;
- Main topic: Development of catalysts materials based on carbon nanofibers for electrochemical cell applications.

10.2011 – 09.2013: Master Degree (M. Sc.)

- Faculty of Industrial Chemistry and Environmental Engineering, Micro and Nano Materials Politehnica University of Timisoara, Romania;
- Main topic: Electrodeposition of Ni-Zn alloys from acid baths on copper substrate.

10.2007 – 07.2011: Bachelor Degree (B. Sc)

- Faculty of Industrial Chemistry and Environmental Engineering, Industrial Chemistry and Environmental Engineering, Inorganic Substances Engineering and Environmental Protection, Politehnica University of Timisoara, Romania
- Main topic: Zinc electrodeposition from acid baths on copper substrate

10.2007 – 07.2010: Bachelor Degree (B. Ec)

- Economics, Accounting and Management Informatics, "Ioan Slavici" University, Timisoara, Romania;
- Main topic: Elaboration of a Project about Rehabilitation, modernization, development and equipping of social services infrastructure based on European Funds, ROP 2007-2013.

Languages: English, German, French.